

**Application of *Sutherlandia flutescens* in cosmetic skin industry (phytochemical fingerprinting and its activity against skin immune diseases.**

**Bongiwe Msebele**

**A thesis submitted in partial fulfilment of the requirements of the degree of Magister Scientiae in Department of Chemistry, University of the Western Cape.**



**Supervisors: Prof. A.M Hussein and Prof. P.G.L Baker**

**2020**

---

# DECLARATION

---

I, Bongiwe Msebele hereby declare that “*Application of Sutherlandia flutescens in cosmetic skin industry (phytochemical fingerprinting and its activity against skin immune diseases.*” thesis is my own work, that it has not been submitted for any degree or examination in any other university, and that all the sources I have used or quoted have been indicated and acknowledged by complete references.

Full name: Bongiwe Msebele

Signed.....

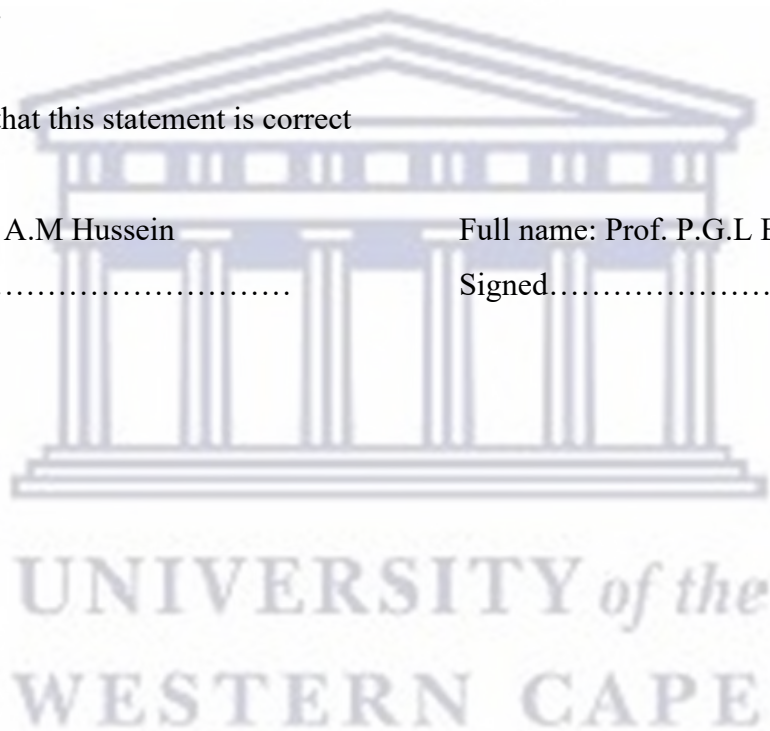
I hereby certify that this statement is correct

Full name: Prof. A.M Hussein

Signed.....

Full name: Prof. P.G.L Baker

Signed.....



---

# DEDICATION

---

Dedicated to my loving family, friends and to those that choose to follow their dreams.



UNIVERSITY *of the*  
WESTERN CAPE

---

# ACKNOWLEDGEMENTS

---

First and foremost, I would like to give all thanks to God for making all things possible and getting me through the hard times.

I want to thank Prof. A.M Hussein and Prof. P.G.L Baker for accepting to be my supervisors for this present work. I will be forever grateful to them for providing me with the opportunity to rejuvenate my research career. Their advice, remarks, guidance and commitment. It is an honour to be one of their postgraduate students at the University of Western Cape.

Thank you to my laboratory colleagues from University of the Western Cape and Cape Peninsula University of Technology.

The National Research Foundation, which financially supported my work. Mr. Lesch, Prof. E. Enthunes and Ms. Jackson for their technical assistance and their human kindness towards me throughout the period of working on this project.

I would like to thank my family and friends for the love they have shown to me, the constant encouragement, support and prayers for the success of my studies.



UNIVERSITY *of the*  
WESTERN CAPE

---

# ABSTRACT

---

Hyperpigmentation disorders such as melasma, freckles and black-pigmented spots on the surface of the skin are often a result of increased over production and accumulation of melanin pigments in the skin. In melanin biogenesis, tyrosinase is the key enzyme that catalysis the synthesis of melanin, thus the most effective and easiest way to reduce melanin synthesis is by inhibiting tyrosinase. There are a large number of reported tyrosinase inhibitors, their identification and isolation from natural sources is highly important because when natural tyrosinase inhibitors are identified in natural sources, their production is relatively low in cost. Tyrosinase inhibitors are highly sought in the cosmetic industry because of their skin – whitening effects. Most common used tyrosinase inhibitors are kojic acid (KA), arbutin, hydroquinone and ascorbic acid. However, these inhibitors have side effects and lack clinical efficiency. These facts led us to focus our research work on the exploration of natural tyrosinase inhibitors. Due to the therapeutic potential of medical plants researchers are not only concerned with validating ethnopharmacological usage of plants, but also with identification, isolation and characterization of bioactive components. *Sutherlandia frutescens* and *Psoralea aphylla* are both examples of indigenous fynbos species, which have been applied by indigenous people for the benefit of their medicinal properties. However, due to limited availability of *Sutherlandia frutescens*, the thesis was focused on *Psoralea aphylla*, using the same research methodology. *Psoralea aphylla* is a leafless fountain bush of the Fabaceae family found in the Cape Floristic Region (CFR) of South Africa. To the best of our knowledge, the chemical components of *Psoralea aphylla* have not been reported in literature, to date. In this study, methanolic extract of *Psoralea aphylla* was subjected to different chromatographic methods which included column chromatography and HPLC, that led to the isolation of four known compounds (C1) Bakuchiol, (C2) 12,13-Dihydro-12,13-epoxybakuchiol , (C3) 3-hydroxybakuchiol and (C4) well-known steroids which are stigmasterol and  $\beta$ -sitosterol . The structures of the isolated compounds were identified by interpretation of 1D ( $^1\text{H}$ ,  $^{13}\text{C}$ ) and 2D (COS Y, HSQC, HMBS) NMR spectrometry, MS, UV and IR data.

The extract and isolated compounds were screened for their inhibitory activities on mushroom tyrosinase using L-tyrosine as substrate. The compounds showed low inhibition activity compared to of kojic acid (KA), a well-known tyrosinase inhibitor. Furthermore, cyclic voltammetry was used to investigate the possibility a pre-screening natural tyrosinase

inhibitors. Our results suggest that the electrochemical method for pre-screening tyrosinase inhibitors and can provide high sensitivity.

Lastly, the cytotoxicity of bakuchiol (C1) was investigated against B16 melanoma cells using the MTT assay. Bakuchiol showed cytotoxicity on B16 melanoma cells with an  $IC_{50}$  value of 11.66  $\mu\text{g}/\text{mL}$ .



---

## TABLE OF CONTENTS

---

<b>DECLARATION</b> .....	<b>ii</b>
<b>DEDICATION</b> .....	<b>iii</b>
<b>ACKNOWLEDGEMENTS</b> .....	<b>iv</b>
<b>ABSTRACT</b> .....	<b>v</b>
<b>LIST OF FIGURES</b> .....	<b>xi</b>
<b>LIST OF TABLES</b> .....	<b>xvi</b>
<b>LIST OF ABBREVIATIONS</b> .....	<b>xviii</b>
<b>CHAPTER 1:</b> .....	<b>20</b>
<b>Introduction</b> .....	<b>20</b>
<b>1.1. Medical plants</b> .....	<b>20</b>
<b>1.2. Bioactive Natural Products</b> .....	<b>21</b>
<b>1.3. Introduction to the Leguminosae/Fabaceae family and genus <i>Psoralea</i></b> .....	<b>22</b>
1.3.1. Leguminosae/Fabaceae family. ....	22
1.3.2. Characteristics of the family Fabaceae .....	23
1.3.3. The genus <i>Psoralea</i> .....	24
1.3.4. Phytochemical studies on genus: <i>Psoralea</i> .....	25
<b>CHAPTER 2:</b> .....	<b>43</b>
<b>Literature Review</b> .....	<b>43</b>
<b>2.1. Cape Florist Kingdom</b> .....	<b>43</b>
<b>2.2. <i>Psoralea aphylla</i></b> .....	<b>45</b>
2.2.1. Taxonomy of <i>Psoralea aphylla</i> .....	45
2.2.2. Historical background of <i>Psoralea aphylla</i> .....	45
2.2.3. Description of <i>Psoralea aphylla</i> .....	45
2.2.4. Distribution, habitat and uses of <i>Psoralea aphylla</i> .....	46
<b>2.3. Biosensors</b> .....	<b>47</b>
2.3.1. Electrochemical biosensors.....	47



2.3.2.    Electrochemical Biosensors Based on Tyrosinase enzyme Inhibition.....	48
<b>CHAPTER 3: .....</b>	<b>50</b>
<b>Methods and Techniques .....</b>	<b>50</b>
<b>3.1. Principle of pre-extraction of plant samples .....</b>	<b>50</b>
<b>3.2. Principle of plant sample extraction .....</b>	<b>50</b>
<b>3.3. Chromatographic techniques in natural product studies .....</b>	<b>51</b>
3.3.1. Thin Layer Chromatography .....	51
3.3.2. Column Chromatography.....	53
3.3.4. Open column chromatography.....	54
3.3.5. High Performance Liquid Chromatography .....	54
<b>3.4. Characterization techniques .....</b>	<b>56</b>
3.4.1. Nuclear Magnetic Resonance (1D and 2D NMR) .....	56
3.4.2. Ultraviolet and visible spectrometry (UV-Vis) .....	57
3.4.3. Fourier-transform infrared spectroscopy (FTIR) .....	57
3.4.4. Mass Spectrometry .....	58
<b>3.5. Tyrosinase Inhibition studies .....</b>	<b>58</b>
3.5.1. Tyrosinase inhibition Assay .....	58
3.5.2. Tyrosinase Inhibition using Cyclic Voltammetry (CV).....	59
<b>3.6. MTT Assay.....</b>	<b>60</b>
<b>CHAPTER 4: .....</b>	<b>62</b>
<b>Materials and Methodology .....</b>	<b>62</b>
<b>4.1. Materials .....</b>	<b>62</b>
4.1.1. Solvents and reagents .....	62
4.1.2. Preparation of 50mM phosphate buffer.....	63
4.1.3. Preparation of tyrosinase enzyme and l-tyrosine standard solutions.....	63
4.1.4. Preparation of kojic acid .....	63
4.1.5. Preparation of constituents for cyclic voltammetry .....	63



4.1.6.	Preparation of electrodes .....	64
4.1.7.	Cell Culture.....	64
4.1.8.	Sub-culturing of cells .....	65
4.1.9.	Cell Counting and Viability Testing .....	65
4.1.10.	Preparation of PBS buffer MTT stock solution.....	65
4.1.11.	Preparation of bakuchiol for MTT Assay .....	65
<b>Part A</b> .....		<b>66</b>
<b>4.2. Methodology of Organic experiment</b> .....		<b>66</b>
4.2.1.	Collection and identification of plant .....	66
4.2.2.	Pre-extraction and extraction of <i>Psoralea aphylla</i> .....	66
4.2.3.	Fractionation of crude extract.....	67
4.2.4.	Isolation of Compound 1 using Column Chromatography.....	69
4.2.5.	Isolation of Compound 2 using HPLC.....	71
4.2.6.	Isolation of compound 3: Column chromatography and crystallization of PA5. <b>Error! Bookmark not defined.</b>	
4.2.7.	Isolation of compound 3: Column chromatography and crystallization of PA5..	77
4.2.8.	Isolation of compound 4: Using the gravity column chromatography and HPLC	81
<b>4.3. Spectroscopic techniques</b> .....		<b>85</b>
4.3.1.	A summary of the Isolation and purification of constituents from <i>Psoralea aphylla</i> 86	
<b>Part B</b> .....		<b>87</b>
<b>4.4. The tyrosinase inhibition assay</b> .....		<b>87</b>
<b>4.5. Electrochemical Tyrosinase Biosensors</b> .....		<b>87</b>
4.5.1.	Standard experiment: Cyclic voltammetry of Tyrosinase and L-tyrosine in PBS buffer	88
4.5.2.	Cyclic voltammetry of Tyrosinase Kojic acid (KA) and L-tyrosine in PBS buffer.	89
4.5.3.	Cyclic voltammetry of Tyrosinase and isolated compounds in PBS buffer.....	90
<b>Part C</b> .....		<b>91</b>

4.6.	<b>Cytotoxicity of Bakuchiol</b> .....	91
4.6.1.	MTT Cytotoxicity Assay.....	91
<b>CHAPTER 5:</b> .....		<b>93</b>
<b>Results and Discussion</b> .....		<b>93</b>
5.1.	<b>Structural elucidation and characterization of the compounds</b> .....	<b>93</b>
5.1.1.	Structural elucidation of Bakuchiol.....	93
5.1.2.	Structural elucidation and characterization of 12,13-Dihydro-12,13-epoxybakuchiol .....	105
5.1.3.	Structural elucidation of 3-hydroxybakuchiol .....	120
5.1.4.	Structural elucidation of Compound 4 - Steroids.....	131
5.1.5.	Summary of analysis of isolated compounds.....	138
5.2.	<b>Tyrosinase inhibition Assay</b> .....	<b>140</b>
5.3.	<b>Tyrosinase solution biosensor</b> .....	<b>141</b>
5.3.1.	Standard experiment: Cyclic voltammetry of Tyrosinase and L-tyrosine in PBS buffer discussion and results .....	141
5.3.2.	Cyclic voltammetry of Tyrosinase, L-tyrosine and Kojic acid (TYR-KA-LTYR biosensor) in PBS buffer.....	143
5.3.3.	Cyclic voltammetry of Tyrosinase and isolated compound in PBS buffer.....	145
5.3.4.	Summary.....	149
5.4.	<b>Cytotoxicity of bakuchiol</b> .....	<b>151</b>
<b>Chapter 6: Conclusion and recommendations</b> .....		<b>153</b>
6.1.	<b>Discussion and Conclusion</b> .....	<b>153</b>
6.2.	<b>Recommendations for further research</b> .....	<b>155</b>
6.3.	<b>References</b> .....	<b>157</b>

---

# LIST OF FIGURES

---

Figure 1: World map showing distribution of <i>Psoralea</i> species, the shaded green parts are where <i>Psoralea</i> is mostly abundant (Koul <i>et al</i> , 2019) .....	24
Figure 2: Schematic representation of human skin layers. ....	37
Figure 3: Example of patients affected by hyperpigmentation on the face and back.....	38
Figure 4:A pathway schematic of the biosynthesis of melanin (Image by Anna Di Cosmo)..	39
Figure 5: A diagrammatic summary of steps in the study of indigenous <i>Psoralea</i> aphylla species, evaluating the phytochemistry and biological activities. ....	42
Figure 6: Location of the Cape Floristic Kingdom shaded with green lines. (Retrieved from <i>Masters 2018: Cape Floristic Region Hotspot Briefing Book 2005</i> ). ....	44
Figure 7: <i>Psoralea</i> aphylla shrub (top left), willow branch with flower (top right), branches and flowers (bottom left) and close up of flower (bottom right).....	46
Figure 8:TLC plate showing the solvent front, spot on spot centre and starting point.....	53
Figure 9: Schematic diagram of silica gel open column chromatography.....	54
Figure 10: Schematic of components of HPLC system.....	55
Figure 11: Example of a three-electrode system.....	59
Figure 12: Example of a cyclic voltammogram for a reversible redox process (Wang, 2006). .....	60
Figure 13: Flow chat of methanolic extraction of <i>Psoralea aphylla</i> . ....	66
Figure 14: Open Column Chromatography set-up.....	67
Figure 15: Picture of main fractions of <i>P. aphylla</i> .....	68
Figure 16: Flow chat of fractionation of methanolic extract. ....	69
Figure 17: TLC chromatograms of main fractions obtained from column chromatography fractionation of <i>P. aphylla</i> methanolic extract. Using Hexane–ethyl acetate (8:2, v/v) solvent system. A: TLC plate visualized under UV light of $\lambda = 254$ nm, B: TLC plate under UV. C: TLC plate after spraying with vanillin solution. ....	69

Figure 18: TLC chromatographs of sub-fractions of PAM1-6-4 eluted in Hex-EtOAc (7:3,v/v) solvent.....	71
Figure 19: HPLC chromatograph fraction PA3, with Compound 2 at 16.0min and TLC chromatograph under UV light of $\lambda = 254$ nm. ....	76
Figure 20: TLC chromatograms of sub fractions obtained from gravity column chromatography fractionation of PA5 + PA6. Plate developed using MeOH-DCM (4:6, v/v) solvent system. ....	78
Figure 21: TLC chromatograms of sub fractions obtained from gravity column chromatography fractionation of PB2 + PB3 + PB4. Plate developed using n-Hexane–ethyl acetate (8:2, v/v) solvent system. ....	80
Figure 22: HPLC chromatograph fraction PAM1-71-1, with Compound 4 at 25min.....	83
Figure 23: Figure 0:12: TLC chromatograms of sub fractions obtained from gravity column chromatography fractionation of PA5 + PA6. Plate developed using MeOH: DCM (4:6, v/v) solvent system. ....	84
Figure 24: Experimental procedure of the isolation and purification of constituents from <i>Psoralea aphylla</i> . ....	86
Figure 25: Schematic presentation of the standard tyrosinase enzyme and L-tyrosine substrate experiment where represents the tyrosinase enzyme and represents the substrate L-tyrosine.....	89
Figure 26: Schematic presentation of the tyrosinase enzyme, kojic acid and L-tyrosine substrate experiment where represents the tyrosinase enzyme, represents the tyrosinase inhibitor K and L- tyrosine. ....	89
Figure 27: Proposed structure of Compound 1. ....	93
Figure 28: $^1\text{H}$ NMR (400 MHz, $\text{CDCl}_3$ ) spectrum of Compound 1. ....	95
Figure 29: Top- DEPT 135 NMR (400 MHz, $\text{CDCl}_3$ ) spectrum of Compound 1, Bottom: $^{13}\text{C}$ NMR (400 MHz, $\text{CDCl}_3$ ) spectrum of Compound 1. ....	96
Figure 30: $^1\text{H}$ - $^1\text{H}$ COSY (400 MHz, $\text{CDCl}_3$ ) spectrum of Compound 1. ....	98
Figure 31: Figure 29: Important $^1\text{H}$ - $^1\text{H}$ correlations represented by <b>————</b> .....	99
Figure 32: Important HMBC correlations of Compound 1. ....	99

Figure 33: HMBC (400 MHz, CDCl <sub>3</sub> ) spectrum of Compound 1. ....	100
Figure 34: FTIR spectrum of bakuchiol, Compound 1.....	103
Figure 35: UV spectrum of bakuchiol. ....	104
Figure 36: Proposed structure of Compound 2.....	105
Figure 37: <sup>1</sup> H NMR (400 MHz, CDCl <sub>3</sub> ) spectrum of Compound 2. ....	106
Figure 38: <sup>1</sup> H NMR (400MHz, CDCl <sub>3</sub> ) spectrum of both Compound 2 and Bakuchiol;. Top: Compound 2, Bottom: Bakuchiol. ....	107
Figure 39: <sup>13</sup> H NMR (400MHz, CDCl <sub>3</sub> ) spectrum of Compound 2.....	109
Figure 40: <sup>13</sup> C NMR (400MHz, CDCl <sub>3</sub> ) spectrum of Compound 1 and Compound 2. Where Red: compound 2 , Blue :Bakuchiol. ....	110
Figure 41: DEPT-135 NMR (400MHz, CDCl <sub>3</sub> ) spectrum of compound 2. ....	111
Figure 42: <sup>1</sup> H- <sup>1</sup> H COSY (400 MHz, CDCl <sub>3</sub> ) spectrum of Compound 2. ....	113
Figure 43: : Important <sup>1</sup> H- <sup>1</sup> H correlations represented by ———. ....	114
Figure 44: Important HMBC correlations of Compound 2. ....	114
Figure 45: HMBC (400 MHz, CDCl <sub>3</sub> ) spectrum of Compound 2.....	115
Figure 46: FTIR spectrum of 12,13-dihydro 12,13-epoxybakuchiol (Compound 2). ....	118
Figure 47: UV spectrum of 12,13-dihydro 12,13-epoxybakuchiol.....	119
Figure 48: Proposed structure of compound 3.....	120
Figure 49: <sup>13</sup> H NMR ( 400 MHz , CDCl <sub>3</sub> ) spectrum of compound 3.....	121
Figure 50: <sup>1</sup> C NMR ( 400 MHz , CDCl <sub>3</sub> ) spectrum of compound. ....	122
Figure 51: DEPT 135 NMR ( 400 MHz , CDCl <sub>3</sub> ) spectrum of compound 3.....	123
Figure 52: HMBC NMR ( 400 MHz , CDCl <sub>3</sub> ) spectrum of compound 3. ....	125
Figure 53: FTIR spectrum of 3-hydroxybakuchiol (Compound 3). ....	128
Figure 54: UV spectrum of 3-hydroxybakuchiol.....	129
Figure 55: The mass spectra of 3-hydroxybakuchiol isolated from the methanolic extract of <i>Psoralea aphylla</i> plan .....	130
Figure 56: Proposed structures of Compound 4 (1a is stigmasterol and 1b is sitosterol).....	131



Figure 57: <sup>1</sup> H NMR ( 400 MHz , CDCl <sub>3</sub> ) spectrum of compound 4. ....	132
Figure 58: <sup>13</sup> C NMR ( 400 MHz , CDCl <sub>3</sub> ) spectrum of compound 4. ....	133
Figure 59: UV spectrum of stigmasterol and β-sitosterol.....	137
Figure 60: A bar graph showing average tyrosinase inhibition percentages of <i>Psoralea aphylla</i> methanol extract and isolated compound in comparison to kojic acid at different concentrations (50 UL= 25 μg/ml and 100UL= 50 μg/ml). Where KA is Kojic acid, MA is the methanolic extract of <i>Psoralea aphylla</i> , C1 is bakuchiol, C2 is 12,13 – dihydro-12,13-epoxybakuchiol.....	140
Figure 61: Cyclic voltammetry of tyrosinase measured using a GCE in response to different concentrations of L-tyrosine in 50 mM PBS pH 6.5, vs Ag/AgCl, at a scan rate of 50mV/s. ....	142
Figure 62: Full calibration curve of current vs concentration of L-tyrosinase at GCE in 50 mM PBS pH 6.5, vs Ag/AgCl, at a scan rate of 50mV/s. , n = 3 measurements. ....	142
Figure 63: Cyclic voltammetry of tyrosinase measured using a GCE in response to a fixed concentration of KA and different concentrations of L-tyrosine in 50 mM PBS pH 6.5, vs Ag/AgCl, at a scan rate of 50mV/s. ....	144
Figure 64: Full calibration curve of current vs concentration of L-tyrosinase at GCE in 50 mM PBS pH 6.5, vs Ag/AgCl, at a scan rate of 50mV/s. , n = 3 measurements. ....	144
Figure 65: Cyclic voltammetry of tyrosinase measured using a GCE in response to different concentrations of bakuchiol in 50 mM PBS pH 6.5, vs Ag/AgCl, at a scan rate of 50mV/s. ....	145
Figure 66: Calibration curve of tyrosinase responding to different concentrations of bakuchiol as a substrate in 50 mM PBS pH = 6,5 at scan rate of 50mV/s using GCE vs Ag/AgCl. ....	146
Figure 67: Cyclic voltammetry of tyrosinase in response to different concentrations of 12,13-dihydro- 12, 13 – epoxybakuchiol in 50 mM PBS pH = 6.5, at scan rate of 50mV/s using a GCE.....	147
Figure 68: Calibration curve of tyrosinase responding to different concentrations of 12,13-dihydro- 12,13- epoxybakuchiol as a substrate in 50 mM PBS pH = 6,5 at scan rate of 50mV/s using GCE vs Ag/AgCl. ....	147

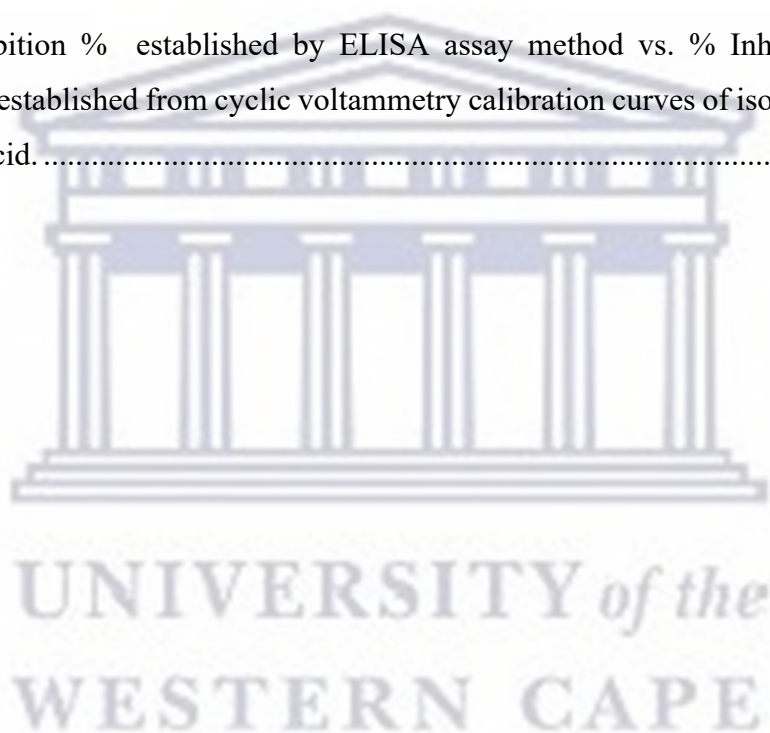
Figure 69: Cyclic voltammetry of tyrosinase in response to different concentrations of 3-hydroxybakuchiol in 50 mM PBS pH = 6.5, at scan rate of 50mV/s using a GCE.....148

Figure 70: Scatter plot tyrosinase in response of different concentrations of 3-hydroxybakuchiol compound using 50 mM PBS electrolyte at scan rate of 50mV/s using a GCE.....149

Figure 71: Cytotoxicity of Bakuchiol on B16 Melanoma cells. The cells were treated with concentration between 1.56 – 100 µg/mL, for 48 hours. Data are expressed as mean ± SEM ( *n* = 3).....151

Figure 72: Dose-Response-Inhibition of Bakuchiol on B16 Melanoma cells. ....152

Figure 73: Inhibition % established by ELISA assay method vs. % Inhibition based on sensitivity established from cyclic voltammetry calibration curves of isolated compounds and kojic acid. ....154





---

# LIST OF TABLES

---

Table 1: Drugs derived from plants, their sources and medical uses.....	21
Table 2: Selected various types of flavonoids including flavones, flavonols, flavanones, isoflavones and chalcones isolated from <i>Psoralea</i> genus.....	25
Table 3: Selected various types of Coumarins isolated from <i>Psoralea</i> genus.....	31
Table 4: Selected various types of phenols isolated from <i>Psoralea</i> genus.....	33
Table 5: Taxonomy of <i>Psoralea aphylla</i> . ....	45
Table 6: Solvent system used for fractionation of the total extract of <i>Psoralea aphylla</i> .....	67
Table 7: Fractions obtained upon fractionation of total extract of <i>P.aphylla</i> . ....	68
Table 8: The sub-fractions from the fractionation of PAM1-6-4. ....	70
Table 9: HPLC conditions for the isolation of Compound 2. conditions*.....	77
Table 10: Collective sub-fractions from the fractionation process of PA5 and PA6.....	77
Table 11: Collective sub-fractions from the fractionation process of PB2, PB3 and PB4. ....	79
Table 12: Solvent system used in the fractionation process fraction PA7.....	81
Table 13: Collective sub-fractions from the fractionation process of PA7. ....	81
Table 14: The gradient mobile phase A: DIW, and mobile phase B: MeOH during profiling of fractions. The run time was 60min. ....	82
Table 15: HPLC conditions for the isolation of Compound 4 conditions*.....	84
Table 16: <sup>1</sup> H [400 MHz: m, J(Hz)] and <sup>13</sup> C (100 MHz) NMR spectral data of Compound 1. Where * presents quaternary carbons. ....	101
Table 17: FT-IR analysis data interpretation of bakuchiol (compound 1).....	102
Table 18: <sup>1</sup> H [400 MHz: m, J(Hz)] and <sup>13</sup> C (100 MHz) NMR spectral data of Compound 2. Where * presents quaternary carbons. ....	116
Table 19: FT-IR analysis data interpretation of 12,13-dihydro 12,13-epoxybakuchiol (compound 2).....	117

Table 20:  $^1\text{H}$  [400 MHz: m, J(Hz)] and  $^{13}\text{C}$  (100 MHz) NMR spectral data of Compound 3.  
The \* represent quaternary carbons. .... 126

Table 21: FT-IR analysis data interpretation of 3-hydroxybakuchiol. .... 127

Table 22:  $^1\text{H}$  [400 MHz: m, J(Hz)] and  $^{13}\text{C}$  (100 MHz) NMR spectral data of Compound 4,  
which is a mixture of stigmasterol and sitosterol..... 135

Table 23: Comparison of analytical electrochemical performance of isolated compounds  
compared to a known tyrosinase inhibitor, kojic acid and substrate L-tyrosine..... 150



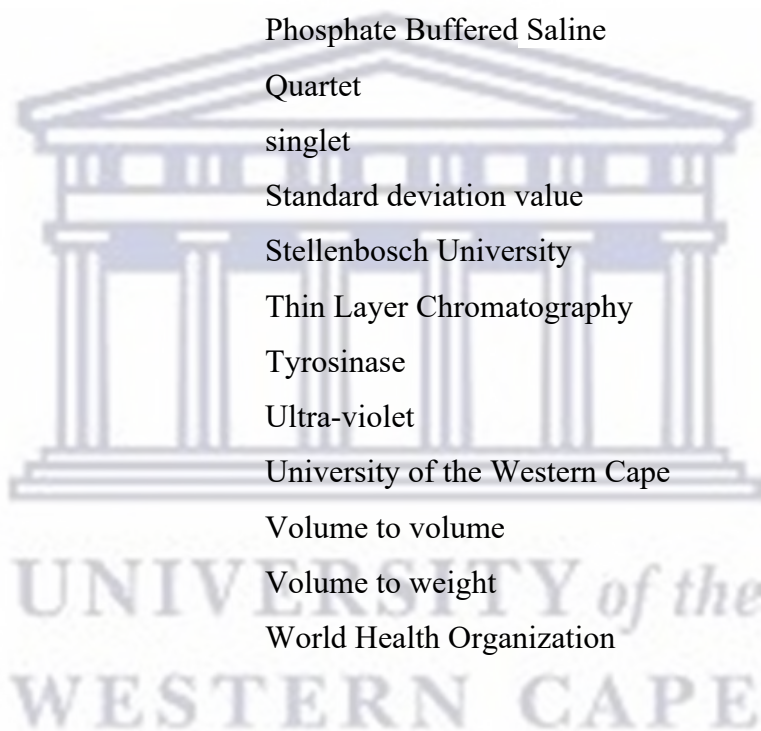
---

# LIST OF ABBREVIATIONS

---

$\mu\text{g}$	Micrograms
$\mu\text{L}$	Microliters
$^{13}\text{C}$	Carbon-13
$^1\text{H}$	Proton
Ace	Acetone
bs	broad singlet
CC	Column Chromatography
$\text{CCl}_3\text{D}$	Deuterated Chloroform
CPUT	Cape Peninsula University of Technology
CV	Cyclic Voltammetry
d	doublet
DCM	Methylene dichloride / Dichloromethane
dd	doublet of doublets
DMSO	Dimethyl sulfoxide
ELISA	Enzyme-linked immunosorbent assay
EtOAc	Ethyl acetate
FTIR	Fourier-transform infrared spectroscopy
gCOSY	Gradient-enhanced correlation spectroscopy
gHMBC	Gradient-enhanced heteronuclear multiple bond coherence
$\text{H}_2\text{O}$	Water
$\text{H}_2\text{SO}_4$	Sulfuric Acid
HPLC	High Performance Liquid Chromatography
hr	Hour/s
$\text{IC}_{50}$	Half maximal inhibitory concentration
J	Coupling constant in Hz
KA	Kojic acid
kg	Kilogram
L-Tyr	L-Tyrosine

LOD	Limit of detection
<i>m/z</i>	Mass to charge ratio
MeOH	Methanol
mg	Milligram
min	Minute
mL	Milliliters
MTT	3-(4,5-Dimethylthiazol2-yl)-2,5-diphenyl tetrazolium bromide
NMR	Nuclear Magnetic Resonance
° C	Degrees Celsius
PBS	Phosphate Buffered Saline
q	Quartet
s	singlet
STD	Standard deviation value
SU	Stellenbosch University
TLC	Thin Layer Chromatography
TYR	Tyrosinase
UV	Ultra-violet
UWC	University of the Western Cape
v/v	Volume to volume
v/w	Volume to weight
WHO	World Health Organization



---

# CHAPTER 1:

## Introduction

---

*This chapter introduces an overview of the importance of medicinal plants, drugs derived from plants, hyperpigmentation of the human skin, causes of hyperpigmentation.. This chapter also presents a review on human skin , tyrosinase inhibition and an introduction to the Fabaceae family and genus Psoralea.*

### 1.1. Medical plants

Medicinal plants are plants used in herbalism and thought to have certain extractable compounds in their leaves, stems, flowers and fruit for medicinal purposes. These extracts are used as inputs in the pharmaceutical, nutraceutical, insecticide and other chemical industries. For several centuries medicinal plants have been used as remedies for human diseases due to their therapeutic properties (Van Wyk *et al.*, 2011; Nastro *et al.*, 2000). The practice of traditional medicine is widespread and has been documented by the ancient Chinese, Indian, Japan, Sri Lanka and Northern and Southern African civilizations. The records of medicinal plants in the Western Cape dates as far back as the 1700s by Lichtenstein and Carl Thunberg (known as the father of South African botany), they noted the use of medicinal plants (Goldblatt *et al.*, 2008). There is a high demand for medicinal plants due to their perceived ability to stop bleeding, speed up healing of wounds, treat burns and alleviate other skin conditions. According to The World Health Organization (WHO), traditional medicine is widely used by about 75-95% of the population in developing countries as part of their primary health care (Mabona and Van Vuuren., 2013). Moreover, using medical plants to treat skin infections is very common in many rural areas. In South Africa, the large proportion of the population uses traditional medicine for the treatment of various ailments in both human and animals (Masika and Afolayan., 2002). There are about 20 000 traditional healers in southern Africa, and up to 60% of the population prefer to consult traditional healers or use traditional healers in addition to western medical doctors (Van Wyk *et al.*, 1997).

Fortunately, in recent years there has been an upsurge in research and development of new medicinal products and new medicinal crops, as is shown by a rapid increase in the number of scientific publications and patents. It is very important and urgent to systematically document

indigenous knowledge on the use of traditional medicinal plants before the knowledge becomes lost and forgotten. Research on medical plants utilization in South Africa used for dermatological purposes is still underdeveloped and relatively little chemical work has been done on medicinal plants from this country (George *et al.*, 2001). An estimated 10% of the world plant diversity is found in southern Africa and only about 20% of known plants in the world have been used in pharmaceutical studies( Van Wyk, 2011).

## 1.2. Bioactive Natural Products

The isolation of bioactive pure compounds and the identification principles of medicinal plant only began in the 19<sup>th</sup> century (Patrick., 2005) Natural products isolated in the 19<sup>th</sup> century included drugs such as aspirin, cocaine, vinblastine, digitoxin, quinine and morphine. Drugs derived from plants as medical agents have been summarized in the Table 1.

**Table 1: Drugs derived from plants, their sources and medical uses.**

Drug name	Plant source	Uses	References
Aspirin	Common name: Willow tree bark Scientific name: <i>Salix</i>	Analgesic, antipyretic and anti-inflammatory	(Newman <i>et al.</i> , 2000; Gilani and Rahman 2005; Gurib-Fakim 2006)
Cocaine	Common name: Coca plant Scientific name: <i>Erythroxylum coca</i>	Anaesthetic	(Gilani and Rahman ,2005; Gurib-Fakim ,2006; Van Wyk <i>et al.</i> , 2000)
Vinblastine	Common name: Madagascar periwinkle Scientific name: <i>Catharanthus roseus</i>	Anticancer	(Hostettman, 1999; Mans <i>et al.</i> , 2000)



Digitoxin	Common name: Fox glove	Cardiotonic	(López-Lázaro et al. 2006).
	Scientific name: <i>Digitalis purpurea</i>		
Quinine	Common name: <i>Cinchona</i> bark	Antimalarial	(Newman et al. 2000, Gilani and Rahman 2005, Gurib-Fakim 2006).
	Scientific name: <i>Cinchona ledgeriana</i>		
Morphine	Common name: Opium poppy	Analgesic	(Newman et al., 2000)
	Scientific name: <i>Papaver somniferum</i>		

Medical plants are a large source of therapeutic phytochemicals that lead to development of novel drugs, making the study of natural products from medical plants be of great importance in worldwide.

### 1.3. Introduction to the Leguminosae/Fabaceae family and genus *Psoralea*.

#### 1.3.1. Leguminosae/Fabaceae family.

The Fabaceae or Leguminosae family, commonly known as the legume family, pea family, bean family or pulse family, is the 3<sup>rd</sup> of the largest land flowering plant families (angiosperms) behind Orchidaceae (orchid family) and Asteraceae (aster family) (Nofel., 2016). Fabaceae is classified under the Plantae kingdom, division of Magnoliophyta, class of Magnoliopsida and order of Fabales (Wanda, Njamen and Gamo, 2015). It comprises 730 genera and more than known 19,400 species without considering the unknown and micro species (Allen and Allen, 1981). Leguminosae is an older name, which refers to the typical fruit of these plants, which are called legumes. The family is now commonly known as Fabaceae, however, the name Leguminosae is still considered to be valid. The name “Fabaceae” comes from a no longer existing genus “*Faba*”, which is now included in *Vicia* (Nofel, 2016). The family is diverse and economically important. Economically, legumes are only second to the grasses



(Gramineae) because of their nitrogen-fixing symbioses (Allen and Allen, 1981). The Fabaceae family is most commonly found in tropical rainforests and dry forests in Africa and America. Many legumes are also found in temperate plains, wood, and deserts (Wanda, Njamen and Gamo, 2015). The family is split based mainly on their floral differences into three distinctive subfamilies, namely Caesalpinioideae, Mimosoideae, Papilionoideae or Faboideae; and taxonomist further separated these families to Mimosoideae, Papilionoideae/Faboideae are considered to be natural groups, and Caesalpinioideae which is considered not natural (Doyle, 2001). The subfamily Mimosoideae has 76 genera and 2000-3000 species. The legumes are primary woody plants of the tropics and in temperate parts of the world few native species are herbaceous. The subfamily Faboideae is the largest group of legumes; it includes 483 genera and close to 14000 species grouped to 28 tribes. The subfamily Faboideae (also called Papilionoideae) legumes are mostly found in tropics, however, unlike the other two subgroups, they are extensively found temperate and arid parts of the world, mostly as herbaceous (Wanda, Njamen and Gamo, 2015). The Papilionoideae subfamily is the largest and is family to the most economically important legumes including pulses and forages (Talukdar, 2013; wojciechowski *et al.*, 2003; Lewis *et al.*, 2005). The subfamily Caesalpinioideae is a heterogeneous group of plants; it includes about 161 genera and 300 species. Caesalpinioideae legumes are found throughout the world but tropical parts of the world are occupied woody plants, while the herbaceous evolutionary derivatives are mostly found in temperate regions. Studies on some of the Fabaceae genera have been found to contain biologically active compounds, for example the species of *Psoralea pinnata* and *Psoralea corylifolia*. (Jiangning *et al.*, 2005; Chopra, Dhingra and Dhar, 2013; Li *et al.*, 2015).

### **1.3.2. Characteristics of the family Fabaceae**

Family Fabaceae is characterized by trees, shrubs, woody vines and by its distinctive (and eponymous) fruit, a two-valve pod whose halves separate to disperse the seeds; however, this form is modified into a wide variety of shapes and sizes, including indehiscent dry or fleshy forms (Allen and Allen, 1981). The family is also characterized by its ability to symbiotically fix nitrogen (Doyle, 2001). Many plant of the Fabaceae family have been found to have antibacterial, antifungal, antioxidant, antiviral, anti-feedant, antihypertensive, hepatoprotective and cytotoxic effects (Wanda, Njamen and Gamo, 2015).

### 1.3.3. The genus *Psoralea*

The name *Psoralea* is derived from the Greek word “*psoraleos*” which means “affected with the itch or with leprosy” (Maisch., 1889). *Psoralea* is a cosmopolitan genus belonging to the tribe *Psoraleae*, which predominantly occurs in southern Africa, North America, Australia, with outliers in South America, Mediterranean Europe and Asia.



**Figure 1: World map showing distribution of *Psoralea* species, the shaded green parts are where *Psoralea* is mostly abundant (Koul *et al*, 2019)**

The genus was first established by Linnaeus in 1742, not up until 1752, only one species native to America called *Psoralea americana* was known, recognised and described by Linnaeus (Koul *et al*, 2019). *Psoralea* genus comprises of 105 accepted species. The genus is related to 6 genera, which includes *Otholobium*, *Bituminaria* and *Cullen*, which are in the same tribe. It is very challenging to determine and identify the genus; in 1981 Striton recognized that there was more than one genus in America, so he left all the American species under the genus *Orbexilum* sensu lato calling for a detailed reassessment. So far, the taxonomy status and identification of the genus is being investigated. Hence, the South African species herein is being referred to as “*Psoralea aphylla* complex”. In South Africa, Europe, North America, South America, India and a few which are native. In Asia there are 130 species from *Psoralea* widely distributed. The genus has been widely used as traditional medicine in China, India and many other countries for treatment of leprosy, psoriasis, leucoderma, tooth decay, kidney problems, indigestion, tuberculosis, constipation and impotence.

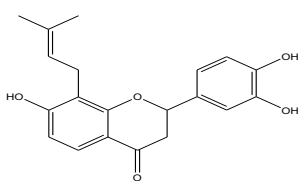
### 1.3.4. Phytochemical studies on genus: *Psoralea*

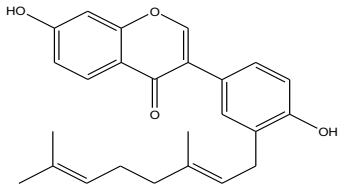
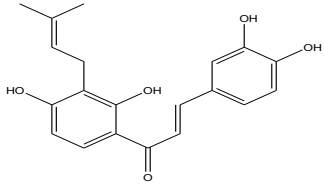
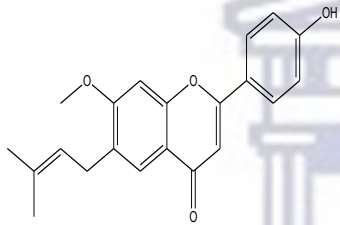
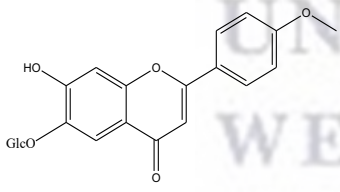
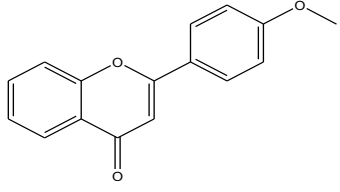
The chemistry of genus *Psoralea* (Fabaceae family) was first investigated in the 1890s when *Psoralea corylifolia* L. (belonging to *Psoralea* genus) was subject to several investigations. More proof of phytochemical studies being done on *P. corylifolia* dates back to 1920. A large number of chemical classes of flavonoids, coumarins, phenols, benzofurans, terpenoids, furanocoumarins, chalcones, steroids, monoterpenes, alcohols, fatty acids, tocopherols, and esters are widely found in different species of *Psoralea* genus (Koul *et al.*, 2018; Li *et al.*, 2016; Alam, *et al.*, 2018). Flavonoids were found to be the most frequently occurring constituents in the genus (Li *et al.*, 2016). The literature available indicates from the genus *Psoralea*, there has been a total of 291 bioactive compounds were isolated and characterized from 06 species. In addition, 150 of those compounds can be isolated from *P. bituminosa* alone. In 1933, the first pure compound called psoralen was isolated from *P. corylifolia* by Jois and co-workers (Koul *et al.*, 2018). Some of the major active constituents and structures of the 291 bioactive compounds isolated from genus *Psoralea* are discussed below. Which includes bakuchiol, isopsoralen, neobavaisoflavone, bavachin, bavachinin, psoralidin and drupanol.

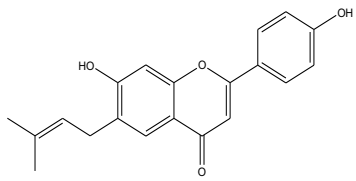
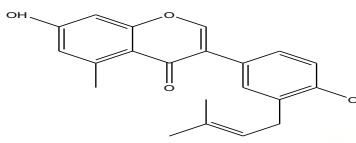
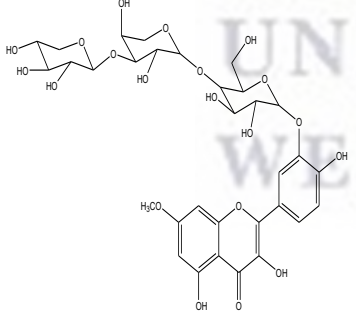
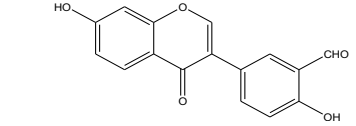
#### Group 1: Flavonoids

Flavonoids are a group of phenolic compounds, which are one of the most diverse and widespread groups of natural constituents. These phenolic compounds are present in all foods of plant origin and are of great importance in human dietary ingredients and health. They cannot be synthesized by humans or animals, but have extensive biological properties that promote human health and help with reducing the risk of diseases.

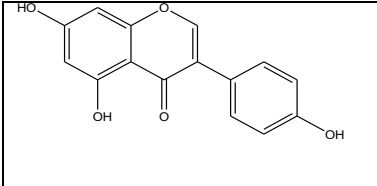
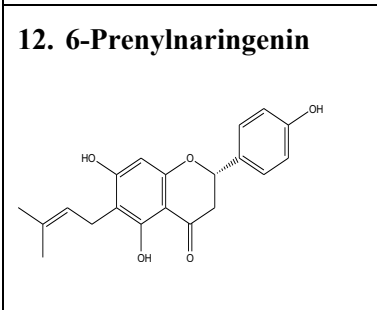
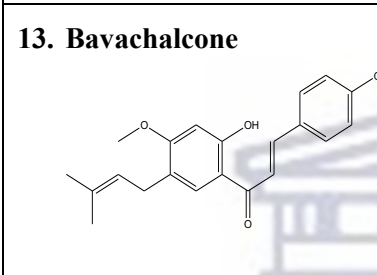
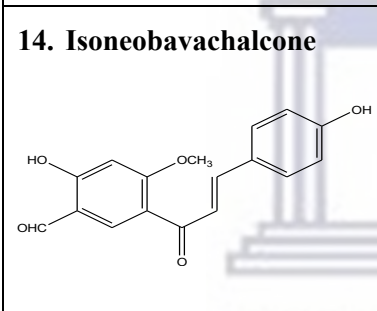
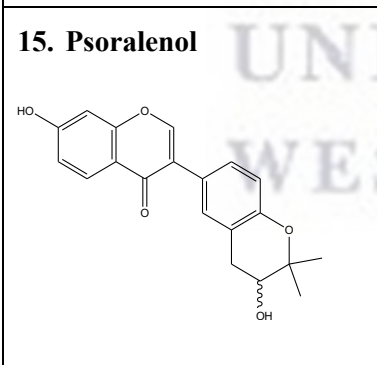
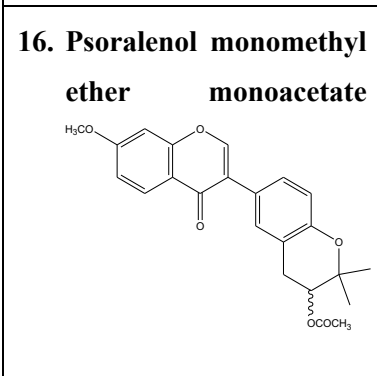
**Table 2: Selected various types of flavonoids including flavones, flavonols, favanones, isoflavones and chalcones isolated from *Psoralea* genus.**

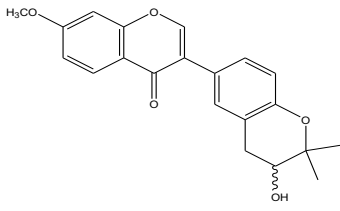
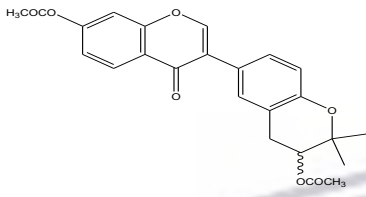
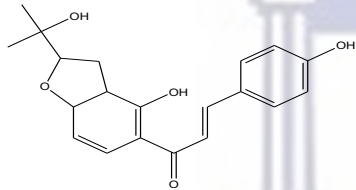
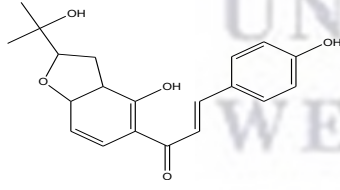
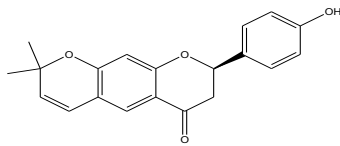
Name and structure of compound	Plant source and part of plant	Biological activity	Reference:
<p><b>1. Corylifol</b></p> 	<p><i>P. corylifolia</i> - Seeds</p>	<ul style="list-style-type: none"> <li>• Anticancer</li> <li>• Protein kinase inhibition</li> </ul>	<p>(Limper <i>et al.</i>, 2013; Alam <i>et al.</i>, 2017)</p>

<p><b>2. Corylifol A</b></p> 	<p><i>P.corylifolia</i> - Seeds/fruits</p>	<ul style="list-style-type: none"> <li>• Carboxylesterase inhibitors</li> </ul>	<p>(Li <i>et al.</i>, 2015)</p>
<p><b>3. Corylifol B</b></p> 	<p><i>P.corylifolia</i> - Seeds</p>	<ul style="list-style-type: none"> <li>• Carboxylesterase inhibitors</li> </ul>	<p>(Li <i>et al.</i>, 2015)</p>
<p><b>4. Bavachinin</b></p> 	<p><i>P.corylifolia</i> - Seeds</p>	<ul style="list-style-type: none"> <li>• Estrogen receptor</li> <li>• Anti-Alzheimer Antibacterial</li> <li>• Lymphangiogenesis inhibition</li> <li>• Carboxylesterase</li> </ul>	<p>(Lim <i>et al.</i>, 2011; Khatune <i>et al.</i>, 2004; Liu <i>et al.</i>, 2014; Chen <i>et al.</i>, 2013; Lin <i>et al.</i>, 2015)</p>
<p><b>5. Isovitexin</b></p> 	<p><i>P.licata</i></p>	<ul style="list-style-type: none"> <li>• Anti-oxidant</li> <li>• Anti-inflammatory</li> <li>• Anti-AD</li> </ul>	<p>Alam <i>et al.</i>, 2017; He <i>et al.</i>, 2016)</p>
<p><b>6. 4'-Methoxyflavone</b></p> 	<p><i>P.corylifolia</i> - Seeds</p>	<ul style="list-style-type: none"> <li>• Antifungal</li> </ul>	<p>(Alam <i>et al.</i>, 2017; Prasad <i>et al.</i>, 2004)</p>

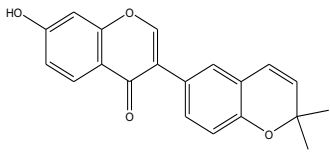
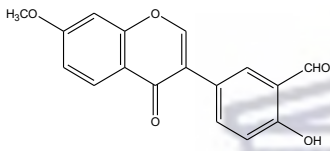
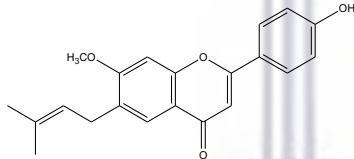
<p><b>7. Bavachin</b></p> 	<p><i>P.corylifolia</i> -Seeds/fruit</p>	<ul style="list-style-type: none"> <li>• Osteoblast</li> </ul>	<p>(Miura &amp; Nishida, 1996)</p>
<p><b>8. Neobavaisoflavone</b></p> 	<p><i>P.corylifolia</i> - Seeds/Fruit</p>	<ul style="list-style-type: none"> <li>• Antibacterial</li> </ul>	<p>(Alam <i>et al.</i>, 2017; Khatune <i>et al.</i>, 2014)</p>
<p><b>9. 3,5,3',4'-Tetrahydroxy-7-methoxyflavone-3'-O-<math>\alpha</math>-L-xylopyranosyl(1<math>\rightarrow</math>3)-O-<math>\alpha</math>-L-arabinopyranosyl(1<math>\rightarrow</math>4)-O-<math>\beta</math>-D-galactopyranoside</b></p> 	<p><i>P.corylifolia</i> - Seeds</p>	<ul style="list-style-type: none"> <li>• Antibacterial</li> <li>• Antifungal</li> </ul>	<p>(Alam <i>et al.</i>, 2017; Yadava <i>et al.</i>, 2005)</p>
<p><b>10. Corylinal</b></p> 	<p><i>P.corylifolia</i> Seeds</p>	<ul style="list-style-type: none"> <li>• No record</li> </ul>	<p>(Alam <i>et al.</i>, 2017; Gupta <i>et al.</i>, 1978)</p>
<p><b>11. Genistein</b></p>	<p><i>P.corylifolia</i> -Fruit</p>	<ul style="list-style-type: none"> <li>• Anti-obesity</li> <li>• Ani-diabetic</li> </ul>	<p>(Shide <i>et al.</i>, 2010;</p>



		<ul style="list-style-type: none"> <li>• Antioxidant</li> </ul>	Behloul & Wu, 2013)
<p><b>12. 6-Prenylnaringenin</b></p> 	<p><i>P.corylifolia</i> - Seeds</p>	<ul style="list-style-type: none"> <li>• Potential Anticancer</li> </ul>	(Alam <i>et al.</i> , 2017; Kim <i>et al.</i> , 2009)
<p><b>13. Bavachalcone</b></p> 	<p><i>P.corylifolia</i> - Seeds</p>	<ul style="list-style-type: none"> <li>• Anticancer</li> <li>• CVS protective effect</li> </ul>	(Dang <i>et al.</i> , 2015; Shan <i>et al.</i> , 2014)
<p><b>14. Isonobavachalcone</b></p> 	<p><i>P.corylifolia</i> - Seeds</p>	<ul style="list-style-type: none"> <li>• No record</li> </ul>	(Alam <i>et al.</i> , 2017; Gupta <i>et al.</i> , 1980)
<p><b>15. Psoralenol</b></p> 	<p><i>P.corylifolia</i> - Seeds</p>	<ul style="list-style-type: none"> <li>• No record</li> </ul>	(Alam <i>et al.</i> , 2017; Suri <i>et al.</i> , 1978)
<p><b>16. Psoralenol monomethyl ether monoacetate</b></p> 	<p><i>P.corylifolia</i> - Seeds</p>	<ul style="list-style-type: none"> <li>• No record</li> </ul>	(Alam <i>et al.</i> , 2017; Suri <i>et al.</i> , 1978)

<p><b>17. Psoralenol methyl ether</b></p> 	<p><i>P.corylifolia</i> - Seeds</p>	<ul style="list-style-type: none"> <li>• No record</li> </ul>	<p>(Alam <i>et al.</i>, 2017; Suri <i>et al.</i>, 1978)</p>
<p><b>18. Psoralenol diacetate</b></p> 	<p><i>P.corylifolia</i> - Seeds</p>	<ul style="list-style-type: none"> <li>• No record</li> </ul>	<p>(Alam <i>et al.</i>, 2017; Suri <i>et al.</i>, 1978)</p>
<p><b>19. Bakuchalcone</b></p> 	<p><i>P.corylifolia</i> - Seeds</p>	<ul style="list-style-type: none"> <li>• No record</li> </ul>	<p>(Alam <i>et al.</i>, 2017; Gupta <i>et al.</i>, 1982)</p>
<p><b>20. Bavachromene</b></p> 	<p><i>P.corylifolia</i> - Seeds</p>	<ul style="list-style-type: none"> <li>• Estrogenic</li> </ul>	<p>(Alam <i>et al.</i>, 2017; Lim <i>et al.</i>, 2011)</p>
<p><b>21. 7,8-Dihydro-8-(4-hydroxyphenyl)-2,2-dimethyl-2H,6H-benzo[1,2-b:5,4-b']dipyrans-6-one</b></p> 	<p><i>P.corylifolia</i> - Seeds</p>	<ul style="list-style-type: none"> <li>• Antimicrobial</li> <li>• Antibacterial</li> </ul>	<p>(Alam <i>et al.</i>, 2017; Yin <i>et al.</i>, 2004)</p>



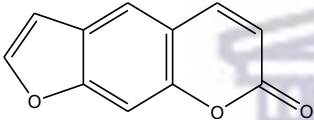
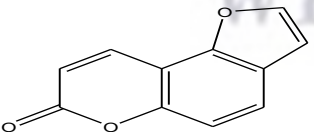
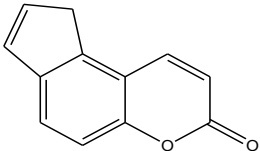
<p><b>22. Corylin</b></p> 	<p><i>P.corylifolia</i> - Whole plant</p>	<ul style="list-style-type: none"> <li>• Antimicrobial</li> <li>• Antibacterial</li> <li>• Osteoblast</li> <li>• Carboxylesterase inhibitors</li> </ul>	<p>(Shan <i>et al.</i>, 2014; Wang <i>et al.</i>, 2001; Miura &amp; Nishida., 1996; Sun <i>et al.</i>, 2016;)</p>
<p><b>23. Corylinal methyl ether</b></p> 	<p><i>P.corylifolia</i> - Seeds</p>	<ul style="list-style-type: none"> <li>• No record</li> </ul>	<p>(Alam <i>et al.</i>, 2017; Gupta <i>et al.</i>, 1978)</p>
<p><b>24. Bavachinin</b></p> 	<p><i>P.corylifolia</i> -Seeds <i>P.fructus</i> - Seeds</p>	<ul style="list-style-type: none"> <li>• Antimicrobial</li> </ul>	<p>(Kelani, 2015; Alam <i>et al.</i>, 2017)</p>

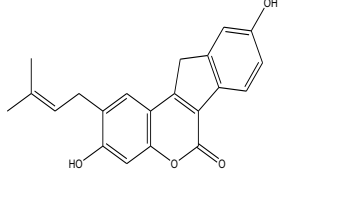
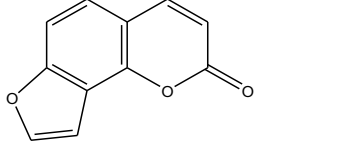
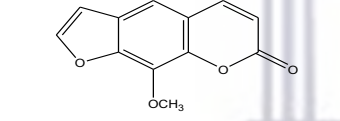
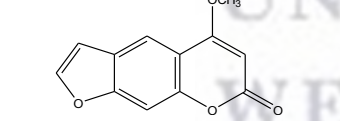
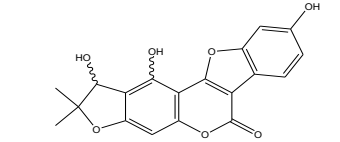
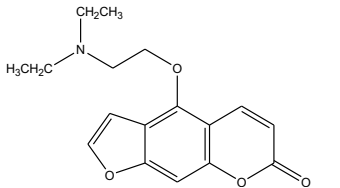
UNIVERSITY of the  
WESTERN CAPE

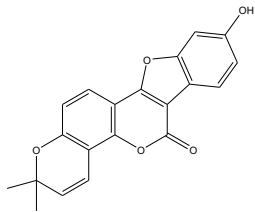
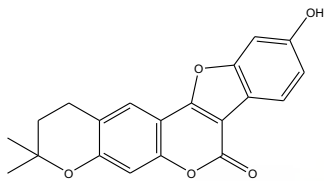
## Group 2: Coumarins

The name “coumarins” comes from a French term the Tonka bean, “*coumarou*”, which are seeds of *Dipteryx odorata* (*Coumarouna odorata*) of the *Fabaceae* family (Matos *et al.*, 2015).

**Table 3: Selected various types of Coumarins isolated from Psoralea genus.**

Name and structure of compound	Plant source and part of plant	Biological activity	Reference:
<p><b>1. Psoralen</b></p> 	<p><i>P. corylifolia</i> - Whole plant and root</p>	<ul style="list-style-type: none"> <li>• Photosensitization</li> <li>• Treatment of vitiligo</li> <li>• Treatment of psoriasis and alopecia areata</li> <li>• Antioxidant</li> <li>• Anti-Alzheimer</li> <li>• Collagen genesis</li> <li>• Leukoderma</li> </ul>	<p>(Li <i>et al.</i>, 2016; Ji &amp; Xu, 1995; Xi-yuan &amp; Jian-xin, 2007)</p>
<p><b>2. Bakuchicin</b></p> 	<p><i>P. corylifolia</i> -Seeds</p>	<ul style="list-style-type: none"> <li>• Topoisomerase inhibitor</li> </ul>	<p>(Sun <i>et al.</i>, 2003; Alam <i>et al.</i>, 2017)</p>
<p><b>3. Bakuchincin</b></p> 	<p><i>P. corylifolia</i> - Seeds <i>P. plicata</i> - Whole plant</p>	<ul style="list-style-type: none"> <li>• Antibacterial activity against Gram (+) and Gram (-) bacteria</li> </ul>	<p>(Khatune <i>et al.</i>, 2004; Alam <i>et al.</i>, 2017; Rasool <i>et al.</i>, 1991)</p>
<p><b>4. Psoralidin</b></p>	<p><i>P. corylifolia</i></p>	<ul style="list-style-type: none"> <li>• Estrogen receptor modulator</li> </ul>	<p>(Liu <i>et al.</i>, 2014; Alam <i>et al.</i>, 2017)</p>

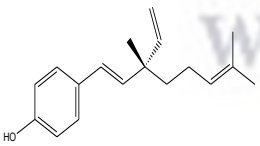
	<p>-Whole plant and seeds</p>	<ul style="list-style-type: none"> <li>• Antibacterial activity against Gram (+) and Gram (-) bacteria</li> </ul>	<p><i>al.</i>, 2017, Li <i>et al.</i>, 2017)</p>
<p><b>5. Psopspralean Angelicin</b></p> 	<p>= <i>P. corylifolia</i>  - Seeds  <i>P. glandulosa</i>  - Whole plant  <i>P. plicata</i>  - Whole plant</p>	<ul style="list-style-type: none"> <li>• Antibacterial activity against Gram (+) and Gram (-) bacteria</li> </ul>	<p>(Kelani, 2015; Li <i>et al.</i>, 2016; Khatune <i>et al.</i>, 2004; Backhouse <i>et al.</i>, 2001; Rasool <i>et al.</i>, 1989).</p>
<p><b>6. 8-methoxy psoralen=Xanthotoxin</b></p> 	<p><i>P. corylifolia</i>  - Seeds</p>	<ul style="list-style-type: none"> <li>• No record</li> </ul>	<p>(Kelani, 2015; Li <i>et al.</i>, 2016)</p>
<p><b>7. 5-methoxy psoralen = Bergapten</b></p> 	<p><i>P. corylifolia</i>  - Seeds</p>	<ul style="list-style-type: none"> <li>• No record</li> </ul>	<p>(Li <i>et al.</i>, 2016)</p>
<p><b>8. Corylidin</b></p> 	<p><i>P. corylifolia</i>  - Fruits</p>	<ul style="list-style-type: none"> <li>• No record</li> </ul>	<p>(Li <i>et al.</i>, 2016; Gupta <i>et al.</i>, 1977)</p>
<p><b>9. Psoralin</b></p> 	<p><i>P. corylifolia</i>  - Seeds</p>	<ul style="list-style-type: none"> <li>• Antimicrobial</li> </ul>	<p>(Li <i>et al.</i>, 2016)</p>

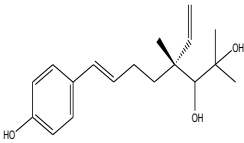
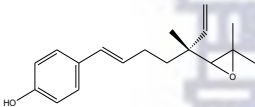
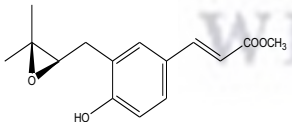
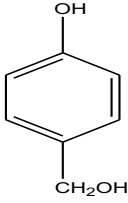
<p><b>10. Plicadin</b></p> 	<p><i>P. corylifolia</i> <i>P. plicata</i> - Whole plant</p>	<ul style="list-style-type: none"> <li>No record</li> </ul>	<p>(Li <i>et al.</i>, 2016; Rasool <i>et al.</i>, 1989)</p>
<p><b>11. Isopsoralidin</b></p> 	<p><i>P. corylifolia</i> - Seeds</p>	<ul style="list-style-type: none"> <li>No record</li> </ul>	<p>(Li <i>et al.</i>, 2016; Khushboo <i>et al.</i>, 2010)</p>

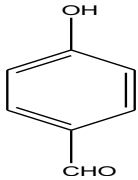
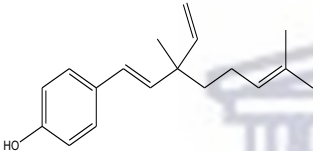
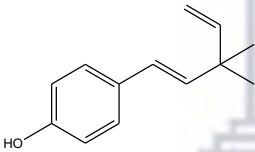
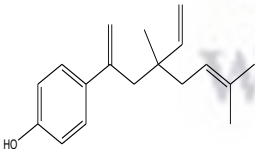
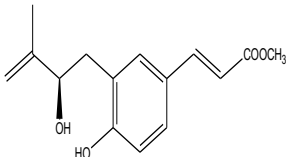
### Group 3: Phenols

Phenols have been reported as one of the major secondary metabolites of *Psoralea* genus and up to 2016, only thirty-two phenols had been identified and documented from the genus *Psoralea* (Li *et al.*, 2016).

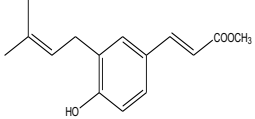
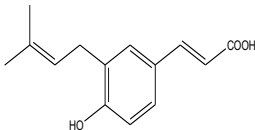
**Table 4: Selected various types of phenols isolated from *Psoralea* genus.**

Name and structure of compound	Plant source and part of plant	Biological activity	Reference:
<p><b>1. Bakuchiol</b></p> 	<p><i>P. corylifolia</i> - Seeds and fruits <i>P. glandulosa</i> - Resinous exudate, young shoots and leaves</p>	<ul style="list-style-type: none"> <li>Anticancer</li> <li>Anti-pyretic</li> <li>Antipregnancy</li> <li>Estrogenic</li> <li>Antibacterial</li> <li>Antioxidant</li> <li>Antiviral</li> <li>Antioxidant</li> <li>Anti-inflammatory</li> <li>Hepatoprotective</li> </ul>	<p>(Iwamura <i>et al.</i>, 1989; Kubo <i>et al.</i>, 1989; Chope <i>et al.</i>, 2013; Pae <i>et al.</i>, 2001; Cho <i>et al.</i>, 2001; Koul <i>et al.</i>, 2018)</p>

		<ul style="list-style-type: none"> <li>• Osteoblastic</li> </ul>	
<p><b>2. 12,13-Dihydro-12,13-dihydroxy bakuchiol</b></p> 	<p><i>P. corylifolia</i> - Whole plant</p> <p><i>P. glandulosa</i> - Resinous exudate, young shoots and leaves</p>	<ul style="list-style-type: none"> <li>• No record</li> </ul>	(Li <i>et al.</i> , 2016; Koul <i>et al.</i> , 2018)
<p><b>3. 12,13-Dihydro-12,13-epoxy bakuchiol</b></p> 	<p><i>P. corylifolia</i> - Seeds</p> <p><i>P. glandulosa</i> - Resinous exudate, young shoots and leaves</p>	<ul style="list-style-type: none"> <li>• No record</li> </ul>	(Li <i>et al.</i> , 2016; Koul <i>et al.</i> , 2018)
<p><b>4. Psoralea=3-(3-methyl-2-3-epoxybutyl)-p-coumaric acid methyl ester</b></p> 	<p><i>P. plicata</i> - Aerial parts</p>	<ul style="list-style-type: none"> <li>• No record</li> </ul>	(Li <i>et al.</i> , 2016; Hamed <i>et al.</i> , 1997)
<p><b>5. p-Hydroxybenzyl alcohol</b></p> 	<p><i>P. corylifolia</i> - No record</p>	<ul style="list-style-type: none"> <li>• Tyrosinase inhibition</li> </ul>	(Peng <i>et al.</i> , 1996; Li <i>et al.</i> , 2016))

<p><b>6. <i>p</i>-Hydroxybenzaldehyde</b></p> 	<p><i>P. corylifolia</i> - Whole plant</p>	<ul style="list-style-type: none"> <li>• No record</li> </ul>	<p>(Li <i>et al.</i>, 2016; Koul <i>et al.</i>, 2018)</p>
<p><b>7. 3-Hydroxy bakuchiol</b></p> 	<p><i>P. glandulosa</i> - Resinous exudate, young shoots and leaves</p>	<ul style="list-style-type: none"> <li>• No record</li> </ul>	<p>(Li <i>et al.</i>, 2016; Koul <i>et al.</i>, 2018)</p>
<p><b>8. Corylifolin</b></p> 	<p><i>P. corylifolia</i> - Whole plant</p>	<ul style="list-style-type: none"> <li>• Antioxidant</li> </ul>	<p>(Li <i>et al.</i>, 2016; Koul <i>et al.</i>, 2018)</p>
<p><b>9. Drupanol</b></p> 	<p><i>P. drupacea</i> - Fruits</p>	<ul style="list-style-type: none"> <li>• Antitumor</li> </ul>	<p>(Li <i>et al.</i>, 2016; Golovina <i>et al.</i>, 1973; Rakhimov <i>et al.</i>, 2016)</p>
<p><b>10. Plicatin-A</b></p> 	<p><i>P. plicata</i> - Leaf, flower and seeds</p>	<ul style="list-style-type: none"> <li>• No record</li> </ul>	<p>(Li <i>et al.</i>, 2016; Koul <i>et al.</i>, 2018; Rasool <i>et al.</i>, 1990)</p>
<p><b>11. Plicatin-B</b></p>	<p><i>P. plicata</i> - Leaf, Flower and Seeds</p>	<ul style="list-style-type: none"> <li>• No record</li> </ul>	<p>(Li <i>et al.</i>, 2016; Rasool <i>et al.</i>, 1990)</p>



	<i>P. bituminosa</i> - Whole plant		
<p><b>12. Drupanin</b></p> 	<i>P. bituminosa</i> - Whole plant <i>P. glandulosa</i> - Resinous exudate, young shoots and leaves <i>P. plicata</i> - Whole plant	<ul style="list-style-type: none"> <li>• RXR<math>\alpha</math> agonistic</li> </ul>	(Li <i>et al.</i> , 2016; Rasool <i>et al.</i> , 1990; Koul <i>et al.</i> , 2018; Nakashima <i>et al.</i> , 2014)

#### 1.4. The human skin

The human skin is the largest organ in the body, located on the outermost layer of a living body (Riviere *et al.*, 2011). Its functions include keeping vital chemicals and nutrients in the body, protection of the underlying body from external environmental factors such as chemicals and harmful effects of ultraviolet radiation emitted by the sun. Making the skin the median between the internal body and the external environment (Casey., 2002; Kanitakis., 2002). Severe exposure of human skin to ultraviolet radiation of sunlight can cause various types of skin damages, including wrinkles, skin cancer, sunburn and hyperpigmentation. The type of skin damage depends on the form and amount of U.V radiation exposure (Clark and Sivamani., 2016).

There are three structural layers to the skin, listing from the outside, which are the epidermis, the dermis and subcutaneous layer (Figure 2). The epidermis is made of four or five layers of epithelial cells; the number of the cells is dependent on the site. The epidermis forms the outermost layer of the skin and is mainly composed of three types of cells that are the keratinocytes, Langerhans cells, Merkel cells and melanocytes. The keratinocytes cells that synthesises the protein keratin and releases a water-repelling glycolipid that helps prevent water loss from the body. Thus, makes the skin relatively waterproof and tough (Riviere and Monteiro-Riviere., 2005). The dermis is found below the epidermis, its thickness ranges from 0.6 mm on the eyelids to 3 mm on the back, palms and soles. It is largely composed of very dense fibre network and is responsible for the mechanical behaviour of the total skin (Riviere and Monteiro-Riviere., 2005; Kanitakis., 2002). The subcutaneous layer or hypodermis is the



inner most layer in the skin. It is composed of loose fatty connective tissue and aids in binding the skin to the skeleton muscle and fascia (Riviere and Monteiro-Riviere., 2005)

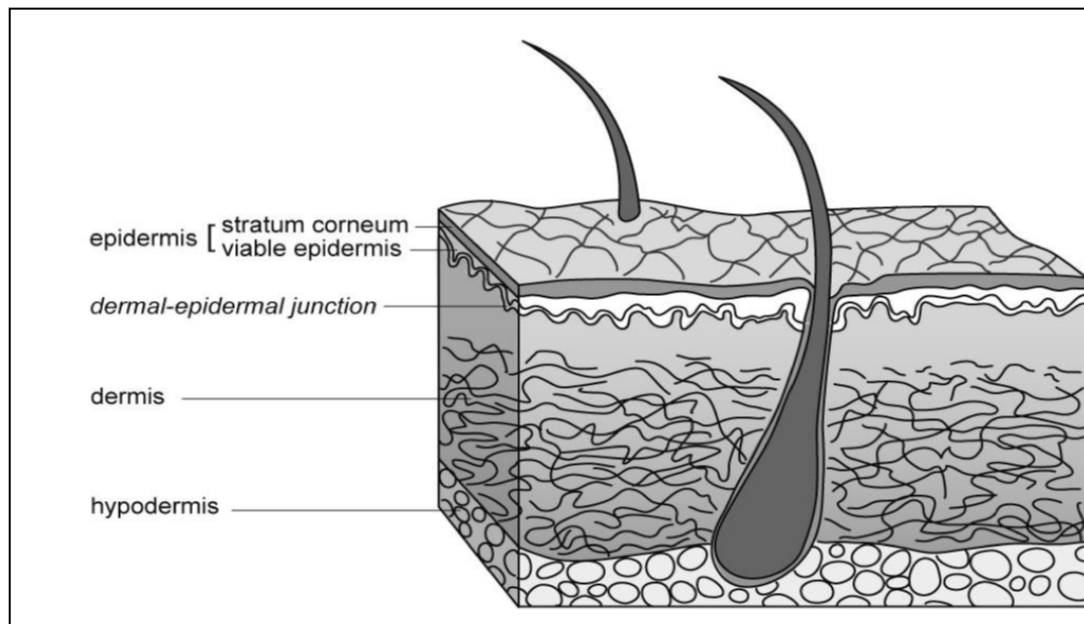


**Figure 2: Schematic representation of human skin layers.**

Melanin is a pigment that is a mixture of biopolymers and is the primary determinant of human skin, eyes and hair colour. Melanin also plays an important role in defending human skin against harmful UV radiation by absorbing UV rays and removing reactive oxygen species (MA punya *et al.*, 2012; Costin and Hearing., 2007). In melanogenesis, melanin is secreted and produced within the melanocyte cells residing in the epidermis of the skin. (MA punya *et al.*, 2012).

Overproduction and accumulation of melanin pigments in the skin, which leads to the development of dermatological hyperpigmentation disorders (MA punya *et al.*, 2012).

## 1.5. Hyperpigmentation

Hyperpigmentation is the most dermatological issue amongst women in South Africa and it affects over 30 million people worldwide caused by various skin disorders (such as eczema and acne), excess skin exposure to sun, chronic inflammation, heredity, rubbing of the skin and abnormal  $\alpha$ -melanocyte stimulating hormone ( $\alpha$ -MSH) release.



**Figure 3: Example of patients affected by hyperpigmentation on the face and back.**

Hyperpigmentation is common in men and women, affecting all ethnic groups. In many countries with a history of slavery, colonization and apartheid; dark skinned people are viewed as unattractive compared to lighter skinned people (Dlova *et al.*, 2015). These countries include India, United States of America, Nigeria and South Africa. Studies show about 91% of the South African population are dark in complexion and about 35% of women in South Africa use skin whitening products consisting of synthetic chemicals (Webstar ., 2014; Dlova *et al.*, 2015). The use of skin lighting products is popular various ethnic groups and highly profitable in South Africa ( Dlova *et al.*, 2015). For instance, a study done in Durban, South Africa reported on 10 top-selling skin-lightening creams sold in supermarkets, cosmetic shops, and hawkers on city streets. They found that nine (90%) of the creams were found to contain banned or illegal compounds, just six (60%) of them were manufactured in South Africa and the rest were illegally imported; and four products (40%) contained mercury as an active ingredient, two (20%) contained corticosteroids, two (20%) resorcinol, and one (10%) a derivative of hydroquinone. The majority of products contained banned substances (Dlova *et al.*, 2012; Dlova *et al.*, 2015).

### **1.6. Tyrosinase Inhibition**

Tyrosinase is a key and rate-limiting enzyme for melanogenesis (Mapunya *et al.*, 2012). This enzyme uses a redox active copper as a cofactor within its active site to oxidize arene rings and it controls two rate – limiting steps: (i) hydroxylation of L-tyrosine (a monophenol) to L- dopa (a *o*-diphenol) and (ii) the conversion of L- dopa to dopaquinone (a *o*-quinone) (Wang *et al.*, 2014; Ullah *et al.*, 2019). The unstable dopaquinone then spontaneously converts to melanin (Lall *et al.*, 2006). As seen in Figure 4.

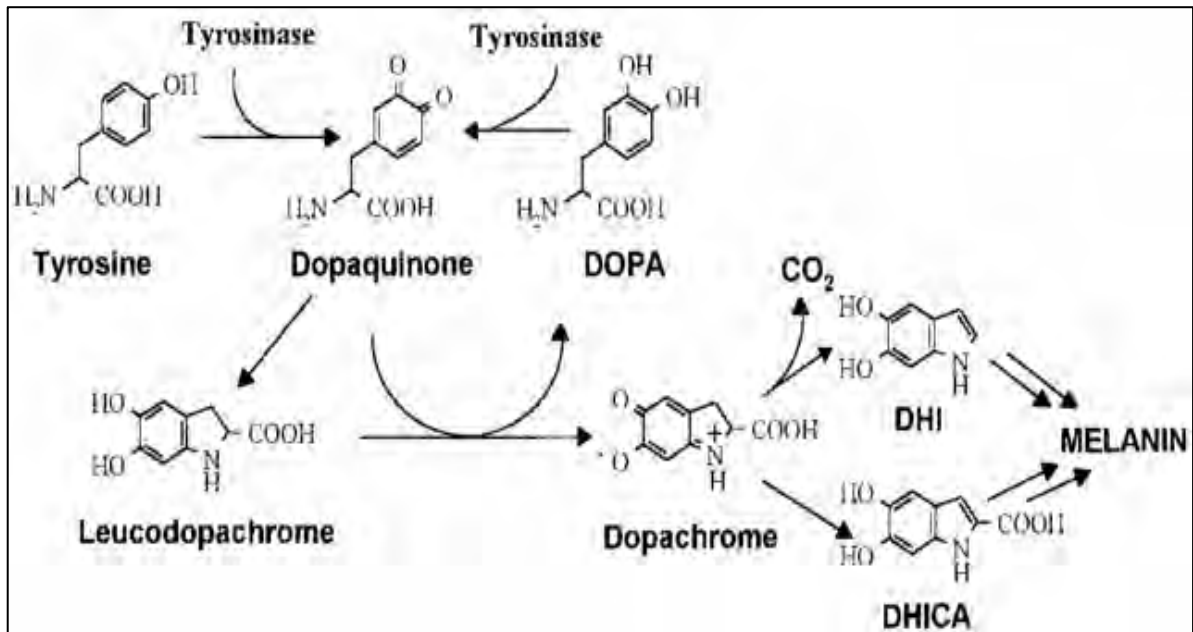


**Figure 4:** A pathway schematic of the biosynthesis of melanin (Image by Anna Di Cosmo).

Current treatment for hyperpigmentation is by reducing melanin production by inhibiting tyrosinase activity (Stapelberg *et al.*, 2019; Deri *et al.*, 2016). Classical tyrosinase inhibitors such as kojic acid, arbutin and hydroquinone are used extensively in topical treatments of skin hyperpigmentation (Deri *et al.*, 2016). Unfortunately, these classical tyrosinase inhibitors have been proven to lack clinical efficacy. Kojic acid is a fungal metabolite commonly used in skin-whitening products, however, it causes side effects such as dermatitis, sensitization and erythema (Chang, 2009). by The Cosmetic Ingredient Review (CIR) Expert Panel recommended the concentrations of 1% of KA for human use after animal experiments found that KA depigmented black guinea pig skin at a concentration of 4% but not a concentration of 1% and that the use of KA promoted tumour and weak carcinogenicity (Burnett *et al.*, 2010). The tyrosinase enzyme was used as subtract and absence of kojic acid as the positive control. Kojic acid is a known tyrosinase inhibitor, however, there is still uncertainty in the full mechanism of kojic acid inhibition (Sendosvski *et al.*, 2011; Lima, *et al.*, 2014); Noh, J.M., et al, 2009). In literature, kojic acid is either a competitive inhibitor or a mixed inhibitor for mushroom tyrosinase by chelating copper in the active site (Lima *et al.*, 2014; Bochot *et al.*, 2014; Noh *et al.*, 2009).

## 1.7. Problem statement

Overproduction of melanin may cause hyper-pigmentation which leads to aesthetic problems, melanoma and age spots (Lall *et al.*, 2006). Tyrosinase inhibitors are well sought after for their importance in medication of dermatological problems and in cosmetic industry to prevent hyperpigmentation (Ullah *et al.*, 2019). There is a global demand for skin whitening agents; increasing the need for research interests focusing on suppressing the accumulation of melanin. Research on medical plants utilization in South Africa used for dermatological issues is still underdeveloped, even though an estimated 10% of the plant species of the world is found in southern Africa (Wyk., 2008). It is imperative to systematically document knowledge from indigenous Southern African plants, increasing the number of scientific publications and patents. There is a high demand for products that reduce the formation of melanin, however, more often, the products are found to have toxic and harmful ingredients (Dlova *et al.*, 2015). Moreover, the more people that becoming aware of plants and their use and there is a higher demand of natural products, both for beauty and for medicinal uses. Thus, in this study, we investigate a possibility of natural alternative tyrosinase inhibitors from plants, most importantly from a South African plant.

## 1.8. Rationale of the study

Hyperpigmentation is a common condition affecting the skin colour of all ethnicities. Prevention of hyperpigmentation requires the suppression of melanogenesis by inhibition of tyrosinase enzyme. There is a high usage of synthetic compounds in the cosmetic industry used in skin lightening products, natural isolated compounds could be a safer alternative source for skin lightening products. The use of known potent tyrosinase inhibitors is rather limited because they show diverse effects (such as rash, dermatitis and impaired wound healing after prolonged use), low stability and insufficient activity (Yang *et al.*, 2012;

In this study, a South African plant, *Psoralea aphylla* was investigated for its tyrosinase inhibition potential. The first compound isolated from the genus was Bakuchiol, which is known a meroterpene phenol abundant in seeds and leaves of the plant *Psoralea corylifolia*. According to a study by Chaudhuri and Bojanowski, bakuchiol was clinically tested to see if it could function as analogue of retinol, even though it has no structural resemblance to retinoids. Their results showed after 12 weeks of treatment, the patients skin showed significant improvement in lines and wrinkles, pigmentation, firmness, elasticity and overall reduction in photo-damage was observed, without retinol therapy-associated negative effects (Chaudhuri and Bojanowsk, 2014).



Other study compared the bakuchiol and retinol for clinical efficacy and side effects. Like the previous study, the results showed that bakuchiol and retinol both decreased wrinkle surface area and hyperpigmentation. However, retinol users reported to have experienced more facial skin scaling and stinging, which made the reporters come into the conclusion that bakuchiol is promising as a more tolerable alternative to retinol (Dhaliwal *et al.*, 2019).

Therefore, since plants from the same genus have been investigated and bioactive compounds were isolated. We investigate the *Psoralea aphylla* in hope to find more interesting bioactive compounds from a local plant and evaluate the potential of the compounds to be tyrosinase inhibitors using bioassay and electrochemistry.

### **1.9. Aim and objectives of study**

To isolate and characterize compounds from the methanolic extract of *Psoralea aphylla*, and investigate the tyrosinase inhibition activity of the methanolic extract and isolated compounds against the mushroom tyrosinase enzyme and melanin production on melanocytes.

**Aim 1:** To isolate and characterize compounds from the methanolic extract of *Psoralea aphylla*.

Objectives are:

- Using methanol for extraction of the plant material.
- Fractionate the main extract using column chromatography
- To determine the components, present in the extracts by Thin Layer Chromatography (TLC).
- To isolate and purify compounds using various chromatographic methods.
- To characterize isolated compounds and elucidate the structure of the compounds, using NMR, FTIR, U.V and MS.

**Aim 2:** To investigate the tyrosinase inhibition activity of the methanolic extract and isolated compounds against the mushroom tyrosinase enzyme and melanin production on melanocyte.

Objectives are:

- To determine the tyrosinase inhibition activity of the crude extract and the isolated compounds.
- Compare the results to kojic acid and well-known tyrosinase inhibitor kojic acid.
- Evaluate the potential use of cyclic voltammetry to determine tyrosinase inhibitions of methanolic extract and isolated compounds.

**Aim 3:** Using electrochemistry to investigate the compounds for tyrosinase inhibition and compare result with that of ELISA assay.

Objectives are:

- Using electrochemical technique (CV) to understand the electrochemistry of tyrosinase in response to different concentrations of L- tyrosine.
- Using electrochemical technique (CV) to investigate the inhibition effect of kojic acid on tyrosinase in response to different concentrations of L-tyrosine.
- Using electrochemical technique (CV) to understand the electrochemistry of tyrosinase in response to different concentrations of isolated compound.
- Compare tyrosinase inhibition activity obtain using electrochemical method with results obtained using ELISA assay.

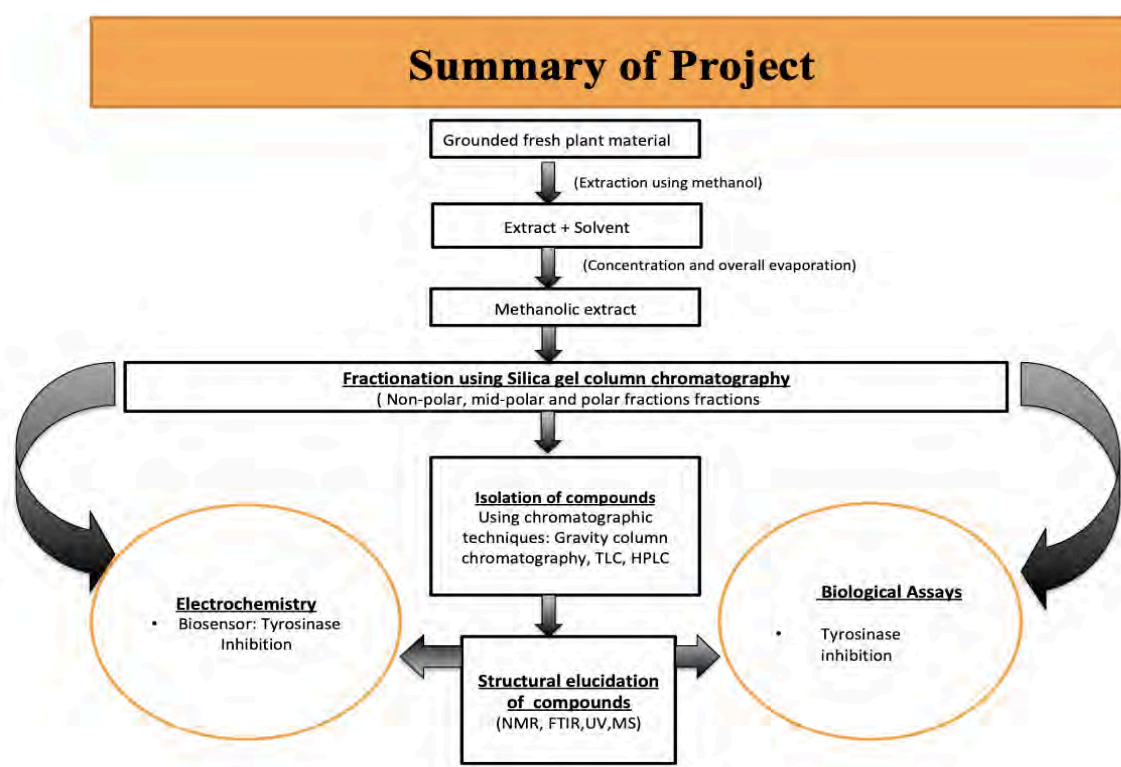


**Figure 5: A diagrammatic summary of steps in the study of indigenous *Psoralea aphylla* species, evaluating the phytochemistry and biological activities.**



---

# CHAPTER 2:

## Literature Review

---

*This chapter provides a literature review of the Cape Florist Kingdom, taxonomy, ecological and historical background of Psoralea aphylla, compounds currently used for tyrosinase inhibition and biosensors that are currently used for detection of tyrosinase inhibitors.*

### 2.1. Cape Florist Kingdom

In the most southern-western tip of South Africa lies the most fertile region on Earth, with the highest density of plant species and approximately 330 species in Africa. This region is called the Cape Floral Kingdom (CFK) and is one of the six Floral Kingdoms across the globe even though it represents less than 0.5% of the area in Africa. The CFK is the world's smallest and most diverse plant Kingdom, found in the southwestern tip of South Africa, from Neiwoudtville in the north to Cape Town in the south, stretching from the Cederberg in the northwest and around the Western Cape coast extending as far as to Port Elizabeth, the region covers an area of 90 000km<sup>2</sup>. This area is a home to approximately 9086 plant species, of which 68.0% are endemic to South Africa and 20% of the genera being endemic; it is comparable to that of the equatorial rain forest (Cowling *et al.*, 1992; Goldblatt *et al.*, 2005). The CFK contain more plant species than bigger than other kingdoms. For instance, the Boreal Kingdom covers 40% of the planet surface, but has less species than the CFR, which contains nearly 3% of the world's plant species on 0.05% of the land area.

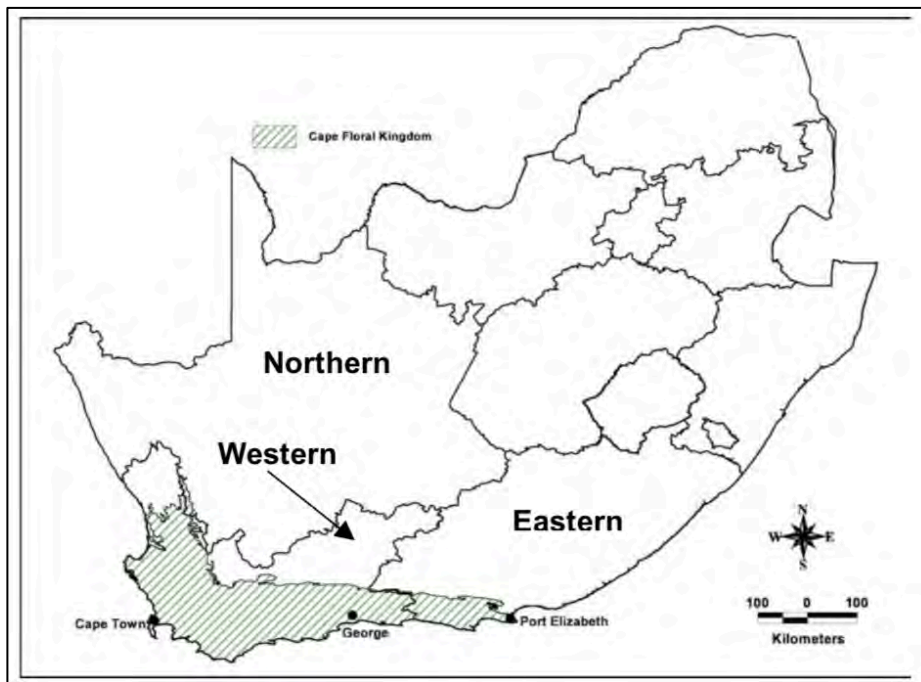


**Figure 6: Location of the Cape Floristic Kingdom shaded with green lines. (Retrieved from Masters 2018: *Cape Floristic Region Hotspot Briefing Book 2005*).**

The vegetation in the area consists of the shrub element is dominated by Proteaceae, the undershrub level which is dominated by Ericaceae, the graminoid element dominated by Restionaceae and the geophytic flora which is very rich (Goldblatt, 1978; Marloth, 1908). The most dominant vegetation type in the Kingdom is fynbos, which contributes to 80% of the species and about 94% of the restios growing in fynbos are indigenous to the CFK (Lee S *et al.*, 2006). There are five main vegetation types of fynbos found in the CFK, which are: mountain fynbos (the largest), grassy fynbos (second largest), laterite (coastal) fynbos, sand-plan fynbos and limestone fynbos. Although the region is better known for its plant species, the region also supports substantial animal diversity, with more than 560 higher vertebrate species. The vegetation in the CFK is under threat and preservation of the region is an urgent priority of the nation.

The rugged topography of the Cape Floristic Kingdom is a mixer of mountains, valleys and coasts.

## 2.2. *Psoralea aphylla*

### 2.2.1. Taxonomy of *Psoralea aphylla*.

Table 5: Taxonomy of *Psoralea aphylla*.

<b>Kingdom</b>	Plantae
<b>Phylum</b>	Tracheophyta
<b>Class</b>	Magnoliopsida
<b>Order</b>	Fabales
<b>Family</b>	Fabaceae/Leguminosae
<b>Tribe</b>	<i>Psoraleae</i>
<b>Genus</b>	<i>Psoralea</i>
<b>Species</b>	<i>Psoralea aphylla</i>

### 2.2.2. Historical background of *Psoralea aphylla*

In 1981 Stirton established the genus *Psoralea sensue stricto* (Stirton, 1981) recognising 20 species that all occurred in southern Africa and mostly diversified and endemic to the Cape Floristic Kingdom. However, when Stirton did more work to revise the genus *Ortholobim*, he discovered more species, at least 47 species of the discovered species belonged to the genus *Psoralea* and then later pointed out that the genus had about 51 species (Stirton 1995). In 2012, Stirton reported about 70 species in *Psoralea* (Stirton and Schutte, 2012). However, in manuscripts that describe the flora of the Cape Floristic Kingdom by Goldblatt & Manning, only about 30 new species are known by informal names, they have no formal descriptions and there is always an ambiguous and subjective use of application of names due to the lack of species delimitation and identification of genus (Goldblatt and Manning, 2000; Manning and Goldblatt 2012). Due to the lack of formal description of the *Psoralea* species it is difficult to identify each species and therefore abstracting the assessment of their conservation statuses.

### 2.2.3. Description of *Psoralea aphylla*

The epithet of the species name of *Psoralea aphylla* is derived from the word ‘aphyllous’, which means ‘leafless’ (Dludlu, 2015). It is also known as ‘Blue Broom Bush’, ‘Founteinbos’ (fountain bush) and to the Afrikaans, its common name is ‘Kaalfonteinbos’ (bare fountain bush) (Maphisa; 2019). *Psoralea aphylla* is a re-seeding, slender, erect to drooping shrub that

grows up to 4m tall with such small scale-like leaves that the willow-like branches appear to be leafless. It appears to have blue and white flowers that are borne towards the ends of the branches. The flowers have a sweet-scented smell and the branches are covered with black hairs. The plant seeds are sowed in autumn in a well-drained medium and flowered between October and February.



**Figure 7: *Psoralea aphylla* shrub (top left), willow branch with flower (top right), branches and flowers (bottom left) and close up of flower (bottom right).**

#### **2.2.4. Distribution, habitat and uses of *Psoralea aphylla***

*Psoralea aphylla* is restricted to lower slopes of the Cape Peninsula and low foothills of mountains. It used to be also found in the Cape Flats however, now it is quite scarce there. Its altitude ranges from 10 to 300m above sea level. It grows in open areas, stream banks, gully and seepages. Flowering takes place from September to April (Dludlu, 2015). The species prefers marshy habitats, mountains, lowland fynbos and stream banks. From our knowledge, there has been no reports on the traditional uses, chemical studies and pharmacological studies on the species.



### 2.3. Biosensors

A sensor is defined analytical device that could serve as a reliable monitoring, detection and quantification device for chemical substances, while a biosensor is a device that uses biomolecules (such as enzymes) to detect analytes. Enzyme-based biosensors have recently been used for selectively detection of target analytes because they are generally considered to be simple and sensitive devices compared to the conventional analytical methods. Researchers found interest in using enzymes in construction of biosensors because enzymes are known as nature's catalysts and could possibly catalyse almost all biochemical processes in a controlled manner and precise specifically (Qu *et al.*, 2018; Yan *et al.*, 2016).

A biosensor is also defined as the device of system used to detect the presence of chemical or biological compounds in a solution or a gas phase, as a result of their interaction with a bioactive substance such as enzymes, antibodies, antigens, living cells, tissues etc (Sawant, 2017). A typical biosensor is composed of three components. (i) The biological sensing element which interacts with the analyte and generates a response signal. The biological sensing element can be enzyme, antibody, DNA probes or microbe (or tissue slice), which interact with the specific targeted analyte and generates responsive signal (Shukla *et al.*, 2016). (ii) The transducer that translates the biological signals generated by the biological element to electrical or optical signals. Thus, the transducer is the most critical component in any biosensing device. (iii) The detector, which amplifies and processes the signals (Parkhey and Mohan 2019). Research related to biosensors has tremendously grown over the last two (some say) three decades because of the capability to be easy to use, portability, cost low, be highly sensible, speed portability and decentralized clinical applications (Yi *et al.*, 2016; Wang, 2006). Highly sensitive biosensors have been used in the advancement of next-generation medicine such as biosensors used for blood glucose monitoring, which is known as the glucose sensor (Grieshaber *et al.*, 2008). Depending on which transducer is used and analysis of signals, biosensors can be classified as electrochemical, optical, thermal, and piezoelectric biosensors (Sewant, 2017).

#### 2.3.1. Electrochemical biosensors

An electrochemical biosensor is a type of biosensors that transforms biochemical information based on the measurements of electric current and charge accumulation or potential carried out by bioelectrodes (Kumar and Upadhyay, 2018; Jothi and Nageswaran, 2019). Typically, electrochemical biosensors require a working electrode, a counter electrode (also known as auxiliary electrode) and a reference electrode (Scognamiglio *et al.*, 2016). The electrochemical

biosensors can be classified as amperometric, potentiometric and conductometric, depending on the type of electrochemical parameters measured (Kumar & Upadhyay, 2018; Sawant, 2017). In amperometric biosensors the current produced during oxidation and reduction of electroactive product or reactant is measured (Sawant, 2017). A constant potential is applied to a working electrode versus a reference electrode promoting a redox reaction and the current is measured (Palchetti *et al.*, 2017; Sawant, 2017). The measured current mostly relies on the continuous turnover of substrate which produces the measured signal. Set optimal conditions, with fixed pH and fixed temperature are best used for analysis of enzyme activity because the redox reaction at electrode interface is directly proportional to concentration of substrate present in the solution. Several amperometric biosensors based on tyrosinase inhibition on the electrode surface have been applied to detect phenolic compounds because of the advantages such as good selectivity, easy automation and low cost (Sanz *et al.*, 2005). Potentiometric biosensors are based on the potential difference between working electrode (usually known as the indicator electrode) and the reference electrode when zero or significant current flows between them, where potential is dependent on concentration of analyte. The transducer in the potentiometric biosensor is sensitive to the solution-based ions, thus potentiometry provides information about the ion activity in an electrochemical reaction. Conductometric biosensors measure the change in electrical conductivity of medium arising due to the biochemical reaction. The biochemical reaction is monitored of the change in conductance of an electrode as a result of, for example the immobilization of enzymes.

### **2.3.2. Electrochemical Biosensors Based on Tyrosinase enzyme Inhibition**

An enzyme biosensor is a sensor that measures the rate of the enzyme-catalysed reaction electronically by detection of target molecules in an appropriate range of concentration. Any optical or electrical change of the surface will reflect the biocatalyst occurring at the conductive surface (Zhu *et al.*, 2019). These types of biosensors have gained great importance due to their potential to detect a target substance/analyte with high specificity via enzyme-catalysed reactions (Wee *et al.*, 2019; Wu *et al.*, 2012). Additionally, they also possess low cost and minimal requirement for sample pre-treatment (Wu *et al.*, 2012).

Tyrosinase is an enzyme known to catalyse the hydroxylation of phenolic substrates to catechol derivatives, which are oxidized into orthoquinone products and the orthoquinone products further undergoes a series of non-enzymatic reactions to form melanin (Heitz and Rupp., 2018; Kim *et al.*, 2019). Different routine methods been used for qualitative and quantitative measurement of tyrosinase activity, which usually means detecting phenolic compounds



(Etsassala *et al.*, 2019). These methods include HPLC, gas chromatography, spectrophotometric essays (including UV-Vis spectrometry), electrophoresis, TLC bioautographic assays, and enzyme-linked immunosorbent assays (ELISA) (Etsassala *et al.*, 2019; Kim *et al.*, 2019; Heitz and Rupp., 2018). However, these methods can be time consuming, require sample pre-treatment and be complex to perform (Qu *et al.*, 2018; Yan *et al.*, 2016; Tsai *et al.*, 2007). ELISA is found to have the best selectivity, sensitivity and versatility. However, it is also time consuming and a relatively enzyme-linked antibody is used (Xia *et al.*, 2013 ). Thus, researchers have been making efforts for simple, selective and sensitive methods for detection of tyrosinase and its activity. Numerous biosensors have been developed for detecting phenols and enzyme activity detections, for example, the fluorescence biosensor, near- infrared biosensor, and different types of amperometric biosensors ( Qu *et al.*, 2018; Yan *et al.*, 2016; Tsai *et al.*, 2007).

The electrochemistry of tyrosinase inhibition has been investigated in previous studies on glassy carbon electrodes. For instance, a study was done using cyclic voltammetry to study the tyrosinase inhibition activity of natural extracts and compounds that possessed hydroxyl groups by measuring the inhibition current with time and compared the inhibition current of each compound to one of KA. The study showed the lower the inhibition current, the higher the tyrosinase inhibitory activity of the extract or compound, the results were compared to the inhibition effect of kojic acid (Etsassala *et al.*, 2019).

Certain tyrosinase based biosensors have been applied to specifically detect phenols, sulfamethoxazole, and tyramine in fermented foods and beverages (Silva *et al.*, 2019; Wee *et al.*, 2012; Tomo-de Román *et al.*, 2016). In most cases, tyrosinase biosensors are used primary for the detection of phenolic compounds. Phenols are present in a broad range of chemical manufacturing processes and are known their inherent toxicity, hence, many researchers have found it essential to develop biosensors for the detection of phenols (Wee *et at.*, 2019; Tsai *et al.*, 2007). Tyrosinase oxidises phenolic compounds to quione species, which can further be reduced at the enzyme electrode to generate electrochemical signals and so, there is a number of electrochemical biosensors are used specifically to detect phenolic compounds (such as catechol) (Tang *et al.*, 2008).

The aim of this work is to develop a considerably highly sensitive, portable, easy to use and selective biosensor, suitable for detection of tyrosinase inhibitors. We evaluated the effects of the *Psoralea aphylla* methanolic extract and compounds isolated from the extract on tyrosinase and compared their efficacies with L-tyrosine substrate and the well-known tyrosinase inhibitor kojic acid.

---

# CHAPTER 3:

## Methods and Techniques

---

*This chapter provides details on instruments, methods, techniques and operation principles used for this work. The experimental methods employed included; chromatography techniques such as extraction, column chromatography, High Performance Liquid Chromatography (HPLC) and Spectroscopic techniques such as UV-visible (UV), Infrared (IR), Nuclear Magnetic Resonance (NMR), and mass spectroscopy are used to determine structures of certain compounds.*

### **3.1. Principle of pre-extraction of plant samples**

Pre-extraction is for preparation of plant samples for preservation of biomolecules in the plant before extraction. Pre-preparation is important for obtaining better quality and high efficiency of extraction.

By grinding the plants, the particle size decreases while the surface contact between the sample and extraction solvents. Powdered samples are smaller in size and homogenized, thus, a better surface contact with extraction solvents.

### **3.2. Principle of plant sample extraction**

Plants are sources of many active compounds such as alkaloids, flavonoids, terpenoids, steroids, tannins, glycosides, volatile oils, fixed oils, resins and phenols, which are from various plant parts such as leaves, seeds, fruits, etc. Extraction is the separation of soluble plant metabolites and living insoluble residue using selective solvents through standard procedure. Solvents used for extraction of phytochemicals are chosen based on the polarity of the solute of interest. Typically, solvents of the same polarity as the solute will dissolve the solute. Thus, polar solvents will extract out polar bioactive components and non-polar solvents will extract out non-polar bioactive components. The bioactive components of medical plants are usually unknown and have different solubility properties in different solvents. Thus, the nature of the solvents used for extraction and the extraction method used affects the composition of the crude extract (Truong *et al.*, 2019). Various solvents such as water, methanol, ethyl acetate, chloroform, acetone, dichloromethane, hexane or a combination of solvents are commonly used in laboratory settings. The polarity, from least most polar to least polar, of a few common

solvents is as follows: Water > Methanol > Ethanol > Acetone > Ethyl acetate > Chloroform > Dichloromethane > Hexane.

Methanol (MeOH) is generally used as the first solvent for extraction because of its polarity, low boiling point and its inexpensive. MeOH consists of molecules having a polar water-soluble group attached to water-insoluble hydrocarbon chain; thus, it can extract both hydrophilic and lipophilic molecules from plant parts. It is easy to remove methanol after extraction because of its low boiling point.

The temperature in which extraction is carried out is important because the activity of plant extracts can be lost due to thermal decomposition. Plant extracts, fractions and isolated compounds should be dried completely, sealed in vials and be stored in the fridge at 4°C to avoid negative chemical reactions due to solvents, high temperature and light. Some bioactive components decompose when subjected to high temperatures, light and water.

In this study, methanol will be used as the solvent for extraction.

### **3.3. Chromatographic techniques in natural product studies**

Chromatography is a general term for a variety of physicochemical separation techniques. The main principle involved in chromatography is based on differential adsorption of substance by the adsorbent. In 1903, Tswett was the first person to separate leaf pigments on a polar solid phase and be able to interpret the process, laying a foundation for all chromatographic techniques known today.

The various chromatographic techniques are subdivided according to the physical states of the mobile phase and the stationary phase.

#### **3.3.1. Thin Layer Chromatography**

Thin layer chromatography (TLC) is a chromatographic method used for analysis mixtures by separating the mixture into different components. It can be used to help determine the number of components in a mixture, identify compounds and for purification of compounds. The technique is widely used to characterize phytochemical compounds in natural product extract analysis, stability tests of extracts and finished products and in sample quality control.

The TLC technique is widely used because it is relatively cheap, highly sensitive, simple, and rapid, and can simultaneously separate complex mixtures.

TLC works on the principle that different components will have different affinities for the mobile and stationary phases, and this affects the differences in distance in which the

components will travel from the original spot. The most common stationary phases are silica (SiO<sub>2</sub>) gel and alumina (Al<sub>2</sub>O<sub>3</sub>), used in the form of a thin layer (about 0.25mm thick) supporting material. When using a silica gel plate separation on the stationary phase occurs by adsorption chromatography. Silica gel plates can be used in identifying steroids, amino acids, alcohols, hydrocarbons, lipids, aflatoxin, acids, vitamins and alkaloids.

To transfer the mixture onto the TLC plate, a very small amount of mixture is dissolved in a suitable volatile solvent, so the after transferring, the solvent can evaporate quickly from the plate leaving the spot. The dilute solution is transferred using a micro pipet on to the one end of a TLC plate. This process is referred to as “spotting”.

The TLC plate is placed vertically in a closed container (containing the mobile phase), with the one end, which the spots were applied down. The mobile phase should just be under the spot. The mobile phase consists of a volatile organic solvent or a mixture of volatile organic solvent. The solvent travels up the thin layer of adsorbent by capillary action, passing the spots and, as it continues up, it tries to move the spot along with it. This procedure is referred to as “developing” the TLC plate.

Choosing the right mobile phase suitable for developing the TLC plate is important and it's by trial and error. Since silica gel has highly polarity, the silica gel tries to retain the polar components. Therefore, the stronger the components are bound to the adsorbent, the slower they move up the TLC plate.

The retention factor ( $R_f$ ) value is used to quantify the movement of the components along the TLC plate. Each spot has a  $R_f$  value that is always between zero and one. Non-polar components have a higher  $R_f$  values; whereas polar components travel up the TLC plate slower, thus, have lower  $R_f$  values. The  $R_f$  formula is:

$$R_f = \frac{\text{distance traveled by component spot}}{\text{distance travelled by solvent}} = \frac{a}{b}$$



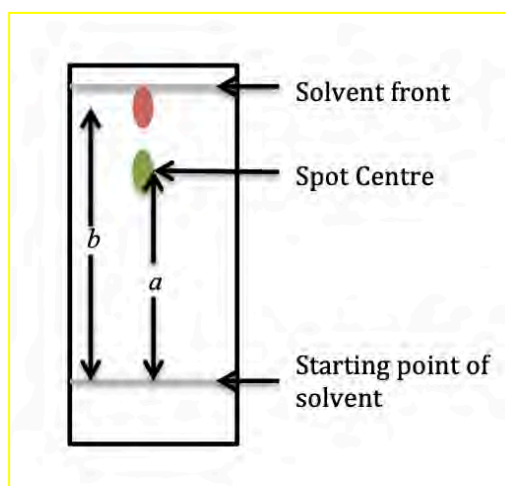


**Figure 8: TLC plate showing the solvent front, spot on spot centre and starting point.**

The TLC plate (shown in Figure 8: TLC plate showing the solvent front, spot on spot centre and starting point.) is an example of how a TLC plate will look after two components (red and green spots) have been separated the mixture. Where  $a$  is the distance travelled by the green component and  $b$  is the distance travelled by the red component. The distance travelled by the solvent use is the difference between the solvent front line and the starting point of solvent line. Developed plates are examined under a light source or sprayed with chemical reagents. Silica gel plate can be impregnated with fluorescent material that glows under ultraviolet (UV) light to identify UV active compounds.

In this study, TLC will be used to identify the number of components in the mixture during the isolation process, identify possible pure compounds and also monitor the progress of isolation during column chromatography.

TLC analysis does not provide information on the structure of the analyte or mass analyte.

### **3.3.2. Column Chromatography**

Column chromatography (CC) is a chromatographic method used to physically separate and purify substantial quantities of components from a mixture. The method is a liquid-solid technique, in which a solvent act as a mobile phase and the stationary phase (absorbents) is a solid. It is based on the same principles that govern TLC, except in CC the stationary phase is packed into in a column and the mobile phase moves through the stationary phase. CC is a type of adsorption chromatography technique. Adsorption is based in the interactions of functional groups in the molecule with the stationary phase, the components with a greater adsorption and affinity to stationary phase will go slower through the stationary phase as compared to the components with lower adsorption and affinity.

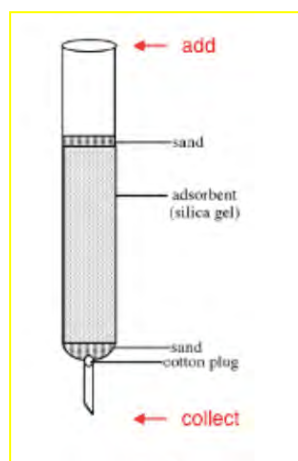


**Figure 9: Schematic diagram of silica gel open column chromatography.**

### **3.3.4. Open column chromatography**

The sample is loaded carefully to the column that is plugged at the bottom by a piece of cotton. The mixture to be separated is dissolved in a suitable volatile solvent then adsorbed on small weight of adsorbent (silica gel) and the solvent allowed to evaporate. Then the dry adsorbent with the mixture is introduced at the top of the column and is packed uniformly to avoid irregular band separation leading to poor separation. More silica gel is added to cover up the mixture to prevent splashing out when the mobile phase added from the top (Figure 9: Schematic diagram of silica gel open column chromatography.). The mobile phase is added to the top of the column and is allowed to pass through the column. As the mixture moves down the column, the rate at which the components of the mixture are separated depends on the activity of the adsorbent and the polarity of the solvent. The strongly adsorbed components will remain close to the top of the column while the weaker adsorbed components will be eluted down the column as per to their affinity of the adsorbent. Eluent is collected in fractions at the bottom, this procedure is also known as fractionation.

In this study, we will be using column chromatography to fractionate compounds with the same polarity and isolate compounds.

### **3.3.5. High Performance Liquid Chromatography**

High Performance Liquid Chromatography (HPLC) was performed on HPLC '1200 series' (Agilent Technologies, United States of America). HPLC is a chromatographic technique is widely used for qualitative and quantitative analysis of each component in a mixture. HPLC can be used for separation of mixtures that cannot be readily volatilized. HPLC can be applied



to just about any sample, such as pharmaceuticals, food, nutraceuticals, cosmetics, environmental matrices, forensic samples, and industrial chemicals.

The technique is suitable for separation of compounds having one or more of the following characteristics:

- High polarity
- Thermal instability
- A tendency to ionize in solution
- High molecular weight

In HPLC, the stationary phase is solid particles while the mobile phase is a liquid. The technique involves injection of a small volume of liquid sample into a column packed with tiny particles (3- 5  $\mu\text{m}$ ) called the stationary phase. Individual components of the injected sample are forced through the column with the mobile phase delivered by the pump.

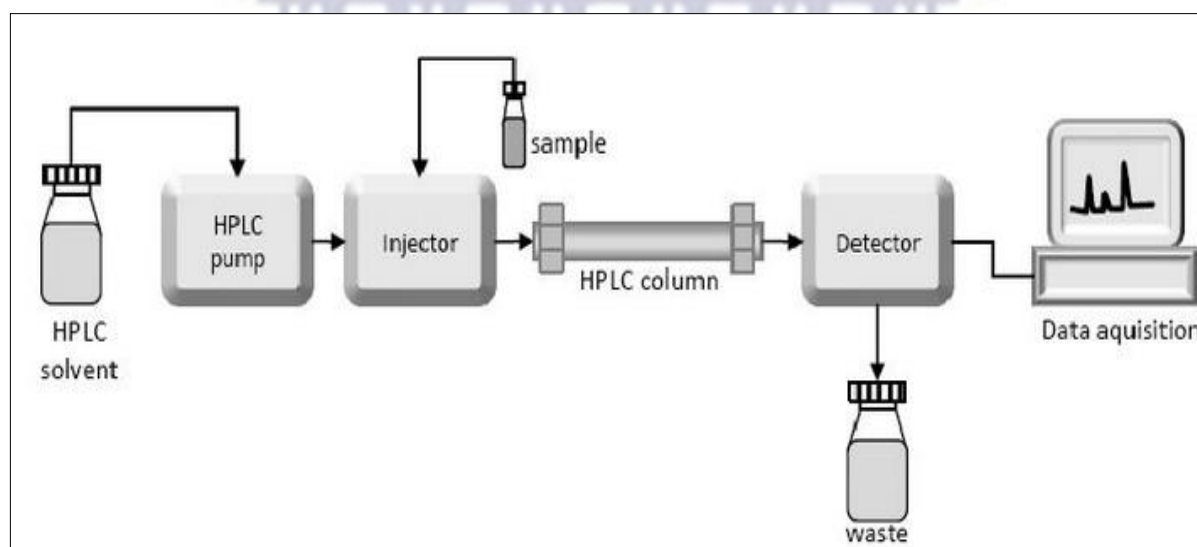


**Figure 10: Schematic of components of HPLC system.**

The components of the HPLC include an HPLC solvent source, pump, injector, column, detector and a data acquisition (Figure 10: Schematic of components of HPLC system.).

There are three types of HPLC techniques, adsorption chromatography, ion-exchange chromatography and size exclusion chromatography.

Adsorption chromatography is divided into two modes, normal phase chromatography and reverse phase chromatography. In normal phase chromatography, the column packing (stationary phase) is polar and the mobile phase is non-polar. In reverse phase chromatography the stationary phase is non-polar or weakly polar and the mobile solvent is more polar. In most cases, the stationary phase is chemically modified silica gel, [for example: Octadecyl (C18)

group-bonded silica gel (ODS)] which binds with alkyl chains and the mobile phase is usually polar mixture of an organic solvent and water. Reverse column chromatography is the most popular mode used because its versatility. It can be used for non-polar, polar, ionisable and ionic molecules.

In ion exchange chromatography, the stationary phase (adsorbent) has a charged surface with opposite charges on it compared to the sample ions. The mobile phase is an aqueous buffer with a controlled pH and ionic strength.

In size exclusion chromatography the stationary phase is made of a porous medium. How the components get separated depends on the pore size of the medium, the molecules diffuse into pore of the porous medium. Larger molecules do not diffuse into the particles and therefore gets elute first, while smaller molecules enter the particle and are separated, thus, gets eluted later. This mode is mainly used for proteins and characterization of polymers.

### **3.4. Characterization techniques**

#### **3.4.1. Nuclear Magnetic Resonance (1D and 2D NMR)**

Nuclear Magnetic Resonance (NMR) technique of high-resolution NMR is a spectroscopic technique used for structure elucidation of pure chemical compounds. The atomic nuclei can be depicted as a positively charged sphere that rotates on its own axis.

The sample is placed in a magnetic field, the sample is then subjected to radiofrequency radiation at the appropriate frequency, allowing for the absorption of energy depending on the type of the nucleus, the chemical environment of the nucleus, whether a methyl or hydroxyl protons are present, molecular conformations, and the spatial location in the magnetic field.

In the classical approach to elucidate a structure by spectral interpretation, reference tables of corresponding measured values, chemical shifts and spin-spin coupling constants, accounting for signal multiplicity, are used. The spectral values are very sensitive to changes in molecular configurations and conformations. So NMR techniques are highly valued in the solution of stereochemical problems.

for signal multiplicity, are used. The spectral values are very sensitive to changes in molecular configurations and conformations. So NMR techniques are of the first value in the solution of stereochemical problems.

Now, there are two advanced approaches to identification/structure elucidation First, a computer spectral simulation is applicable. NMR spectra are easily predictable for hypothetical structures, and can be used for comparison with spectra recorded for analyte. Second, such

comparisons can be performed if reference databases comprising of experimental NMR spectra are available. Both approaches are rapidly developed, and well deserve more attention from the analytical chemist. Nevertheless, relatively low (a) sensitivity and (b) identification power in relation to individual components of complicated mixtures still limit NMR applicability in qualitative analysis I. In this study, NMR is used as a tool to confirm the purity of compounds and elucidation of chemical structures using the data.

### **3.4.2. Ultraviolet and visible spectrometry (UV-Vis)**

Ultraviolet (UV) and visible (Vis) spectrometry is a method used for identification and quantification of organic and inorganic compounds across a wide range of products and processes. It is one of the most popular techniques because of its simplicity, versatility, speed, accuracy and cost-effectiveness.

In UV-Vis spectrometry, consist of three main elements which are a light source, a monochromator and detector. A beam of light is passed through a sample, the monochromator uses diffraction grating to dispense the beam of light into various wavelengths and the detector records the intensity of the transmitted beam of light. The amount of absorbance at any wavelength is due to the chemical structure of the molecule. Before samples are run, a reference should be taken to calibrate the spectra and cancel out spectral interferences. Molecules with different chemical structures have different absorption spectra. Thus, it can be used to identify functional groups or confirm the identity of a compound by matching the absorbance spectrum. UV-Vis spectrometry is used to provide the knowledge about  $\pi$ -electron systems, conjugated unsaturation, aromatic compounds and conjugated non-bonding electron systems, etc. For aromatic compounds the electronic levels involved are this of  $\pi \rightarrow \pi^*$  (Lampman *et al.*, 2001). In this study, UV-Vis will be used to obtain information on the chemical structure of isolated compounds, such as the functional groups present, the number of molecules.

### **3.4.3. Fourier-transform infrared spectroscopy (FTIR)**

Infrared (IR) spectrometry is a non-destructive method used for identifying vibrational structures of various materials. In classical IR spectroscopy, pure organic compounds can be elucidated/identified by means of spectral interpretation using reference tables containing specific wavenumber of absorption bands of different functional groups and specific band absorption. IR is widely used because it requires minimal or no sample preparation, fast and inexpensive. The technique is used for analysis of foodstuff, pharmaceuticals, chemicals, polymers and etc. FT-IR is a tool used to identify types of functional groups present in the

organic compounds. The chemical structural fragments within molecules absorb infrared radiation in the same wavelength range and regardless of the structure of the molecule, the absorbance will occur. Interpreting the infrared absorption spectrum can identify the chemical bonds in a compound (Coleman, 1993).

In this study, The AT- FTIR analysis of isolated compounds, in range 400 to 4000  $\text{cm}^{-1}$  will be used provide more information about the chemical structures of the compounds isolated from *Psoralea aphylla*.

#### **3.4.4. Mass Spectrometry**

Mass spectrometry is a powerful tool for the characterization of various biomolecules, that separates molecular ions based on their mass and charge, or exactly according to their mass to charge ratio (Vandell *et al.*, 2017; Chandler *et al.*, 2014). This technique helps identify the amount and type of chemicals present in the sample by measuring the mass-to-charge ratio and abundance of gas-phase ions. The sample is directly injected to the ion source, in vacuum, the sample molecules are bombed with a high energy beam of electrons from a heat filament to form a radical cation known as the molecular ion. If the molecular ion is too unstable it can be fragment into smaller cations and neutral fragments. The charged particles are focused into a beam, accelerated into the magnetic field and separated according to their masses of the ions. Ions of the same mass-to-charge ratio will undergo the same amount of deflection, thus, by adjusting the magnetic field, the ions can be focused on the detector. A mass spectrum displaying the result in the form of a plot of ion abundance (signal intensity) versus mass-to-charge ratio ( $m/z$ ). The sample is identified by correlating known masses to the identified masses or through a characteristic's fragmentation pattern.

### **3.5. Tyrosinase Inhibition studies**

#### **3.5.1. Tyrosinase inhibition Assay**

The tyrosinase inhibition assay was performed on a MULTISKAN SPECTRUM spectrometer, which is used to measure the absorbance of solution in 6, 12, 24, 48, 96 or 384-well plates. The instrument is ideal for measuring the absorbance in end point, kinetic and spectral scanning applications. Due to its flexibility for photometric research applications, it is used for DNA, RNA and protein analysis.

The enzyme activity is determined by measuring the absorbance of *o*-dopachrome at 490 nm using a plate reader. The tyrosinase inhibition percentage is calculated as follows:



$$[(A - B) - (C - D)] / (A - B) \times 100 \quad \text{Equation 1}$$

Where, A is the absorbance of control with the enzyme, B is the absorbance of the control without the enzyme, C is the absorbance of the test sample with the enzyme and D is the absorbance of the test sample without the enzyme.

In this study we will be measuring the tyrosinase inhibition of the main extract and each compound after the reaction mixture has been incubated for 30 minutes at room temperature.

### 3.5.2. Tyrosinase Inhibition using Cyclic Voltammetry (CV)

Cyclic voltammetry (CV) experiments were performed using PalmSens 4.4 electrochemical workstation (Bioanalytical systems, USA). CV is one of the most widely used analytical techniques for studying electrochemical reactions. The potential is scanned at a potential controlled rate between two values at a fixed rate, and the current produced by oxidations or reduction is continuously recorded. The scan rate is a critical factor because the duration of the scan must provide sufficient time to allow a significant chemical reaction to take place.

The CV system consists of electrolysis cell, which consists of a conventional three-electrode potentiostat connected to three electrodes immersed in an electrolytic solution (Figure 11). The three electrodes are the working electrode, reference electrode and counter (auxiliary) electrode (Grieshaber *et al*, 2008; Wang, 2006)



**Figure 11: Example of a three-electrode system.**

To obtain a cyclic voltammogram, a linear potential sweep (that is, a potential that increases or decreases linearly with time) is applied to the working electrode, while the reference electrode

maintains a constant potential, while current is measured between the working electrode and the counter electrode. A voltammogram is the obtained measurement that are plotted as current vs. potential. The current depends on the electron transfer reaction the movement of electroactive material (Grieshaber *et al.*, 2008; Wang, 2006; Mabbott, 2006).

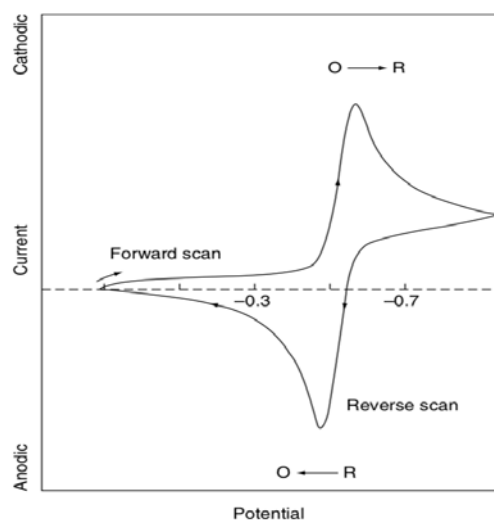


**Figure 12: Example of a cyclic voltammogram for a reversible redox process (Wang, 2006).**

CV can be used to study compounds, the voltammogram for a given compound depends on the scan rate, electrode surface (which differs in each adsorption step) and on the catalyst concentration. For certain specific enzymes, studies show by increasing the concentration of the enzyme at a constant scan rate, the current will be higher for a catalysed reaction compared to the non-catalysed reaction (Grieshaber *et al.*, 2008; Wang, 2006)

In this study, the glassy carbon electrode was used to understand the electrochemical response of tyrosinase enzyme to extracts and compounds isolated from *Psoralea aphylla*. The results will be compared to the tyrosinase inhibition assay results using Tyrosinase Inhibition ELISA method.

### 3.6. MTT Assay

MTT assay, an enzyme based method is a standard colorimetric assay that is widely used for estimating the number of viable cells reduced that the MTT formazan (Riss *et al.*, 2019). In this assay, MTT is a positively charged compound that readily penetrates viable cells. Viable cells with active metabolism produce NADH within the mitochondria and the NADH acts as



an oxidizing agent that convert MTT into formazan (Riss *et al.*, 2019; Morgan, 1998) . The formation of formazan is indicated by purple needle-like crystals within the cell. The crystals are impermeable to cell membranes and can be solubilized by detergents. The number of living cells is directly proportional to the level of the formed formazan and the absorbance of the purple formazan solution can be quantified using a spectrophotometer by at 570 – 690 nm (Morgan, 1998). In order to determine the viability and cytotoxicity levels of bakuchiol an MTT cell viability assay was performed using POLARstar Omega microplate reader (BMG LABTECH, Germany).



---

# CHAPTER 4:

## Materials and Methodology

---

*This chapter presents the materials used to perform all experiments. The chapter is separated into three parts; Part A, B and C. Part A focuses on the collection, extraction and isolation of compounds from *Psoralea aphylla*, while part B focuses on the tyrosinase inhibition assay to screen the main extract and isolated compounds as potential tyrosinase inhibitors using an spectrophotometric method, and the behaviour of compounds isolated from *Psoralea aphylla* was investigated using cyclic voltammetry to monitor the each compounds behaviour with tyrosinase enzyme and compare to a known inhibitor, kojic acid. In Part C we also investigated to cytotoxicity of bakuchiol using MTT assay.*

### 4.1. Materials

#### 4.1.1. Solvents and reagents

Analytical grade organic solvents such as methanol (MeOH), ethanol (EtOH), hexane (*n*-Hex), dichloromethane (DCM), ethyl acetate (EtOAc), and dimethyl sulfoxide (DMSO) were used for all purposes, HPLC grade solvents were used for HPLC and deuterated chloroform (CD<sub>3</sub>OD, 99.9% purity) was used for NMR sample preparation. The analytical solvents supplied by Merck (Cape Town, South Africa) were stored at room temperature and transferred to 2.5L bottles for routine use. The vanillin reagent was prepared using 15g of vanillin powder dissolved in 250mL of 96% ethanol and 2.5mL of sulfuric acid (concentrated H<sub>2</sub>SO<sub>4</sub>) was carefully added, while stirring the mixture under vacuum. The mushroom tyrosinase (EC 1.14.18.1) 5771 Unit/mg, L-tyrosine and kojic acid were purchased from Sigma Aldrich (Cape Town, South Africa). Sodium phosphate dibasic dihydrate (HNa<sub>2</sub>O<sub>4</sub>P•2H<sub>2</sub>O) and Sodium phosphate monobasic dehydrate (H<sub>2</sub>NaO<sub>4</sub>P•H<sub>2</sub>O) were purchased from Sigma-Aldrich (Cape Town, South Africa). The Dulbecco's Modified Eagle Medium (DMEM) medium, penicillin-streptomycin and phosphate buffered saline (PBS) were purchased from Lonza (Cape Town, South Africa). 0.05% trypsin-EDTA was purchased from Thermo Fisher Scientific (Cape Town, South Africa).

The MTT assay experiments were carried out in a model NU-5510E NuAire DHD autoflow automatic CO<sub>2</sub> air-jacketed incubator and an AireGard NU-201-430E horizontal laminar

airflow table-top work station that provides a HEPA-filtered clean work area we all purchased from NuAire (Minnesora, USA). 96-well culture plates and 25 cm<sup>2</sup> cell culture flasks were purchased from SPL Life Sciences (Gyeonggi-da, Korea), PrimoVert phase-contrast microscope was purchased from Carl Zeiss Microscopy LCC (New York, United States USA), TC20™ automated cell counter Bio-Rad, USA) and POLARstar Omega microplate reader purchased from BMG LABTECH (Ortenberg, Germany) was used in this experiment. Deionized water purified by Milli-QTM system (Millipore) was used throughout the experiment.

#### **4.1.2. Preparation of 50mM phosphate buffer**

8.159mM of sodium phosphate dibasic dihydrate and 0.04184 mM of sodium phosphate monobasic dihydrate were dissolved in separate 0.5L distilled water. To obtain the pH of 6.5 the two solutions were mixed and the pH of the buffer was 6.8. The pH was adjusted by adding the sodium phosphate monobasic dihydrate until a pH of 6.8 was achieved.

#### **4.1.3. Preparation of tyrosinase enzyme and l-tyrosine standard solutions**

2mM of L-tyrosine prepared by dissolving 2.0 mg in 5.52mL of 50 mM PBS solution. 500 units of tyrosinase enzyme solution was prepared by dissolving 0.700 mg of 5771 units tyrosinase in 8.08mL 50mM PBS solution. The enzyme stock solution was stirred gently for 1 min and stored in the refrigerator at -5 °C.

#### **4.1.4. Preparation of kojic acid**

The standard stock solution kojic acid was prepared by dissolving 1.0 mg in 1mL DMSO to yield a concentration of 1.00mg/ml. The stock solutions were kept in the refrigerator at -5 °C.

#### **4.1.5. Preparation of constituents for cyclic voltammetry**

The preparation of plant extract and isolation of compounds was mentioned in Chapter 3. The extract and compounds were dissolved in DMSO to a concentration of 1.00mg/ml for the tyrosinase inhibition assay.

#### 4.1.6. Preparation of electrodes

The glassy carbon electrode of area  $0.071 \text{ cm}^2$  was pre-cleansed by polishing the electrode surface with three alumina slurries of particle sizes ( $3.0 \mu\text{m}$ ,  $1.0 \mu\text{m}$  and  $0.03 \mu\text{m}$ ) respectively in glassy polishing pads or a minimum time of 10 min on each pad. After polishing, the glassy carbon electrode was sonicated for 10 min in ethanol and for another 10 min in deionized water to remove any possible residual alumina powder; this was followed by rinsing the electrode again with double distilled water. Before each experiment, the cleanness of the electrode was checked by potential scanning the cleansed glassy carbon electrode from the potential of  $E = 1500 \text{ mV}$  to  $E = -1500 \text{ mV}$  at scan rate of  $50 \text{ mV s}^{-1}$  over 1 cycle from negative to positive potentials, in a 10mL solution containing 50 mM PBS purged with argon gas for 5 min.

#### 4.1.7. Cell Culture

B16 melanoma cells were kindly provided by Prof. Davids Lester of Department of Medical Bioscience, University of the Western Cape, South Africa. The B16 cells were cultured in DMEM medium. All media were supplemented with 20% heat-activated and gamma-irradiated Fetal Bovine Serum (FBS) and 1% Streptomycin plus Penicillin (100U/mL Streptomycin and 100U/mL Penicillin). The melanoma cell lines were grown and kept at  $37 \text{ }^\circ\text{C}$ , 80% - 90% relative humidity with 5%  $\text{CO}_2$  atmosphere, respectively (Yáñez *et al.*, 2014). Cryovials containing the cells were taken from a  $-80 \text{ }^\circ\text{C}$  fridge and slowly thawed to  $37 \text{ }^\circ\text{C}$ , in a humidified  $\text{CO}_2$  incubator at of  $37 \text{ }^\circ\text{C}$  in 5%  $\text{CO}_2$  atmosphere, the cells were placed into 15 mL conical centrifuge tubes and fresh culture medium were then added to neutralize the effect of DMSO used for preservation of cells. The tubes were then centrifuged at 3000 rpm for 3 min at  $25 \text{ }^\circ\text{C}$  temperature. After centrifugation, the supernatant was discarded and the cell pellet were recovered. The cell pellets were re-suspended in 5 mL fresh complete culture medium and transferred into a T-25 tissue culture flask. The flask was viewed under a PrimoVert phase-contrast microscope to ascertain presence of cells. Then, the flask was placed in a humidified  $\text{CO}_2$  incubator at of  $37 \text{ }^\circ\text{C}$  in 5%  $\text{CO}_2$  atmosphere. After 24 hr the cells were observed under a microscope to confirm attachment. The flask was placed in a humidified  $\text{CO}_2$  incubator at  $37 \text{ }^\circ\text{C}$  in 5%  $\text{CO}_2$  atmosphere until about 80%-90% cell confluency was reached (Yáñez *et al.*, 2014); Elbagory *et al.*, 2015).

#### **4.1.8. Sub-culturing of cells**

After reaching 80-90% confluency, the culture medium was discarded and the cells were washed with 1 mL of PBS for 1 min. PBS was removed and 0.05% trypsin-EDTA was added for the purpose of trypsinization. The flask was incubated at 37 °C for 2 min to allow the cells to detach from the bottom of the flask, after which it was transferred to the laminar flow safety cabinet. 2 mL of growth medium were added to the flask to deactivate the action of trypsin and the mixture was aspirated and transferred into sterile 15 mL conical centrifuge tube. The tube was centrifuged at 3000 rpm for 3 min at 25 °C to separate cells from the medium-trypsin solution and the supernatant was discarded. The cell pellets were dislodged at the bottom of the conical centrifuge tube by adding 4 mL of fresh complete medium. The cell pellets were gently mixed to ensure a homogenous suspension and the suspension was then transferred into T-25 culture flask and stored at -80 °C to maintain stock cultures.

#### **4.1.9. Cell Counting and Viability Testing**

TC20™ automated cell counter was used for cell counting as recommended manufacturer's procedure. To determine whether cells are viable, TC20™ uses images acquired from multiple focal planes during the focusing step in liquid medium within counting slide. The cells in a 96-well plate were treated with 0.4 % of trypan blue stain in 1:1 ratio (v/v) and the solution was carefully mixed. After mixing 10 µL of the trypan blue stained cell suspension was counted using a TC20™ automated cell counter and the desired concentration of viable cells was determined based on displayed calls using the cell counter calculator.

#### **4.1.10. Preparation of PBS buffer MTT stock solution**

A stock solution of MTT was prepared by dissolving 5mg/ml of MTT 3-(4, 5-dimethyl-thiazol-2-yl)-2, 5-diphenyltetrazolium bromide in PBS.

#### **4.1.11. Preparation of bakuchiol for MTT Assay**

1.0 mg of bakuchiol was dissolved in 1 mL DMSO, then was diluted in complete growth medium to reach a concentration of 1000 µg/ mL. After dilution, the final DMSO concentration was not greater than 1% (v/v) in all experiments.



## Part A

### 4.2. Methodology of Organic experiment

#### 4.2.1. Collection and identification of plant

*Psoralea aphylla* plant was collected in Paarl, Western Cape, South Africa in the month of February 2018. The plant was collected by Prof. Ahmed Mohammed Hussein (Chemistry Department, CPUT) and was identified by Prof. Christopher Cupido (Fort Hare University).

#### 4.2.2. Pre-extraction and extraction of *Psoralea aphylla*

For this study the fresh *Psoralea aphylla* plant (leaf, stem and flower) was cut into smaller pieces, ground and weighed (664.5g).

For this study, plant was subjected to methanol extraction at constant temperature heat of 60°C for 2 hours, and left outside for 24 hours. Extraction using methanol was repeated twice to obtain optimum soluble extract.

The combined methanol soluble extract was filtered under suction using Whatman's No. 1 filter paper in Buckner funnel and was concentrated on a rotary evaporator. The evaporated methanolic extract was preserved in labelled vials and left under fume hood for proper solvent evaporation to afford 200 g of total crude methanolic extract.

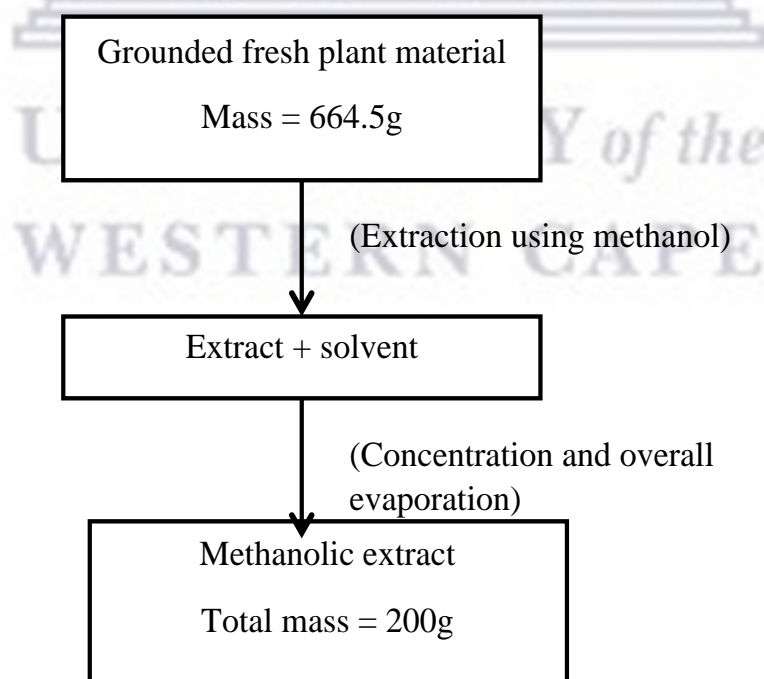


Figure 13: Flow chat of methanolic extraction of *Psoralea aphylla*.

### 4.2.3. Fractionation of crude extract

The whole crude methanolic extract was subjected into open column chromatography (Figure 14) using a glass column packed with either silica gel 60 (0.040 –0.06mm) purchased from Merck (Cape Town, South Africa) or Sephadex<sup>®</sup> LH-20 purchased from Sigma-Aldrich (Cape Town, South Africa) using different solvents from non – polar to polar i.e. *n*-hexane to ethyl acetate and then methanol (Table 6: Solvent system used for fractionation of the total extract of *Psoralea aphylla*.).



Figure 14: Open Column Chromatography set-up.

Table 6: Solvent system used for fractionation of the total extract of *Psoralea aphylla*.

Solvent Volume	Solvent System
1 L	Hexane
3 L	Hexane : Ethyl acetate 9:1
3 L	Hexane : Ethyl acetate 7:3
3 L	Hexane : Ethyl acetate 1:1
3 L	Hexane : Ethyl acetate 3:7
2 L	Methanol
2 L	Ethyl acetate : Methanol 1: 9
2 L	Ethyl acetate : Methanol 7:3
2 L	Ethyl acetate : Methanol 1:1

The gradient elution was very efficient for elution of different fractions with different polarities and different compounds. Fractions (volume = 250.0 mL) were collected, concentrated on the rotary evaporator and then underwent TLC analysis. The TLC analysis was performed on silica gel 60 F<sub>254</sub> pre-coated plates with 0.2mm thickness (Merck, Germany), eluents were spotted on pre-coated TLC plate by using a capillary tube. The dried plate was run in *n*-Hexane–ethyl acetate (7:3, v/v) mobile phase. Once developed, the plate was taken out from the TLC chamber and air-dried. The spots on the plate were visualized using UV light of wavelength  $\lambda_{254}$  and  $\lambda_{365}$ , respectively ( Figure 17) . The plate was dipped in the vanillin reagent and heated using a heating gun. The eluents with the same R<sub>f</sub> values were pooled together into one fraction. 7 fractions afforded after pooling were given designated codes ( Table 7: Fractions obtained upon fractionation of total extract of *P.aphylla*.).

**Table 7: Fractions obtained upon fractionation of total extract of *P.aphylla*.**

Fraction number	Designated number
1	PAM1-1
2	PAM1-2
3	PAM1-3
4	PAM1-4
5	PAM1-5
6	PAM1-6
7	PAM1-7

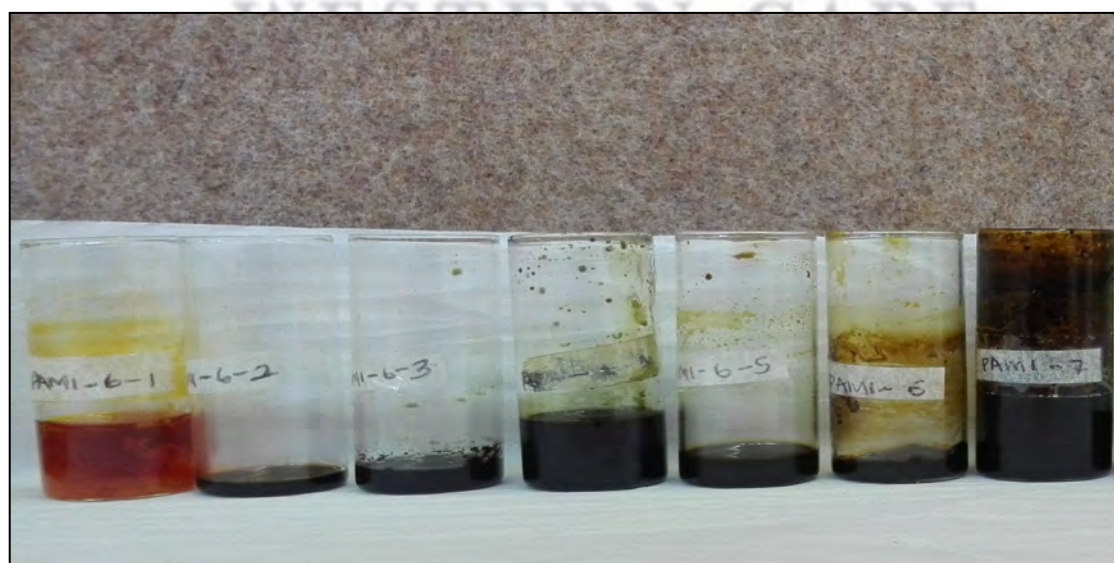


**Figure 15: Picture of main fractions of *P.aphylla*.**

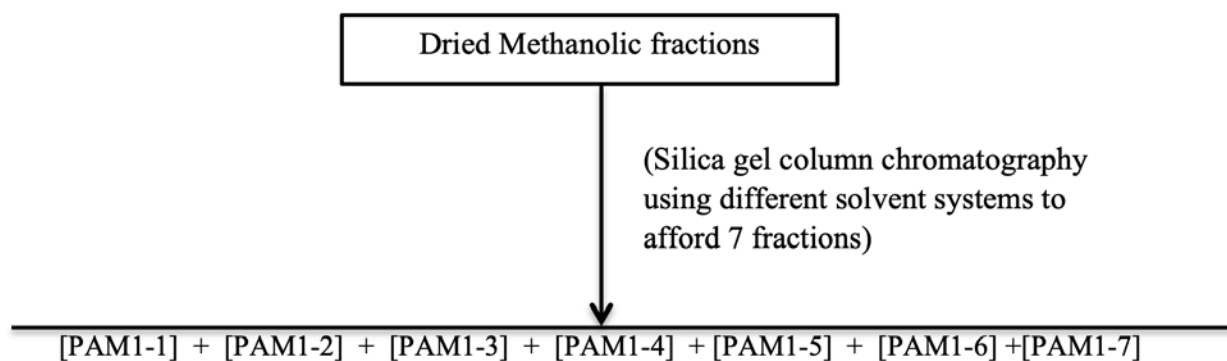


**Figure 16: Flow chat of fractionation of methanolic extract.**

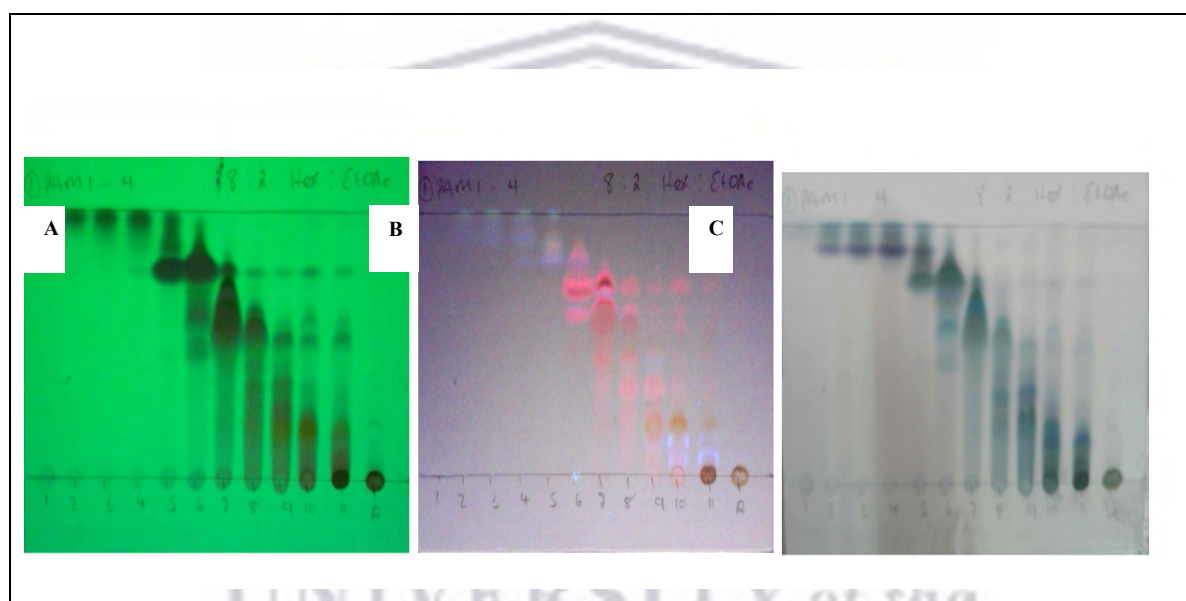


**Figure 17: TLC chromatograms of main fractions obtained from column chromatography fractionation of *P. aphylla* methanolic extract. Using Hexane–ethyl acetate (8:2, v/v) solvent system. A: TLC plate visualized under UV light of  $\lambda = 254$  nm, B: TLC plate under UV. C: TLC plate after spraying with vanillin solution.**

Using a tip of a spatula, each fraction was dissolved using 1ml methanol in a micro tube and stored at room temperature.

#### **4.2.4. Isolation of Compound 1 using Column Chromatography**

A glass column was clamped upright and packed with silica gel. Fraction 4 (PAM1-6-4) weighing 21.25g was subjected to gradient silica gel column chromatography using *n*-Hexane–ethyl acetate (95:5, to 80:20) increasing in 2% (v/v) was used as an eluent and 10 ml fractions were collected into test tubes. Using Hexane–ethyl acetate (7:3, v/v), and dichloromethane-



methanol (97:3, v/v) solvent systems for TLC analysis. Similar fractions were pooled together to give 11 sub-fractions, in which sub-fractions PA1, PA2 and PA3 showed a single spots on the TLC plate (Table 8: The sub-fractions from the fractionation of PAM1-6-4.; Figure 18: TLC chromatographs of sub-fractions of PAM1-6-4 eluted in Hex-EtOAc (7:3,v/v) solvent.). The sub-fractions were each combined in a round bottom flask and were concentrated on the rotary vapor, sub-fraction PA1 yielding 85 mg of orange product, sub-fraction PA2 yielding 50mg of orange product and sub-fraction PA3 yielding 53.3 mg of orange product. The  $R_f$  values of all 3 sub-fractions (as indicated in Figure 18: TLC chromatographs of sub-fractions of PAM1-6-4 eluted in Hex-EtOAc (7:3,v/v) solvent.) were measured to be 0,7 in Hex-EtOAc (7:3,v/v). To determine the purity of the obtained sub-fractions, PA1, PA2 and PA3 were subjected to NMR spectroscopy. The spectroscopy data analysis revealed PA1 and PA2 were pure compounds and PA3 was contained impurities. PA1 and PA2 were there same, therefore, were combined and named **Compound 1**.

**Table 8: The sub-fractions from the fractionation of PAM1-6-4.**

Combined fractions	Code	Mass (mg)
1-10	PA1	85.0
11-15	PA2	50.0
16-17	PA3	53.5
18-19	PA4	25.6
20-21	PA5	1411
24-29	PA6	1399
30-33	PA7	669.4
34-39	PA8	208.7
40-45	PA9	36.7
46-47	PA10	560.2
48-53	PA11	27.9



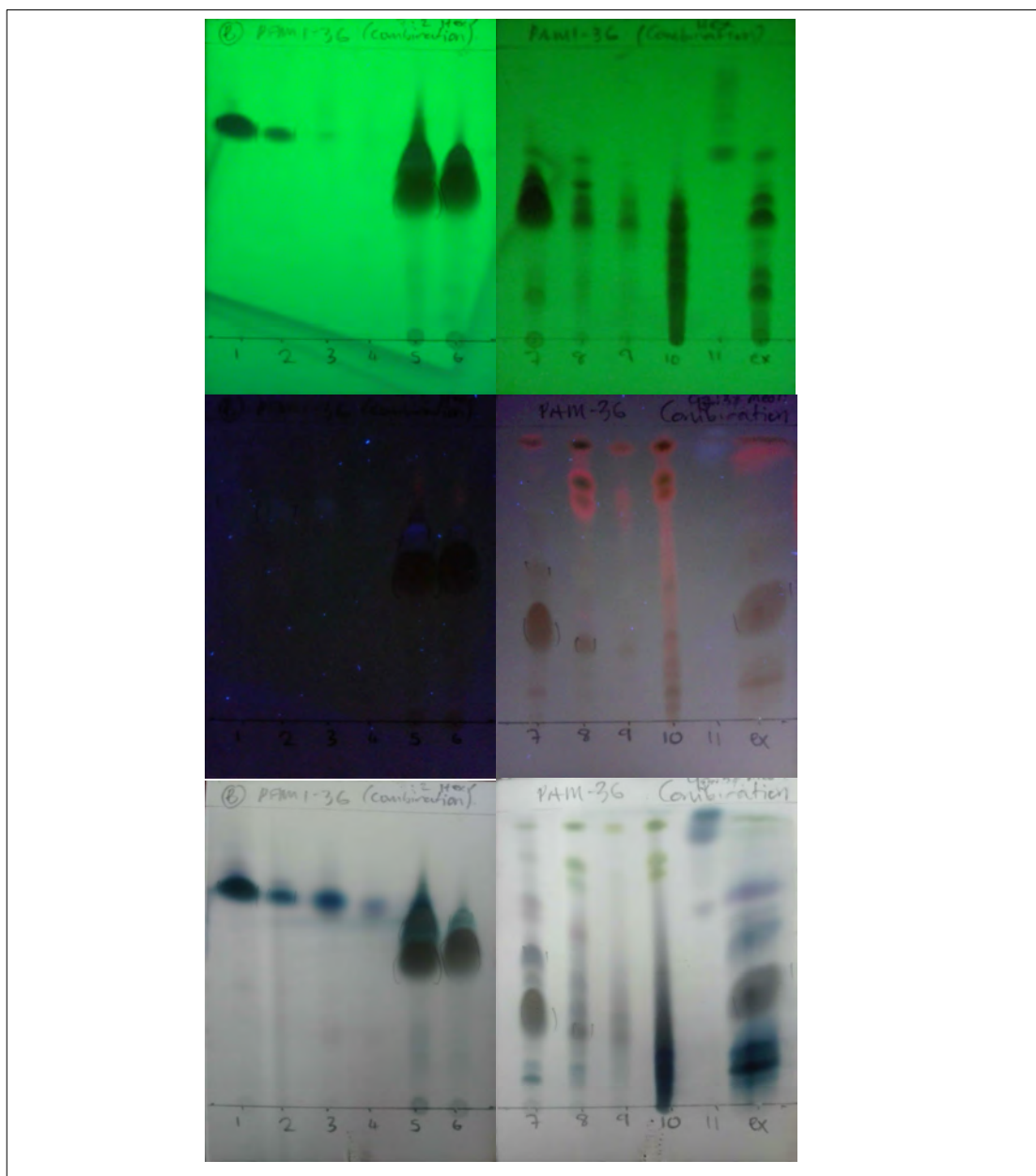


**Figure 18:** TLC chromatographs of sub-fractions of PAM1-6-4 eluted in Hex-EtOAc (7:3,v/v) solvent.

#### 4.2.5. Isolation of Compound 2 using HPLC

A dried PA3 (mass = 50mg) was dissolved in 2ml DMSO before it was injected in the HPLC; 50uL was injected each time onto the HPLC. The utilized mobile phases can be seen in Section 3.3.3, Table 3.3. The mobile phase A: DIW and mobile phase B: MeOH. The total run time was 60 min. The peak at 16.0 min (see

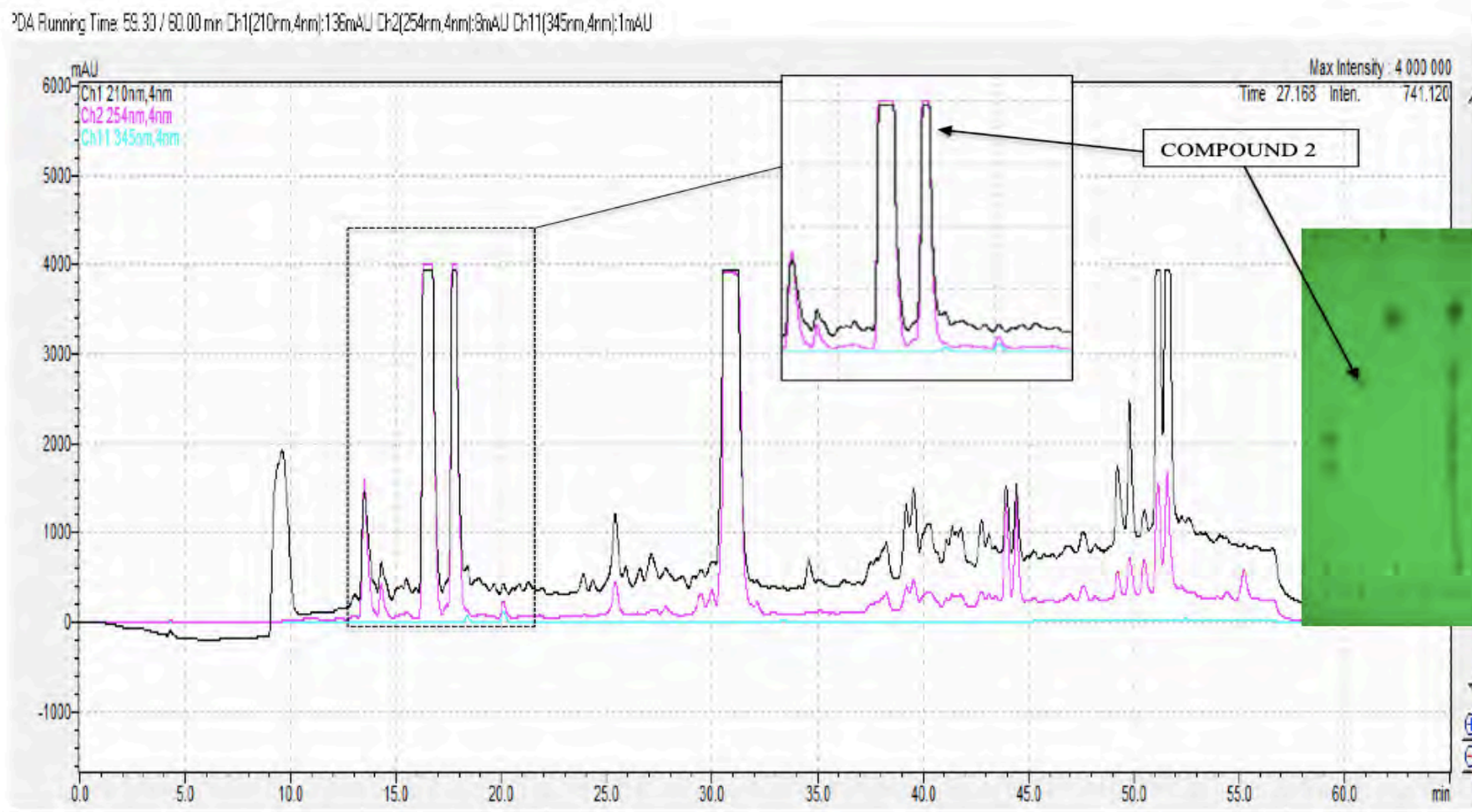


Figure 19: HPLC chromatograph fraction PA3, with Compound 2 at 16.0min and TLC chromatograph under UV light of  $\lambda = 254$  nm.

**Table 9: HPLC conditions for the isolation of Compound 2. conditions\*.**

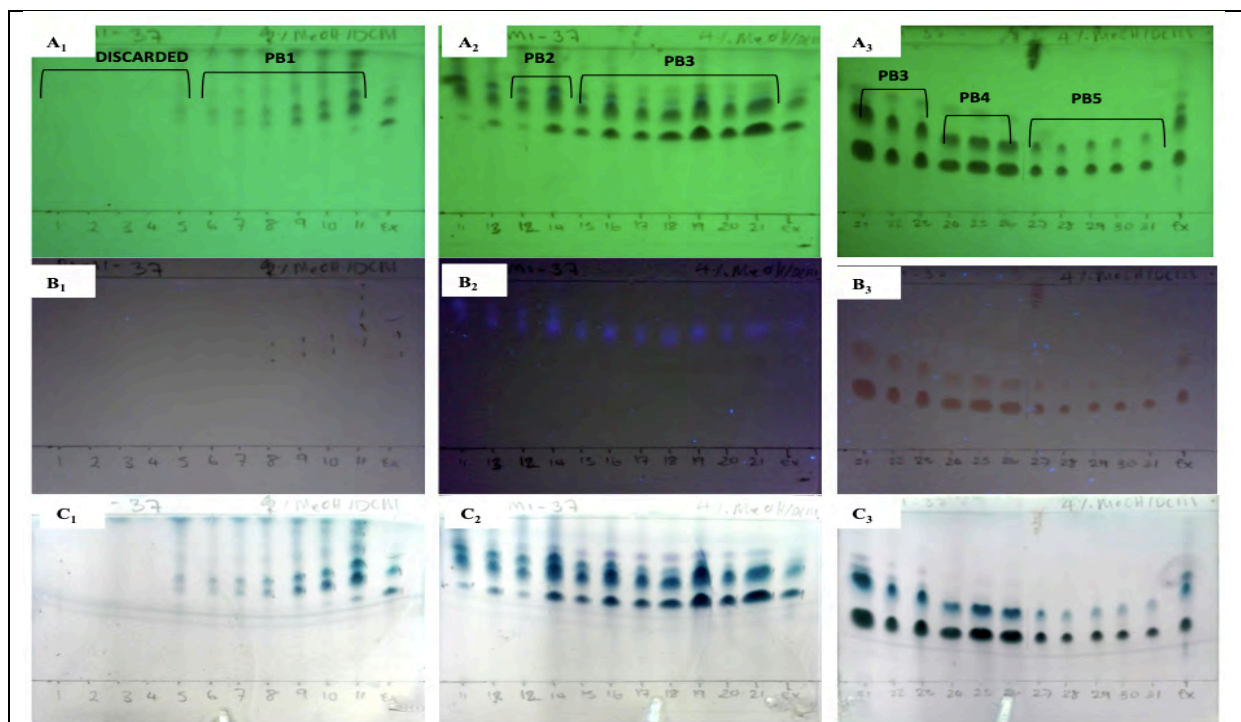
Compound	Column	Gradient	Flow rate (mL/min)	Detector	Mass (mg)
Compound 2	C18 column SUPELCO (25 x 2.1 cm, 5µm)	MeOH: DIW 80:20(v/v) to 100% MeOH in 40 minutes	1.5	UV at: Black = λ210 Pink = λ254 Blue =λ345	5.3

#### 4.2.6. Isolation of compound 3: Column chromatography and crystallization of PA5.

Sub-fraction PA5 (mass = 1411.0 mg) and PA6 (mass = 1399 mg) were combined weighing 2810.0 mg (= 2.81g) were subjected to isocratic silica gel column and eluted with *n*-Hexane–ethyl acetate (91:9, v/v) solution. Similar fractions were pooled together to give 5 sub-fractions, in which sub-fractions PB1 to PB5 (Table 10: Collective sub-fractions from the fractionation process of PA5 and PA6.)

**Table 10: Collective sub-fractions from the fractionation process of PA5 and PA6.**

Combined fractions	Code	Mass (mg)
1-5	Discarded	-
6-11	PB1	256,7
12-14	PB2	272,1
15-23	PB3	799,3
24-26	PB4	176,7
27-31	PB5	121.0



**A: A1, A2 and A3: TLC plate visualized under UV light of  $\lambda = 254$  nm,**

**B: B1, B2 and B3: TLC plate under UV light of  $\lambda = 356$  nm,**

**C: C1, C2 and C3: TLC profile of the main fractions after dipping with vanillin/H<sub>2</sub>SO<sub>4</sub> reagent.**

**Figure 20: TLC chromatograms of sub fractions obtained from gravity column chromatography fractionation of PA5 + PA6. Plate developed using MeOH-DCM (4:6, v/v) solvent system.**

Then sub-fraction PB2, PB3 and PB4 were combined giving a total mass of 1248.1mg and fractionated using a deactivated silica gel column. The fraction was eluted with *n*-Hexane–ethyl acetate (85:15, v/v) solution. Using TLC analysis, in *n*-Hex-EtOAc (8:2,v/v) and MeOH-DCM (2:8,v/v) solvent system and vanillin reagent for visualization, similar fractions were pooled together to give 11 sub-fractions (Table 11: Collective sub-fractions from the fractionation process of PB2, PB3 and PB4., Figure 21: TLC chromatograms of sub fractions obtained from gravity column chromatography fractionation of PB2 + PB3 + PB4. Plate developed using *n*-Hexane–ethyl acetate (8:2, v/v) solvent system. ).

) was collected respectively to give **Compound 2** (mass = 5.3mg).





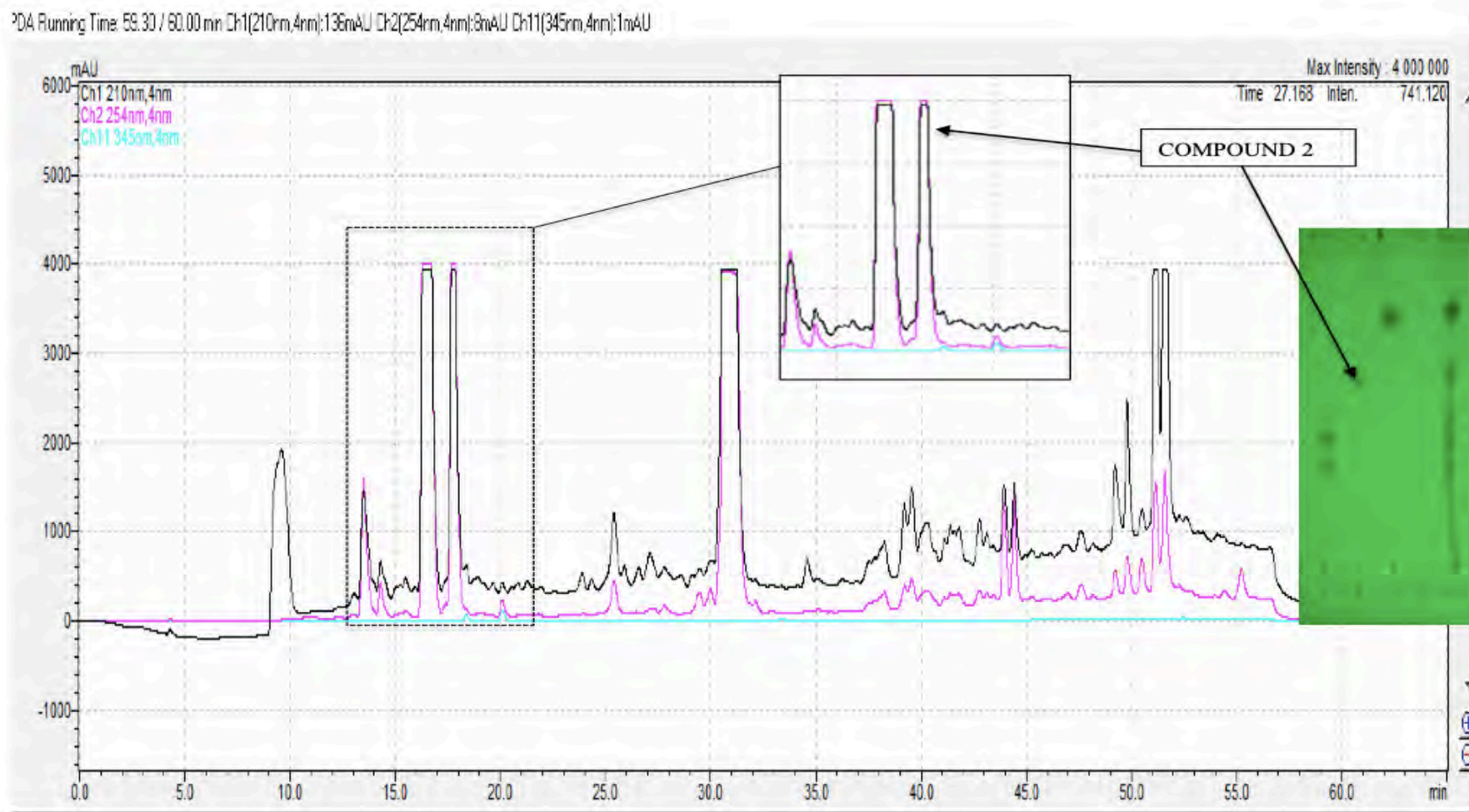


Figure 19: HPLC chromatograph fraction PA3, with Compound 2 at 16.0min and TLC chromatograph under UV light of  $\lambda = 254$  nm.

**Table 9: HPLC conditions for the isolation of Compound 2. conditions\*.**

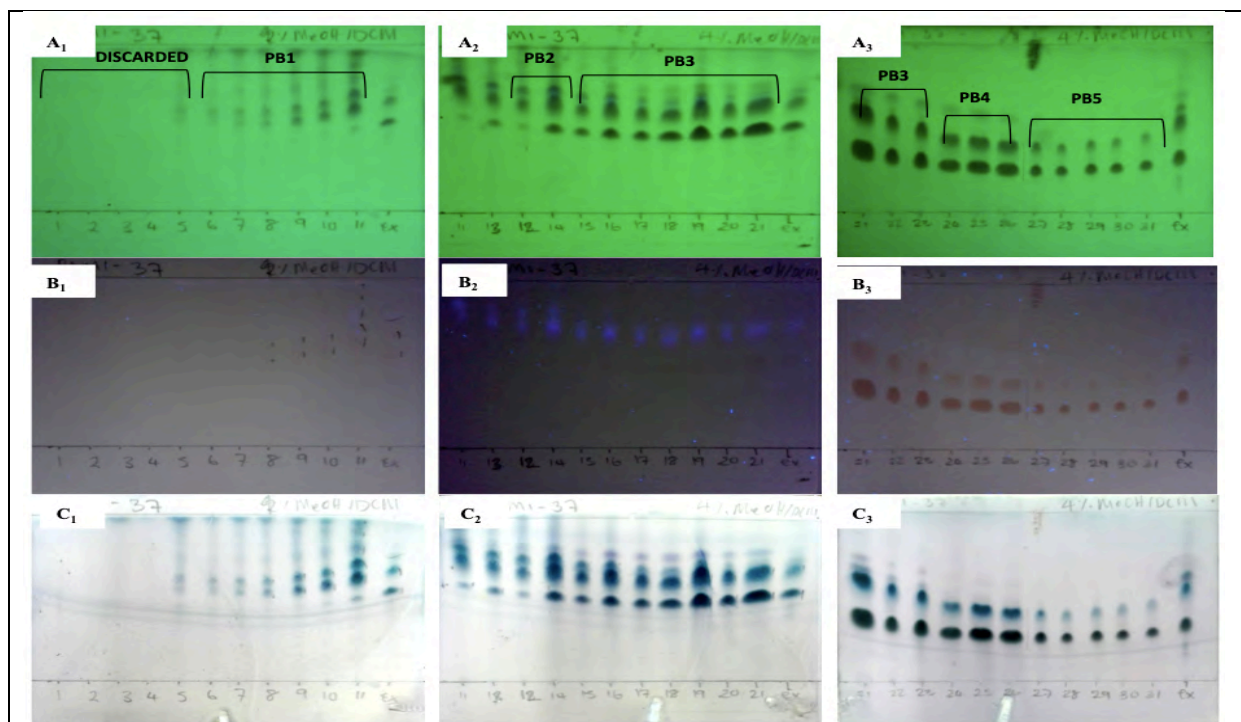
Compound	Column	Gradient	Flow rate (mL/min)	Detector	Mass (mg)
Compound 2	C <sub>18</sub> column SUPELCO (25 x 2.1 cm, 5µm)	MeOH: DIW 80:20(v/v) to 100% MeOH in 40 minutes	1.5	UV at: Black = λ <sub>210</sub> Pink = λ <sub>254</sub> Blue = λ <sub>345</sub>	5.3

#### 4.2.7. Isolation of compound 3: Column chromatography and crystallization of PA5.

Sub-fraction PA5 (mass = 1411.0 mg) and PA6 (mass = 1399 mg) were combined weighing 2810.0 mg (= 2.81g) were subjected to isocratic silica gel column and eluted with *n*-Hexane–ethyl acetate (91:9, v/v) solution. Similar fractions were pooled together to give 5 sub-fractions, in which sub-fractions PB1 to PB5 (Table 10: Collective sub-fractions from the fractionation process of PA5 and PA6.)

**Table 10: Collective sub-fractions from the fractionation process of PA5 and PA6.**

Combined fractions	Code	Mass (mg)
1-5	Discarded	-
6-11	PB1	256,7
12-14	PB2	272,1
15-23	PB3	799,3
24-26	PB4	176,7
27-31	PB5	121.0



**A:** A<sub>1</sub>, A<sub>2</sub> and A<sub>3</sub>: TLC plate visualized under UV light of  $\lambda = 254$  nm,

**B:** B<sub>1</sub>, B<sub>2</sub> and B<sub>3</sub>: TLC plate under UV light of  $\lambda = 356$  nm,

**C:** C<sub>1</sub>, C<sub>2</sub> and C<sub>3</sub>: TLC profile of the main fractions after dipping with vanillin/H<sub>2</sub>SO<sub>4</sub> reagent.

**Figure 20:** TLC chromatograms of sub fractions obtained from gravity column chromatography fractionation of PA5 + PA6. Plate developed using MeOH-DCM (4:6, v/v) solvent system.

Then sub-fraction PB2, PB3 and PB4 were combined giving a total mass of 1248.1mg and fractionated using a deactivated silica gel column. The fraction was eluted with *n*-Hexane–ethyl acetate (85:15, v/v) solution. Using TLC analysis, in *n*-Hex-EtOAc (8:2,v/v) and MeOH-DCM (2:8,v/v) solvent system and vanillin reagent for visualization, similar fractions were pooled together to give 11 sub-fractions (Table 11: Collective sub-fractions from the fractionation process of PB2, PB3 and PB4., Figure 21: TLC chromatograms of sub fractions obtained from gravity column chromatography fractionation of PB2 + PB3 + PB4. Plate developed using *n*-Hexane–ethyl acetate (8:2, v/v) solvent system. ).

**Table 11: Collective sub-fractions from the fractionation process of PB2, PB3 and PB4.**

<b>Combined fractions</b>	<b>Code</b> <b>(Code in lab book PAM1-63)</b>	<b>Mass</b> <b>(mg)</b>
1-6	Discarded	-
7	PC1	32.0
8-9	PC2	13.7
10-11	PC3	14.0
12	PC4	49.0
13-14	PC5	15.7
15-16	PC6	24.6
17	PC7	20.0
18-20	PC8	13.5





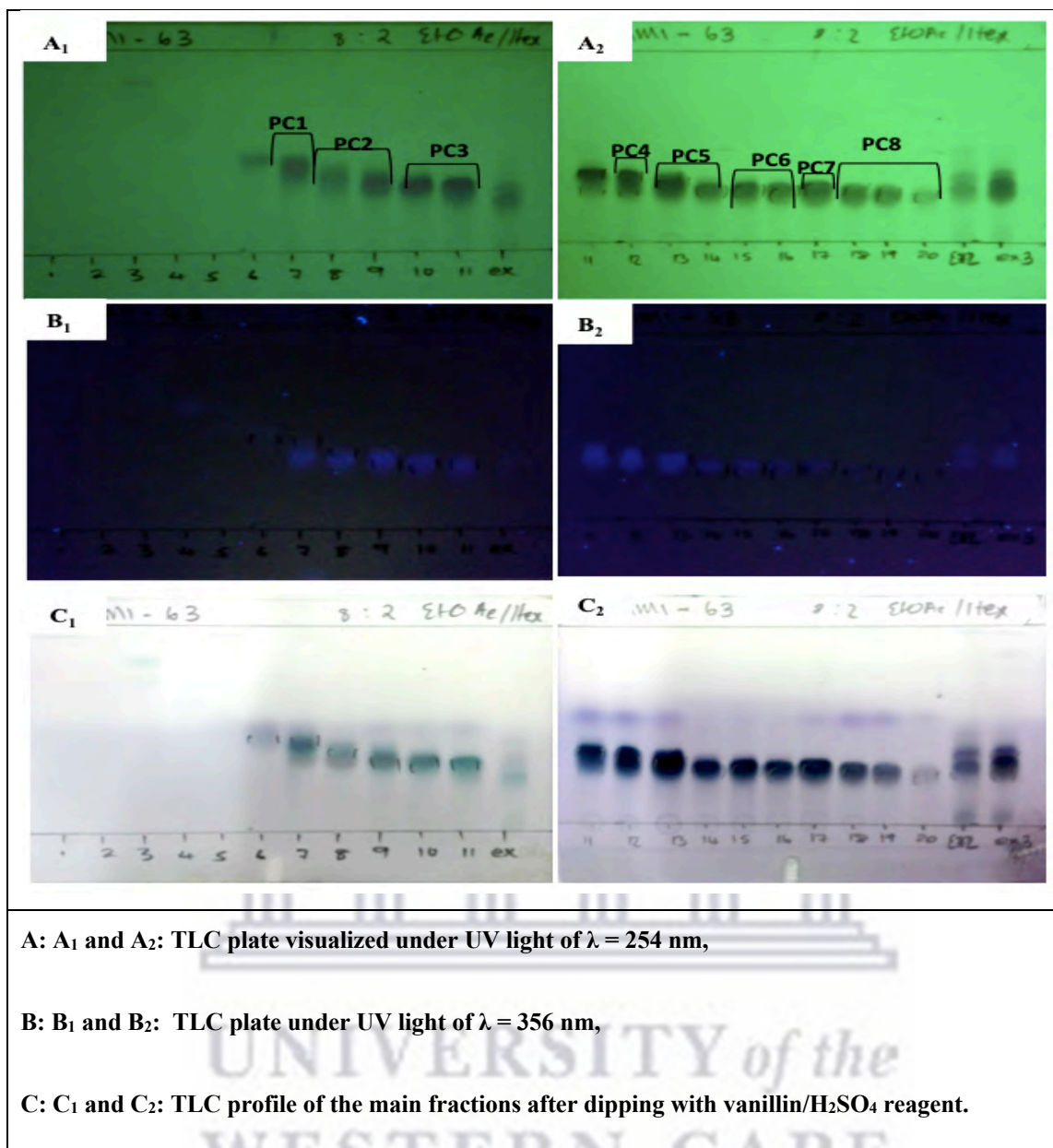


**Figure 21: TLC chromatograms of sub fractions obtained from gravity column chromatography fractionation of PB2 + PB3 + PB4. Plate developed using n-Hexane–ethyl acetate (8:2, v/v) solvent system.**

Fraction PC4 (mass = 49.0mg) when dry formed white sharp crystals in orange precipitate. To separate the white crystals, the MeOH was used to dissolve the orange precipitate, once dissolved, the yellow solution was removed using glass pipette leaving the white sharp crystals in a vial. Once dry, the orange precipitate weighed 37.5mg and the white crystals weighed 8.7mg. The two samples were subjected to NMR spectroscopy to determine content and purity of each sample. Thus, it was confirmed from the NMR spectrometer that the white crystals sample was a pure compound (**Compound 3**) and the orange precipitated was not pure.



#### 4.2.8. Isolation of compound 4: Using the gravity column chromatography and HPLC

A dried PA7 (mass= 669.4 mg) was subjected to gradient silica gel column and eluted using Hex: A mixture. Where A is DCM-MeOH (99:1, v/v). The solvent system is shown in Table 12. Similar fractions were combined together to give the sub-fractions PD1 – PD5.

**Table 12: Solvent system used in the fractionation process fraction PA7.**

Solvent Volume	Solvent System
	(Where A is DCM-MeOH 99:1,v/v)
0.1 L	Hexane
0.3 L	Hexane : A 4:6
0.4 L	Hexane : A 7:3
0.7 L	Hexane : A 8:2
0.7 L	Hexane : A 9:1
0.5 L	A

**Table 13: Collective sub-fractions from the fractionation process of PA7.**

Combined fractions	Code	Mass (mg)
1-12	Discarded	-
13-16	PD1	99.6
17-19	PD2	96.0
20	PD3	36.0
21-24	PD4	23.1
24-34	PD5	20.8

Fraction PD1 (mass = 99.6 mg) from silica gel chromatography was dissolved in 5mL DMSO. To determine the optimal purifications conditions, 10µL of sample was injected into the HPLC. High Performance Liquid Chromatography (HPLC) analysis were performed on a HPLC ‘1200 series’ purchased from Agilent Technologies (California, United States of America) equipped with a variable wavelength UV/Vis detector, manual injector, quaternary pump (G1311A),

vacuum degasser (G1322A), column compartment (G1316A), (Shimadzu Corporation, Japan), and reverse phase C<sub>18</sub> column SUPELCO (25 cm x 10 mm, 5µm). The flow rate employed was 1.500mL/min. The total run time was 60 min. The peak at 25min (Figure 3.6.3) was collected and gave **Compound 4 (mass = 23.3mg)**.

**Table 14: The gradient mobile phase A: DIW, and mobile phase B: MeOH during profiling of fractions. The run time was 60min.**

Time (min)	Mobile phase B (MeOH)	Column	Flow rate (mL/min)	Detector
0.01	80	C <sub>18</sub> column	1.5	UV at:
40	80	SUPELCO (25 x 2.1 cm, 5µm)		Black = λ <sub>210</sub>
45	100			Pink = λ <sub>254</sub>
50	80			Blue = λ <sub>345</sub>
60	Stop			

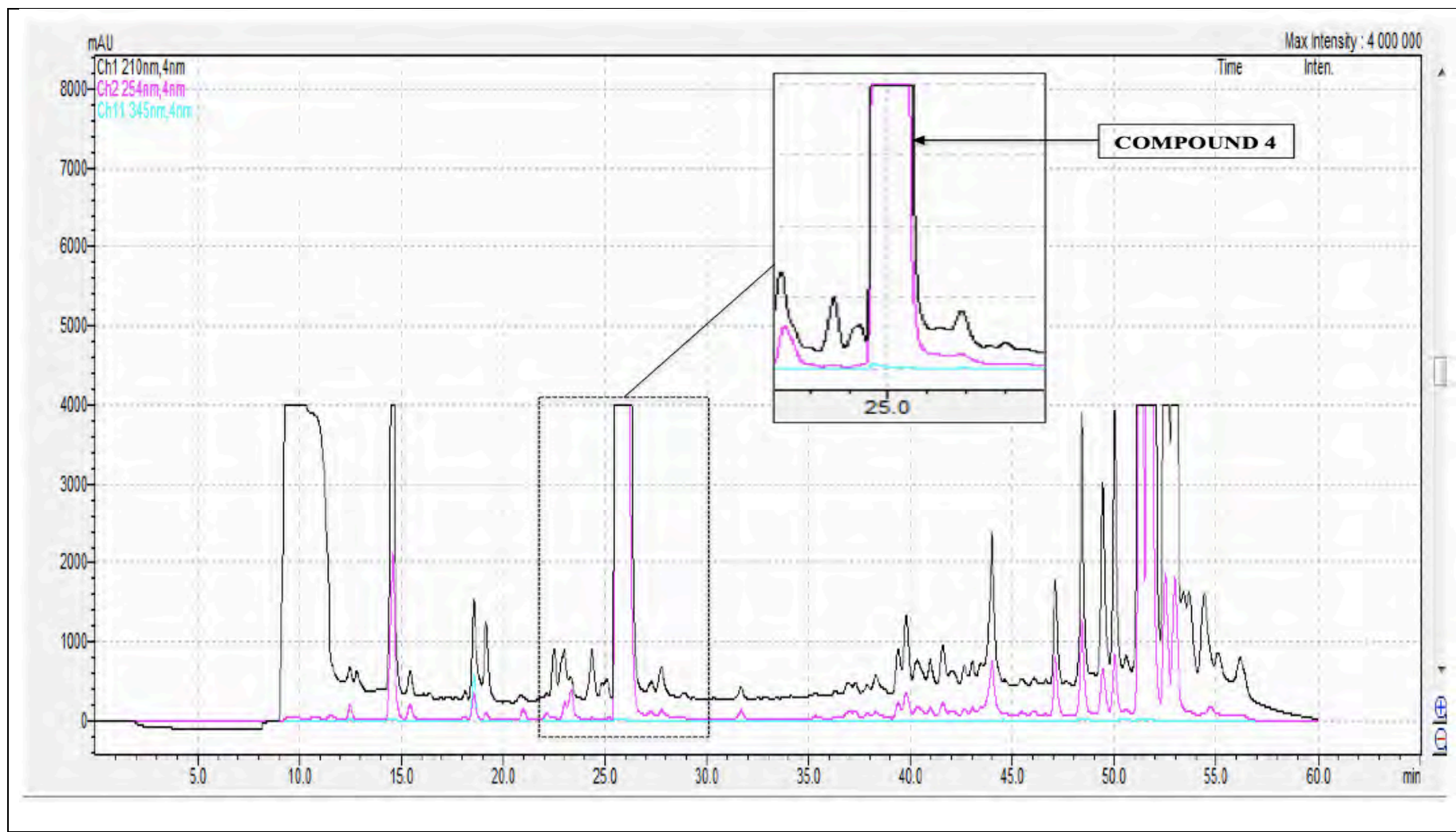
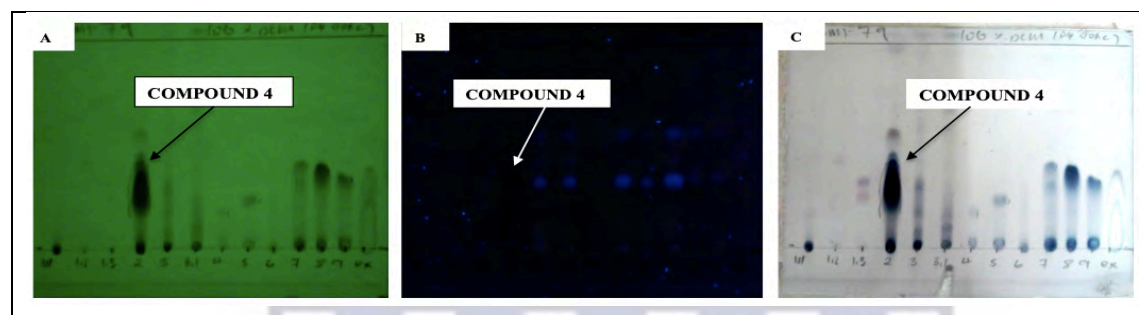


Figure 22: HPLC chromatograph fraction PAM1-71-1, with Compound 4 at 25min.

**Table 15: HPLC conditions for the isolation of Compound 4 conditions\*.**

Compound	Column	Gradient	Flow rate (mL/min)	Detector	Mass
Compound 4	C <sub>18</sub> column SUPELCO (25 x 2.1 cm, 5µm)	MeOH-DIW 85:15(v/v) to 100% MeOH in 40 minutes	1.5	UV at: Black = λ <sub>210</sub> Pink = λ <sub>254</sub> Blue = λ <sub>345</sub>	23.3mg



**Figure 23: Figure 0:12: TLC chromatograms of sub fractions obtained from gravity column chromatography fractionation of PA5 + PA6. Plate developed using MeOH: DCM (4:6, v/v) solvent system.**

The isolated compounds were subjected to spectroscopic techniques, which included NMR, sometimes FTIR, UV, and MS.

UNIVERSITY of the  
WESTERN CAPE

### **4.3. Spectroscopic techniques**

#### **4.3.1. NMR spectrometry**

NMR spectra were recorded at 25°C on a Bruker Avance III HD 400 MHz NMR spectrometer (Bruker Avance, Germany) that uses a 5mm BBO probe, based at the Department of Chemistry, University of the Western Cape, South Africa.

For NMR analysis, deuterated chloroform (CD<sub>3</sub>OD, 99.9% purity) was used to prepare samples as a solvent. For <sup>1</sup>H and <sup>13</sup>C NMR analysis, tetramethylsilane (TMS) solution was used as internal standard and the coupling constants (J) are reported in Hz. The <sup>1</sup>H shift (multiplicity) and <sup>13</sup>C shift (multiplicity) for chloroform were 7.24 and 77.0 ppm respectively. Standard 1D and 2D NMR pulse sequences were used to obtain 1D and 2D data respectively.

#### **4.3.2. Infrared (IR) Spectrometry**

Attenuated total internal reflectance (ATR) FTIR characterization was performed on a PerkinElmer (FT-IR Spectrometer), Model: SPECTRUM TWO. Spectra recording were accomplished using the interface “Spectrum”.

#### **4.3.3. UV Spectrometry**

Ultraviolet–visible spectroscopy (Uv-vis) analysis was performed on a NICOLET EVOLUTION 100 instrument. The VISIONpro software was used for recording the spectra.

#### **4.3.4. Mass Spectrometry**

LC-MS spectra were recorded using a Waters Synapt G2 instrument, ESI probe, ESI probe, ESI Pos and Cone Voltage 15 V. Analysis of the compound isolated was performed at the Central Analytical Facilities, Stellenbosch University, South Africa.



4.3.1. A summary of the Isolation and purification of constituents from *Psoralea aphylla*

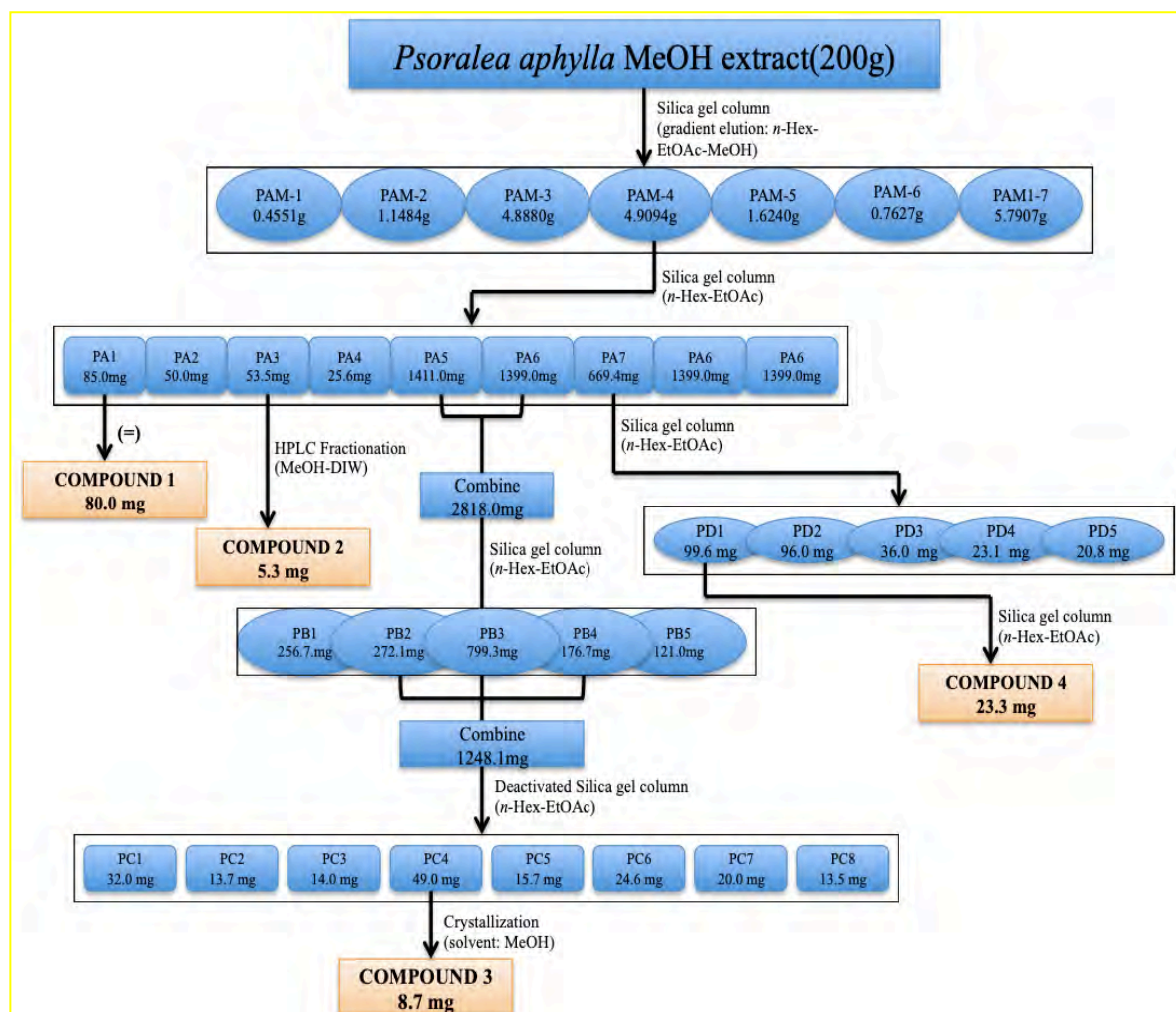


Figure 24: Experimental procedure of the isolation and purification of constituents from *Psoralea aphylla*.

## Part B

We assumed since the structure of compounds C1, C2, and C3 had OH functional groups just like kojic acid, they would also have an inhibition effect on tyrosinase.

### 4.4. The tyrosinase inhibition assay

The assay was performed using a method described by (Papoola *et al.*, 2015) with slight modifications. The extract and isolated compounds were dissolved in DMSO to a final concentration of 1 mg/mL(w/v) for isolated compounds. These fractions were further diluted with 50mM PBS (pH 6.5) to obtain working solution of 25 and 50 µg/mL. From each sample (at each concentration) 70 µL of each sample was eluted to different sample microtubes on a 96-well plate. Kojic acid (KA) was used as a positive control. For all the samples (including the KA), 30µl of the prepared mushroom tyrosinase enzyme (500 Units/mL in PBS) were then aliquoted into each well in triplicate. The plate was incubated for 5 min at room temperature. After the incubation, 110 µl the L-tyrosine (2mM) substrate was added to the wells and the plate was further incubated in a dark place at room temperature for 30 min.

The tyrosinase activity was determined by measuring the absorbance at 465nm using the MULTISKAN SPECTRUM plate reader.

The tyrosinase inhibition percentage was determined using the following equation:

$$\text{Inhibition \%} = \frac{(A - B)}{A} \times 100\%$$

#### Equation 2: Percentage of tyrosinase inhibition.

Where *A* is control inhibition difference and *B* is the sample or positive control inhibition difference. *A* is the difference between the absorbance of the control with the enzyme and the absorbance of the control without the enzyme, *B* is the difference between the absorbance of the test sample with the enzyme and the absorbance of the test samples without the enzyme.

### 4.5. Electrochemical Tyrosinase Biosensors

Electrochemical experiments were carried out with a PalmSens Ptrace work station and some were carried out using a BAS100W integrated and automated chemical work station purchased from Bio Analytical Systems (Lafayette, USA). A 10 mL electrochemical cell was used with a conventional three electrode configuration consisting of: (1) a glassy carbon electrode (GCE),

(2) Pt wire counter electrode and Ag/AgCl (3M NaCl salt bridge) as a reference electrode , all purchased from Sigma Aldrich (Cape Town, South Africa).

All experimental solutions were purged using Argon gas for 10 min and carried out at a controlled room temperature of 25 °C.

In this study, in order to investigate the electrochemical properties of the *Psoralea aphylla* methanolic extract and of each compound with tyrosinase enzyme on a GCE electrode, it was important to first understand the electrochemistry of tyrosinase enzyme and L-tyrosine in PBS buffer. The tyrosinase inhibitory activity of kojic acid (KA) was evaluated to prove the accuracy of the method. The experiments were carried out at controlled room temperature of 25 °C.

The inhibition percentage (%) for each sample was calculated as follows:

$$\% \text{ Inhibition} = 1 - \left( \frac{A_{\text{sample}}}{A_{\text{standard}}} \right) \times 100\% \quad \text{Equation 3}$$

Where  $A_{\text{sample}}$  and  $A_{\text{Standard}}$  are the sensitivity values of the sample biosensor and standard biosensor. Tyrosinase inhibitory activities of isolated compounds were evaluated with the same method using the same mixture without KA as an inhibitor.

#### **4.5.1. Standard experiment: Cyclic voltammetry of Tyrosinase and L-tyrosine in PBS buffer**

A standard experiment to evaluate enzyme and substrate reaction was performed using cyclic voltammetry from a start potential of  $E = 1500 \text{ mV}$  to  $E = -1500 \text{ mV}$  at a scan rate of  $50 \text{ mV/s}$ . The test solution was made out of  $5 \text{ mL}$  solution of  $50 \text{ mM}$  PBS buffer, to which was added  $350 \mu\text{L}$  of  $500$  units tyrosinase enzyme. The substrate, L- tyrosinase was added in increments of  $50 \mu\text{L}$  which correspond to  $0.02 \text{ mM}$  in final solution. This experiment gives an idea of how L-tyrosinase behaves as a catalyst. In Figure 25 is a schematic presentation of how the standard procedure enzyme and substrate will be done.

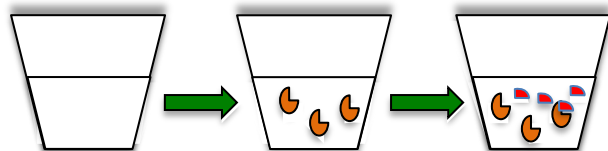


**Figure 25:** Schematic presentation of the standard tyrosinase enzyme and L-tyrosine substrate experiment where represents the tyrosinase enzyme and represents the substrate L- tyrosine.

#### 4.5.2. Cyclic voltammetry of Tyrosinase Kojic acid (KA) and L-tyrosine in PBS buffer.

Kojic acid (KA) is a well-known competitive tyrosinase inhibitor of tyrosinase in the presence of L-tyrosine substrate. In this study, an experiment was performed to evaluate the reaction between enzyme, KA and L-tyrosine at different concentrations in order to understand the inhibition effects of KA on tyrosinase enzyme. CV is used to demonstrate the changes of inhibition current of tyrosinase and KA at different concentration of L-tyrosine. Thus, testing how KA behaves as an inhibitor. The experiment was performed using cyclic voltammetry from a start potential of  $E = 1500 \text{ mV}$  to  $E = -1500 \text{ mV}$  at a scan rate of  $50 \text{ mV/s}$ . The test solution was made out of  $5 \text{ mL}$  solution of  $50 \text{ mM}$  PBS buffer, to which  $350 \text{ }\mu\text{L}$  of  $500 \text{ units}$  tyrosinase enzyme and  $350 \text{ }\mu\text{L}$  of  $7.04 \text{ mM}$  KA were added, respectively. For each run, L-tyrosine was added in increments of  $50 \text{ }\mu\text{L}$  which corresponds to  $0.02 \text{ mM}$  in final solution. Figure 26 shows a schematic presentation of how the procedure will be done. Since KA is a competitive inhibitor, it is expected to inhibit tyrosinase in the presence of L-tyrosine. The sensitivity of this experiment is expected to be less than of the standard procedure, due to the inhibition of tyrosinase by KA.

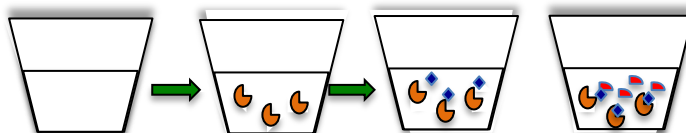


**Figure 26:** Schematic presentation of the tyrosinase enzyme, kojic acid and L- tyrosine substrate experiment where represents the tyrosinase enzyme, represents the tyrosinase inhibitor K and L- tyrosine.

### 4.5.3. Cyclic voltammetry of Tyrosinase and isolated compounds in PBS buffer

Three compounds were isolated from a Southern African plant called *Psoralea aphylla*. Cyclic voltammetry was applied to investigate the effect of the isolated compounds on tyrosinase. For each experiment, a clean and polished glassy carbon electrode was connected as a working electrode. The potentials were scanned from  $E = 1500$  mV to  $E = -1500$  mV at a scan rate of 50 mV/s. The test solution was made out of 5 mL solution of 50 mM PBS buffer, to which 350  $\mu$ L of 500 units tyrosinase enzyme was added. For each run, a compound was added in increments of 50  $\mu$ L, which corresponds to 0.20 mM for each compound.

Each compound will be expected to react with tyrosinase as catalysis or an inhibitor. If the current response increases with each incremented addition of compound that would imply the compound is catalysed by the a tyrosinase enzyme. However, if the current response shows a decrease in oxidation peak, then that would mean the compound is a potential tyrosinase inhibitor. The compounds will be compared to the response of tyrosinase to different concentrations of L- tyrosine without KA (Section 4.5.1) and the response of tyrosinase to L-tyrosine in the presence of KA (Section 4.5.2). If the compound is an inhibitor we expected decrease in oxidation peak at 0.8 V. For compounds that are catalysts, an increase in the oxidation peak at 0.8V.



UNIVERSITY of the  
WESTERN CAPE



## Part C

### 4.6. Cytotoxicity of Bakuchiol

Bakuchiol is a prenylated phenolic monoterpene commonly known to be isolated from the seed of *Psoralea corylifolia* belonging to the Leguminosae (Fabaceae) family (Bequette *et al.*, 2016). This compound is made up of styryl moiety in conjunction with a monoterpene. Literature indicates that bakuchiol [(1E,3S)-3-ethenyl-3,7-dimethyl-1,6-octadien-1-yl]phenol] has been commonly used in traditional Chinese and Indian folkloric medicine as a kidney-tonifying agent and for alleviation of asthma, osteoporosis and diarrhoea (Chen *et al.*, 2010; Park *et al.*, 2016). In Sri Lanka, bakuchiol is widely used in the treatment of vitiligo, by applying the oil to the affected areas and exposing those areas to sunlight (Mahendra *et al.*, 2012). Bakuchiol is also known to exhibit pharmacological activities, such as anti-oxidant, anti-inflammatory, hepatoprotective, antimicrobial, osteoblastic, anti-pregnancy and estrogenic (Li *et al.*, 2016; Cho *et al.*, 2011). Bakuchiol has been also demonstrated to have anti-tumour effect on lung cancer cells, reported to have cytotoxic effect towards breast cancer (Park *et al.*, 2016; Chen *et al.*, 2010; Majeed *et al.*, 2012). According to Chaudhuri and Bojanowski, bakuchiol is a retinol-like functional compound because it has a similar gene expression profile, even though there is no structural resemblance. In their study, Bakuchiol was formulated in a skin care product and a clinical study was done over a period of 12 weeks. The clinical study results showed an observed improvement in lines and wrinkles, pigmentation, firmness, elasticity and reduction in photo-damage (Chaunduri and Bokanowski, 2014). Compared to retinol, bakuchiol was found to have excellent photochemical and hydrolytic stability; easy to use in formulations because of its miscibility with a wide variety of emollients and solubilizes; because of its photostability it can be used during the day (Chaunduri and Bokanowski, 2014; Chaunduri, 2010; Chaudhuri and Marchio, 2011).

#### 4.6.1. MTT Cytotoxicity Assay

In this study we evaluate the cytotoxicity effects of bakuchiol isolated from a *Psoralea aphylla* methanolic extract on B16 melanoma cells to further evaluate the effect of bakuchiol on the pigmentation of skin.

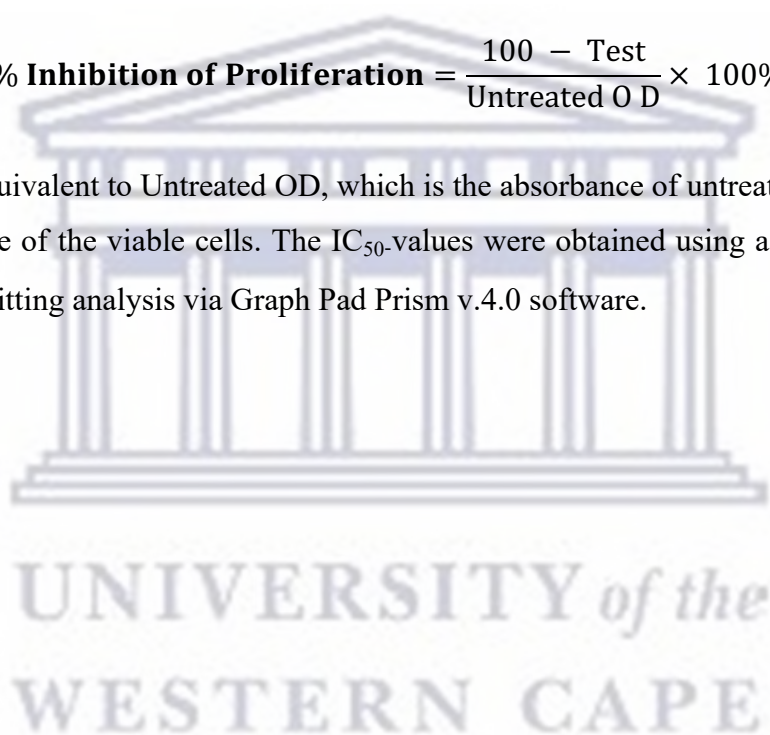
The cytotoxicity effect of bakuchiol on the melanoma cells was done using the MTT colorimetric assay. The cells were seeded at density of  $6 \times 10^4$  cells per well in a 96-well plate

and incubated in a humidified atmosphere of 37 °C and 5% CO<sub>2</sub> a for 24 hr. The growth medium was then removed and the cells was then treated with different concentrations (1.56 µg/mL - 100 µg/mL) of bakuchiol for 48 hrs. Negative controls cells were treated with fresh growth medium and 6 % DMSO was used as positive control. To measure the viability of the cells, 10 µL of MTT (5 mg/ml in PBS) was added to the treated cells and the plate was incubated for another 3 hr. MTT was carefully and DMSO was then added to dissolve the insoluble formazan and its absorbance at 570 nm was measured using POLARstar Omega microplate reader.

The percentage inhibition of cell growth was calculated using the formula below:

$$\% \text{ Inhibition of Proliferation} = \frac{100 - \text{Test}}{\text{Untreated O D}} \times 100\%$$

Where 100 is equivalent to Untreated OD, which is the absorbance of untreated cells and Test is the absorbance of the viable cells. The IC<sub>50</sub>-values were obtained using a non-linear dose-response curve fitting analysis via Graph Pad Prism v.4.0 software.



---

# CHAPTER 5:

## Results and Discussion

---

*This chapter presents the results and discussion of identification and characterization of the isolated compounds by analysis of physical, chemical and spectral characteristics; and possible identification of tyrosinase inhibitors using an ELISA assay and cyclic voltammetry. The spectroscopic techniques were used to elucidate the structure of isolated compounds, this included NMR, FTIR, UV and MS.*

### 5.1. Structural elucidation and characterization of the compounds

#### 5.1.1. Structural elucidation of Bakuchiol

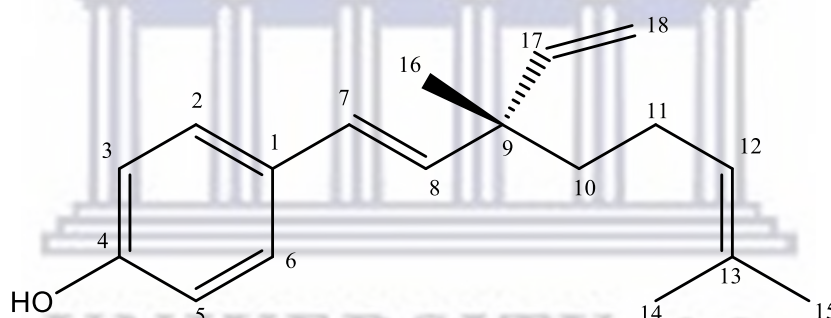


**Figure 27: Proposed structure of Compound 1.**

#### a) NMR analysis of bakuchiol

The  $^1\text{H}$  NMR spectrum (Figure 28) showed two aromatic signals at  $\delta$  7.22 (*d*,  $J= 8.50$  Hz, H-2,H-6) and  $\delta$  6.75 (*d*,  $J= 8.52$  Hz, H-3,H-5) which indicated 1,4- *para*-substituted aromatic ring; the presence of a *trans* double bond (C-7 - C-8) is supported by the two doublets at  $\delta$  6.24 (*d*,  $J=16.25$  Hz,H-7) and  $\delta$  6.04. (*d*,  $J=16.24$  Hz, H-8). The vinylic olefinic proton at C-12 was indicated by doublet of doublets at  $\delta$  5.89 (*dd*,  $J=17.41$  Hz, 10.77 Hz, H-17) and two doublets at  $\delta$  5.02 (*d*,  $J=17.41$  Hz, H-18a) and at  $\delta$  5.05 (*d*,  $J=10.77$  Hz, H-18b). Two methylenes at  $\delta$  1.95 (*m*, H-11) and  $\delta$  1.49 (*m*, H-10), and three intense singlets each integrating to three

hydrogens each at  $\delta$  1.59 (s, H-15) and  $\delta$  1.69 (s, H-14) can be assigned to geminal dimethyl group while the other singlet at  $\delta$  1.20 (s, H-16) can be assigned to tertiary methyl group.

$^{13}\text{C}$  NMR spectrum (Figure 29) showed sixteen peaks corresponding to 18 carbons. DEPT-135 NMR spectrum (Figure 29) revealed four quaternary carbons at  $\delta_{\text{c}}$  154.6, 131.2, 130.9 and 42.4 ppm, six methine carbon signals at  $\delta_{\text{c}}$  145.9, 135.8, 127.3 (two carbons), 126.4, 115.3 (two carbons) ppm; three methylene carbons at  $\delta_{\text{c}}$  111.7, 41.2 and 23.1 and three methyl carbons at  $\delta_{\text{c}}$  25.6, 23.3 and 17.5 ppm.



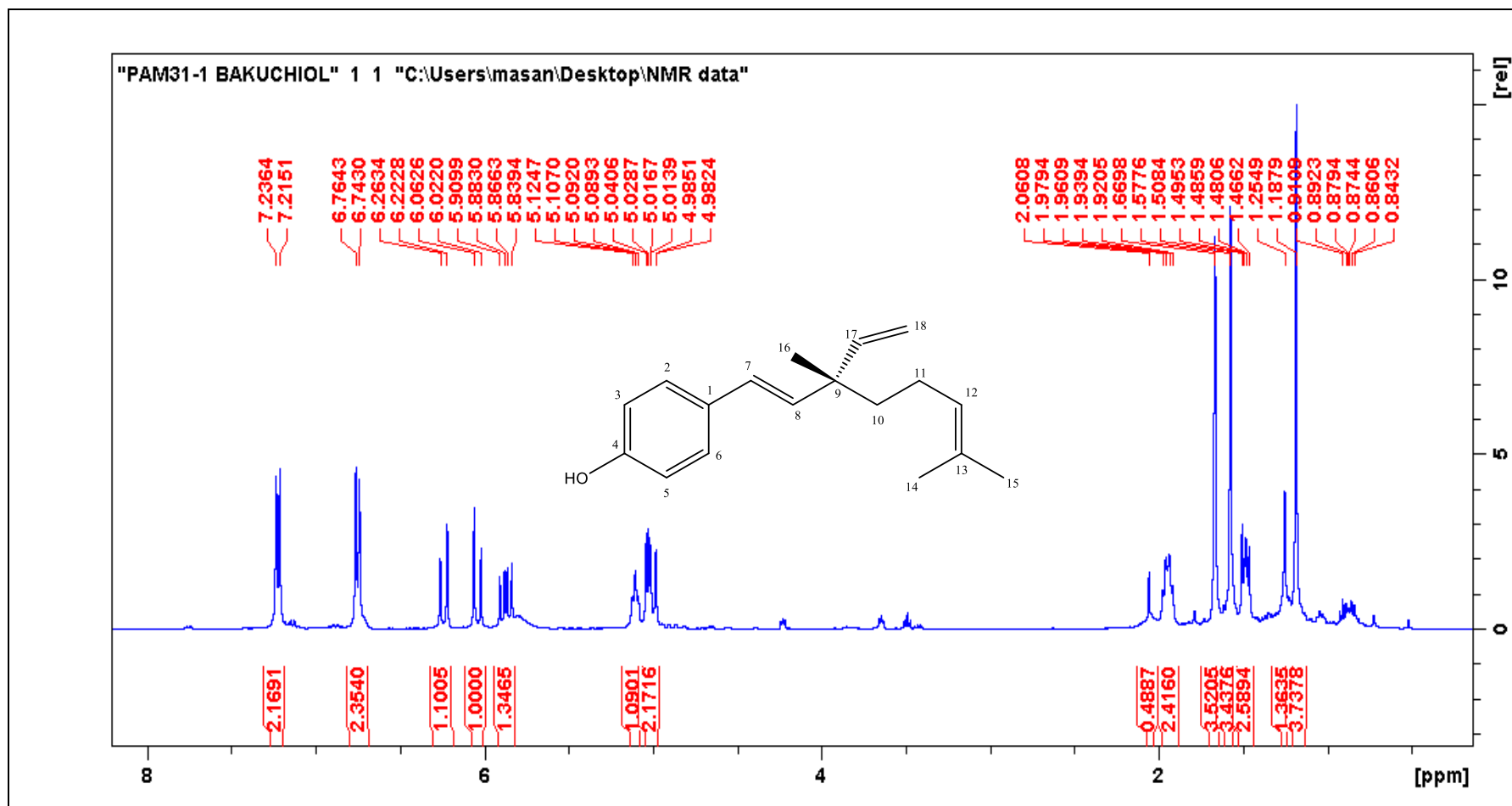


Figure 28: <sup>1</sup>H NMR (400 MHz, CDCl<sub>3</sub>) spectrum of Compound 1.





Inspection of  $^1\text{H}$ - $^1\text{H}$  COSY (Figure 30) was observed between the two aromatic doublets H-2, H-6 and H-3, H-5 which also confirmed the presence of a *para*-substituted benzene ring. The doublet of doublet appearing at  $\delta$  5.88 ppm (H-17) also showed a  $^1\text{H}$ - $^1\text{H}$  correlation to the doublets at  $\delta$  5.03 ppm (H-18a) and  $\delta$  4.92 ppm (H-18b).  $^1\text{H}$ - $^1\text{H}$  COSY spectrum revealed a connection between doublet appearing at  $\delta$  6.24 ppm (H-7) and the doublet at  $\delta$  6.24 ppm (H-8). Another  $^1\text{H}$ - $^1\text{H}$  correlation between  $\delta$  5.10 ppm (assigned as H-12) and a multiplet at  $\delta$  1.95 ppm which was already assigned as H-11; and two methyl proton singlets at  $\delta$  1.56 ppm (already assigned as H-15) and  $\delta$  1.67 ppm (already assigned as H-14).



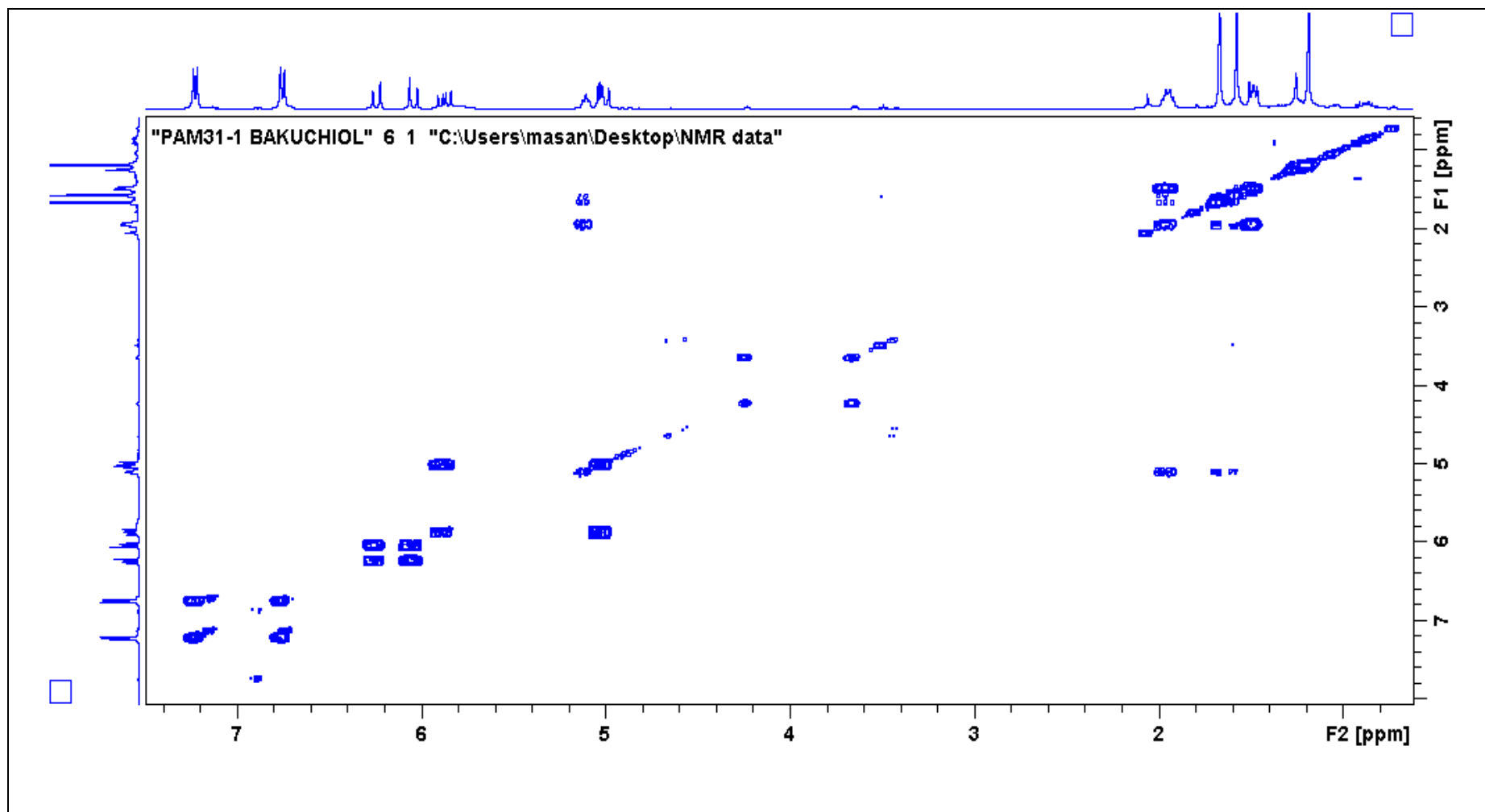
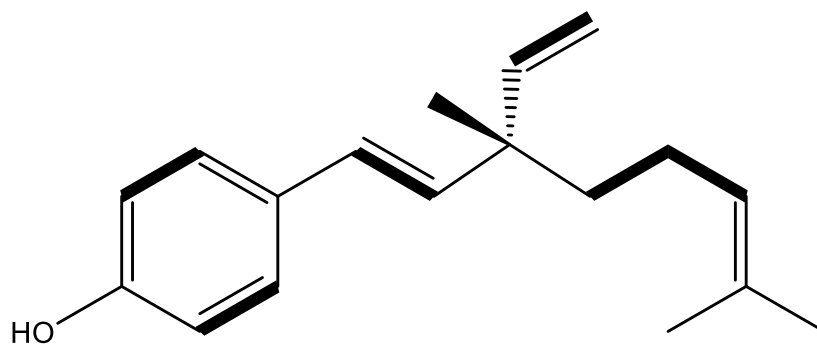
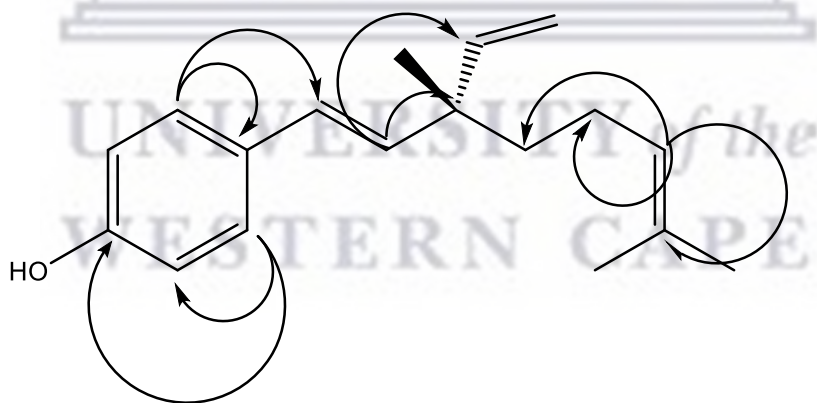


Figure 30:  $^1\text{H}$ - $^1\text{H}$  COSY (400 MHz,  $\text{CDCl}_3$ ) spectrum of Compound 1.



**Figure 31: Figure 29: Important  $^1\text{H}$ - $^1\text{H}$  correlations represented by —.**

The correlations of the HSQC spectrum allows interpretation of the  $^1\text{H}$ - $^{13}\text{C}$ . The HMBC spectrum (Figure 30) was used to further confirm the structure of Compound 1. The following correlations were observed: H-2 to C-3, C-4 and C-5 and the same correlations were observed for H-6 to the same carbons suggesting that H-2 and H-6 are two equivalent protons. Similar pattern was observed for H-3 to C-1, C-2 and C-4, which also suggested that H-3 and H-5 are two equivalent aromatic protons. Other correlations observed include H-7 to C-1, C-2/6, C-8 and C-9 confirming its close proximity to the benzene ring and H-8 to C-1, C-7, C-9, C-10, C-16 and C-17 which also assisted in establishing the assignment of C-10 ( $\delta_c$  41,37 ppm) and C-11 ( $\delta_c$  23.2 ppm).



**Figure 32: Important HMBC correlations of Compound 1.**

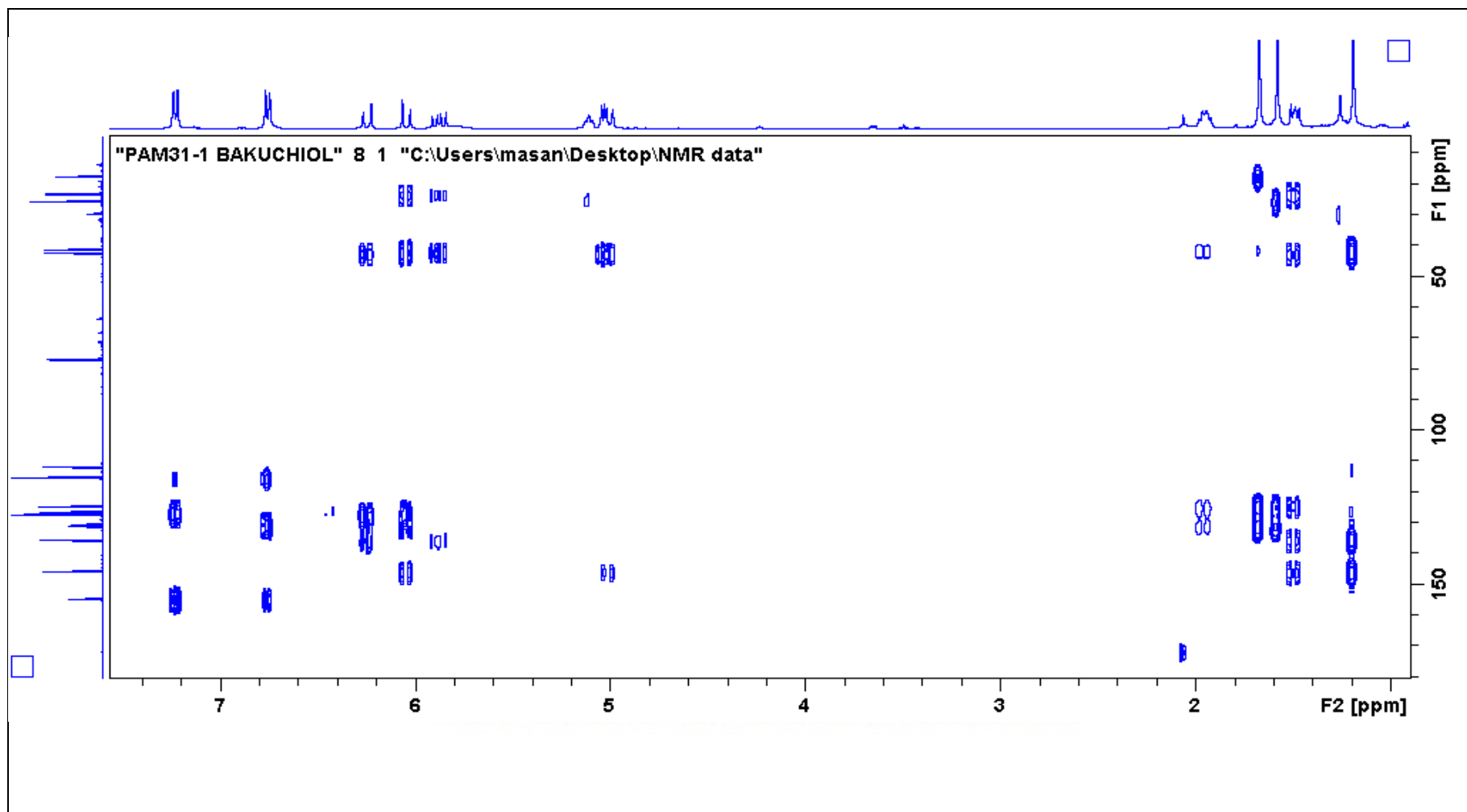


Figure 33: HMBC (400 MHz, CDCl<sub>3</sub>) spectrum of Compound 1.



From the HMBC spectrum (Figure 33) correlation the structure of this compound was fully established. The structure was confirmed by comparing the data with those published in literature (Hsu *et al.*, 2009; Labbe *et al.*, 1996).

**Table 16:  $^1\text{H}$  [400 MHz: m, J(Hz)] and  $^{13}\text{C}$  (100 MHz) NMR spectral data of Compound 1. Where \* presents quaternary carbons.**

Position	$^{13}\text{C}$ (ppm)	$^1\text{H}$ (ppm)
1*	130.9	-
2	127.3	7.22 (d, 8.5 Hz)
3	115.5	6.75 (d, 8.5 Hz)
4*	154.6	-
5	115.4	6.75 (d, 8.6 Hz)
6	127.3	7.22 (d, 8.5 Hz)
7	135.7	6.24 (d, 16.2 Hz)
8	126.4	6.04 (d, 16.2 Hz)
9*	42.4	-
10	41.3	1.95 (m)
11	23.2	1.95 (m)
12	124.8	5.10 (bt)
13*	131.2	-
14	17.5	1.61 (s)
15	25.7	1.59 (s)
16	23.3	1.20 (s)
17	146.9	5.89 (dd, 17.41 Hz)
18a	111.7	5.02 (bt)
18b	111.7	5.05 (d, 10.8 Hz)

The above data confirmed the structure of Compound 1 to be 4-(3,7-dimethyl-3-vinyl-octa-1,6-dienyl) phenol, common name Bakuchiol. Bakuchiol has also been reported to possess a variety of other activities such as antimutagenic, anti-inflammatory, insect juvenile hormone,

anti-helmenthic, and cytotoxic activities (Haraguchi, H., 2002; Katsura, H. *et al.*, 2001; Bapat, K. *et al.*, 2005).

**b) FTIR analysis of bakuchiol.**

The ATR-FTIR spectra (Figure 34) were recorded over the range of 4000  $\text{cm}^{-1}$  to 400  $\text{cm}^{-1}$ . The prominent peaks are described in Table 15. The broad peak at 3302  $\text{cm}^{-1}$  represents the OH stretch attached to the benzene ring. The peaks at 1603 and 1514  $\text{cm}^{-1}$  can be attributed to the C=C aromatic stretch and the peak 1376  $\text{cm}^{-1}$  represent the alkene stretch. The results were compared to literature (Labbé *et al.*, 1996).

**Table 17: FT-IR analysis data interpretation of bakuchiol (compound 1).**

Experiment frequency ( $\text{cm}^{-1}$ )	Intensity	Assignment
3302	B, M	-OH stretch
3082	W	C-H stretch (Aromatic)
2917 and 2845	N,S	C-H stretching in $\text{CH}_2$ and $\text{CH}_3$
1605 and 1514	N, M	C=C stretch (Aromatic)
1462	N, M	$\text{CH}_2$ bending (methylene group)
1376	N, M	C=C stretch
1236	N, M	C-O stretch
971	N, M	C=C stretch

Key words: S=strong, N=narrow, B= broad, M= medium, W = weak.

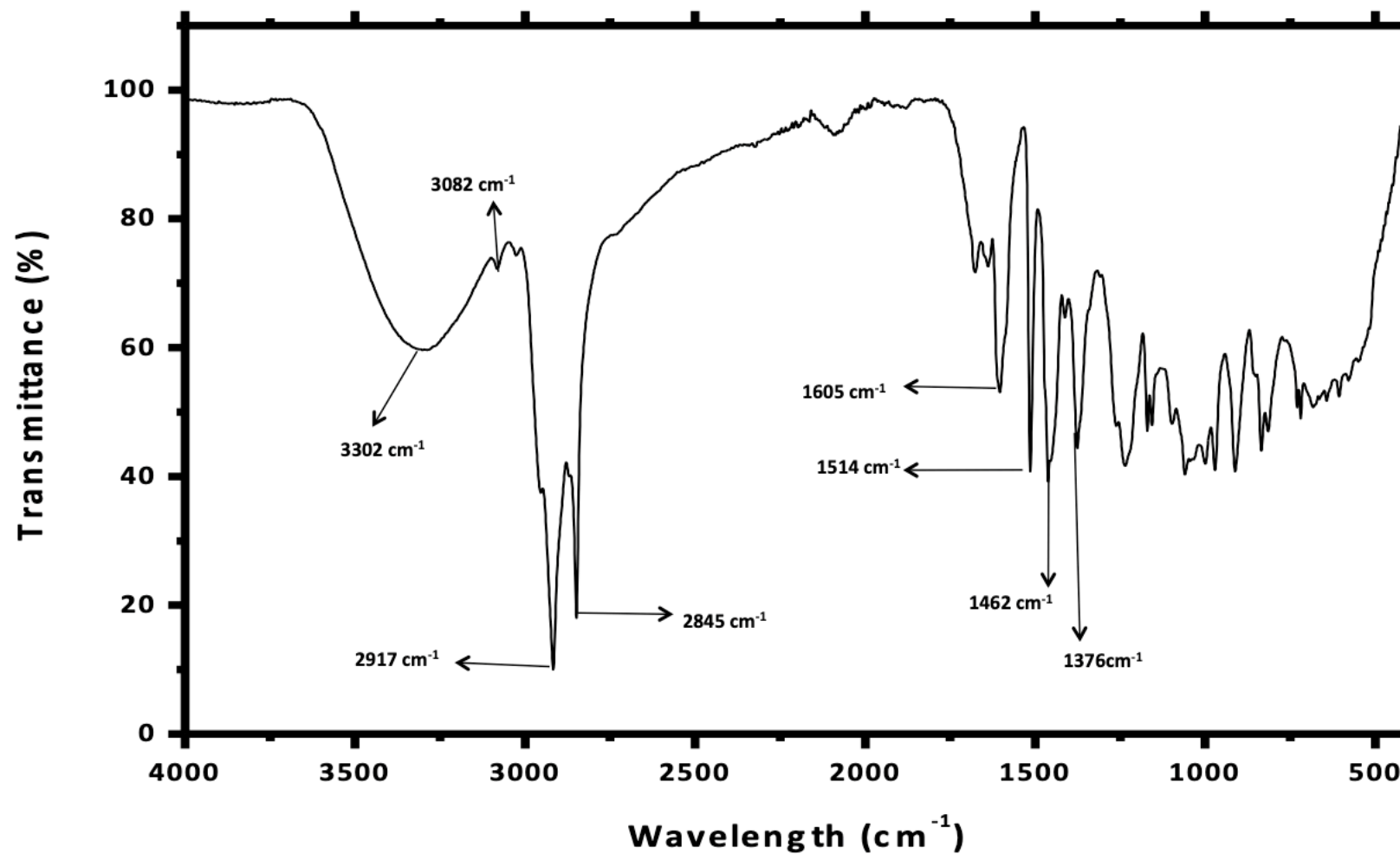
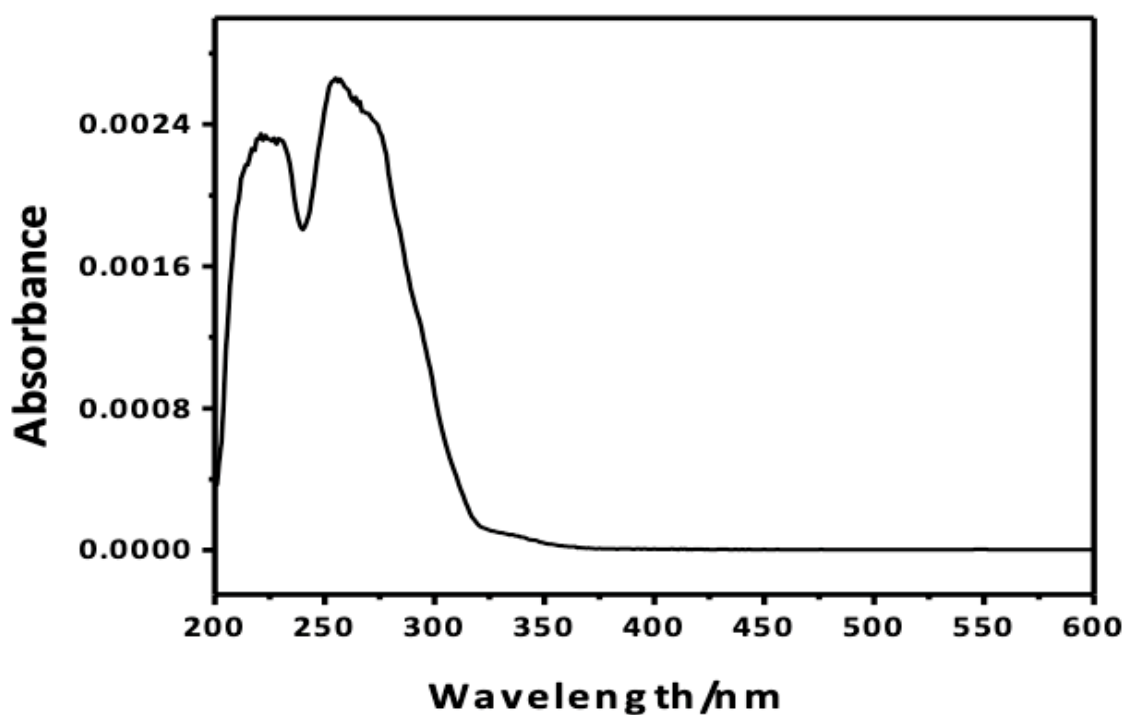


Figure 34: FTIR spectrum of bakuchiol, Compound 1.

**c) UV analysis of Bakuchiol**

Ultraviolet (UV) spectra were recorded using a NICOLET EVOLUTION 100 instrument, and methanol was used as solvent and a quartz cuvette was used. Bakuchiol has maximum absorption at 275nm in its UV spectrum.



**Figure 35: UV spectrum of bakuchiol.**

### 5.1.2. Structural elucidation and characterization of 12,13-Dihydro-12,13-epoxybakuchiol

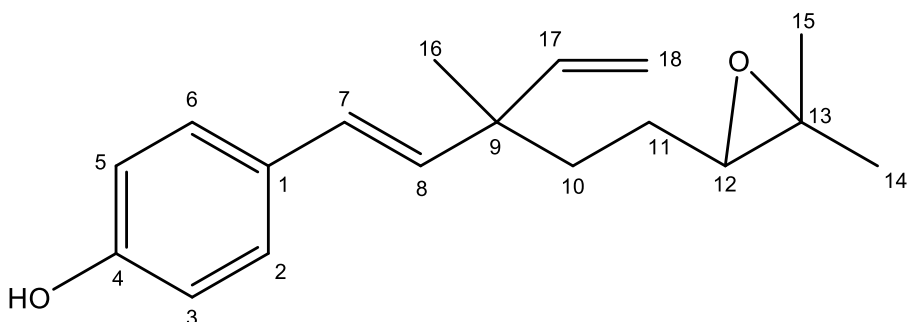


**Figure 36: Proposed structure of Compound 2.**

#### a) NMR analysis of 12,13-dihydro 12,13-epoxybakuchiol

The NMR spectroscopic data of Compound 2 showed a similar spectrum to those of Compound 1 (Bakuchiol), the differences are expressed below.

$^1\text{H}$  NMR data of compound 2 (Figure 37) were quite similar to those of Bakuchiol except for the main differences being signal  $\delta$  2, 71 (bt, 1H), attributed to H-12 methine attached to the secondary carbon of the oxirane ring (as shown in Figure 38). The two singlets at  $\delta$  1.32 (s, Me-15) and  $\delta$  1.26 (s, Me-14) assigned to the methyl groups had a larger chemical shift as compared to of bakuchiol because of the electron withdrawing epoxide ring.

UNIVERSITY of the  
WESTERN CAPE



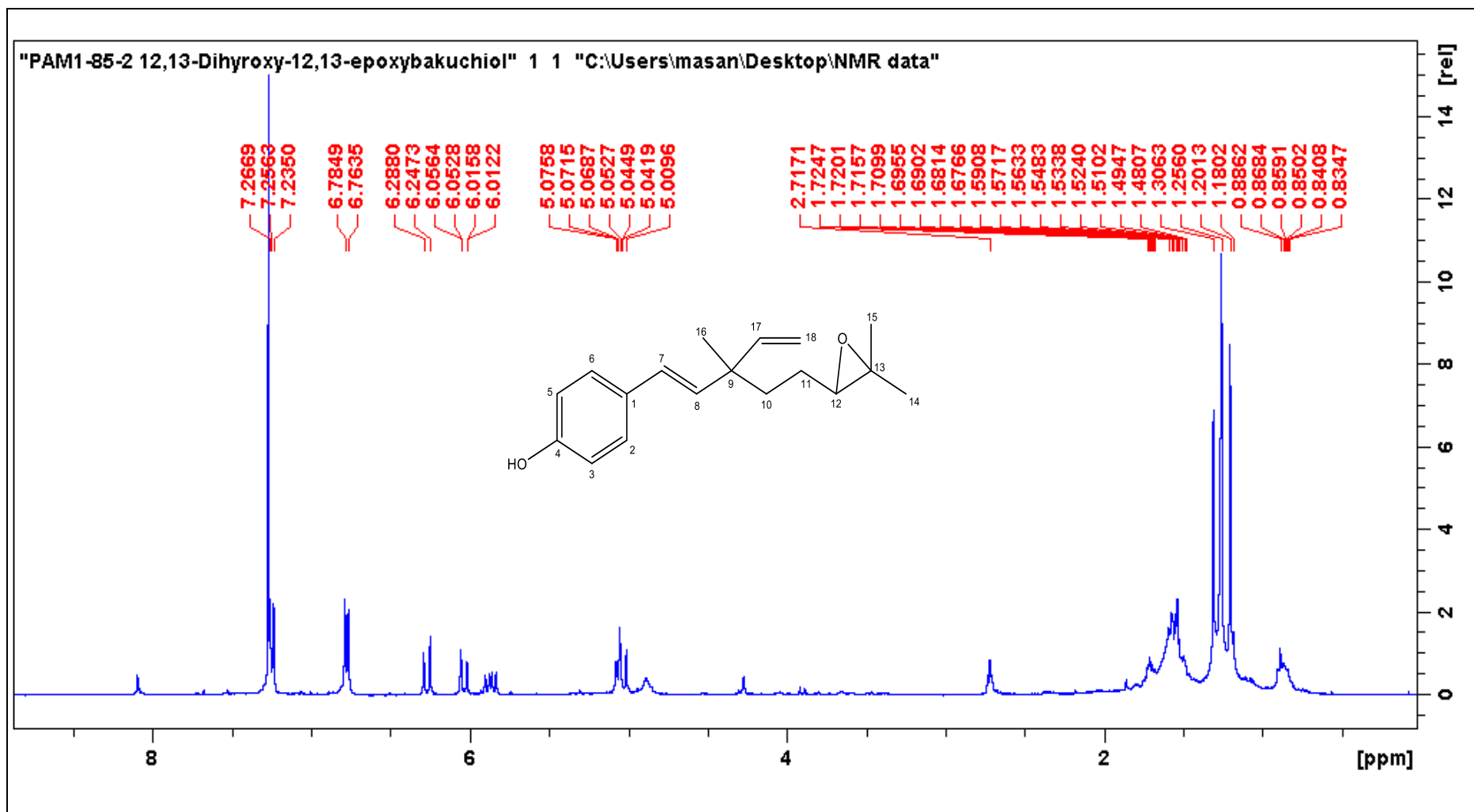


Figure 37: <sup>1</sup>H NMR (400 MHz, CDCl<sub>3</sub>) spectrum of Compound 2.

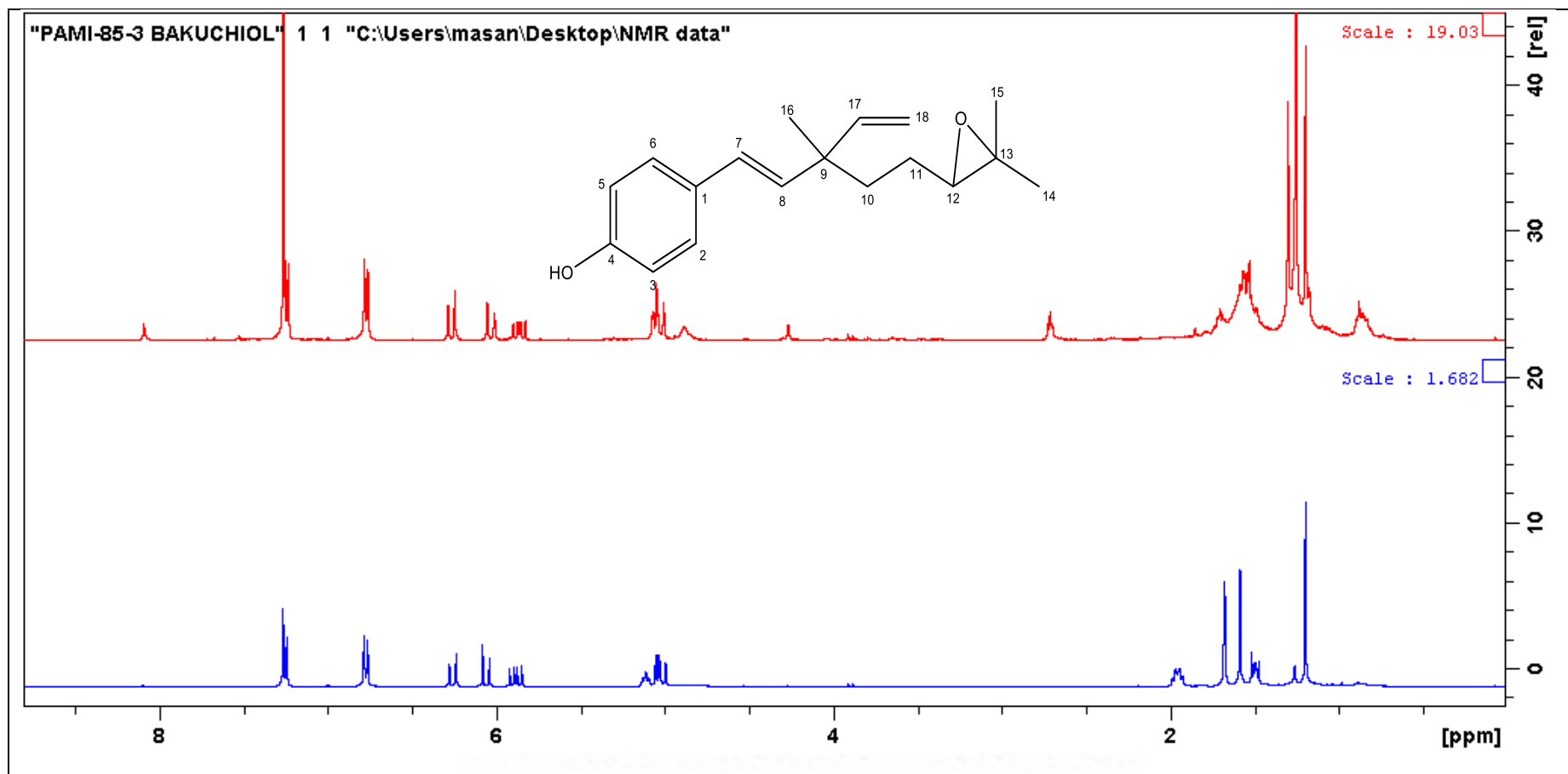


Figure 38:  $^1\text{H}$  NMR (400MHz,  $\text{CDCl}_3$ ) spectrum of both Compound 2 and Bakuchiol;. Top: Compound 2, Bottom: Bakuchiol.

$^{13}\text{C}$  NMR spectrum (Figure 39) shown sixteen peaks which corresponded to 18 carbons. The spectrum revealed a doublet at  $\delta_{\text{c}}$  65.0 ppm and  $\delta_{\text{c}}$  58.6 ppm indicating a presence of a trisubstituted epoxide ring assigned to C-12 and C-13, respectively. In addition, the DEPT 135 NMR spectrum ( as shown Figure 41) revealed four quaternary carbons at  $\delta_{\text{c}}$  154.8, 130.6 , 58.6 and 42.2 ppm and confirmed C-13 to be quaternary carbon of the oxirene ring.



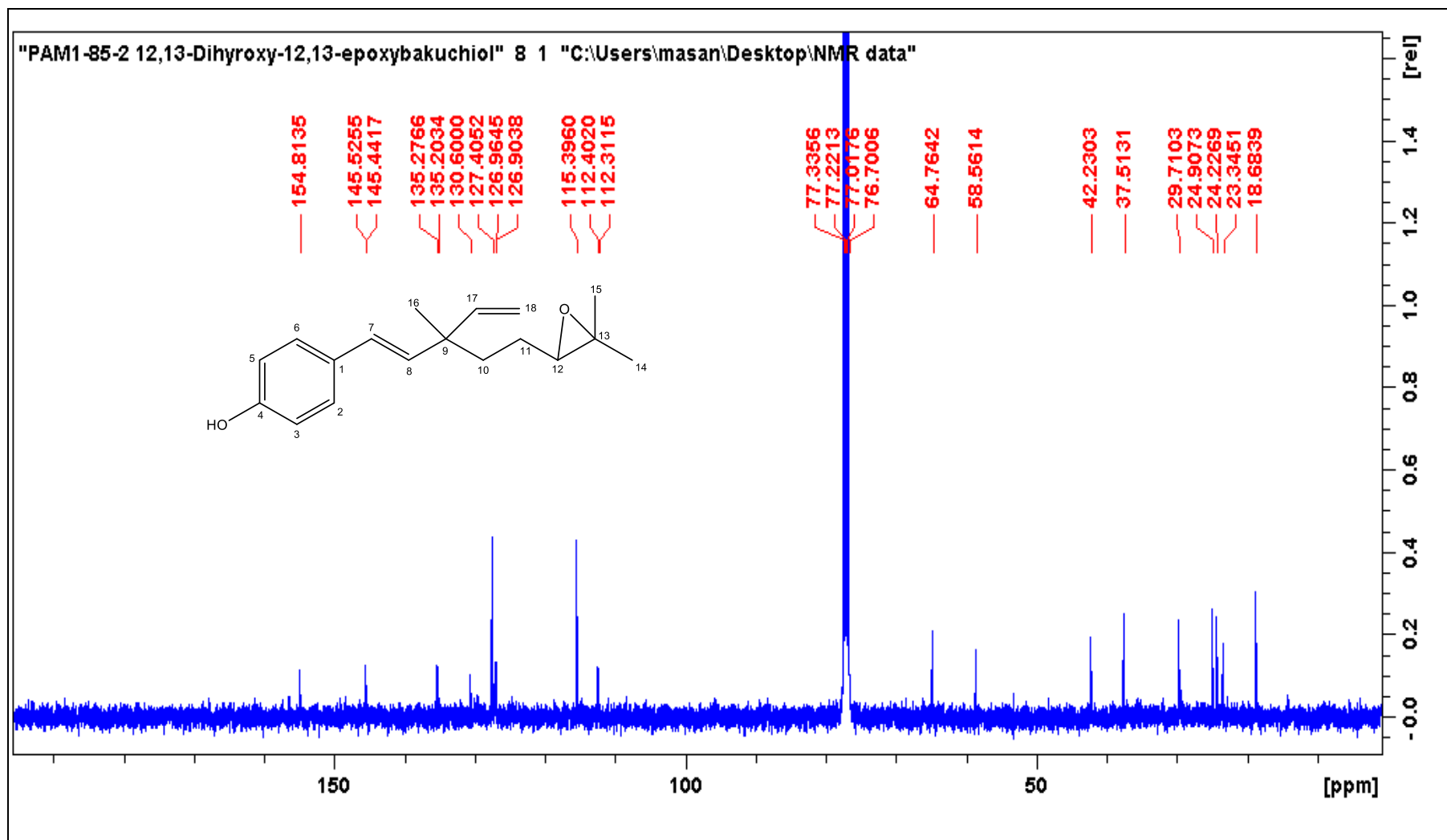


Figure 39:  $^{13}\text{C}$  NMR (400MHz,  $\text{CDCl}_3$ ) spectrum of Compound 2.

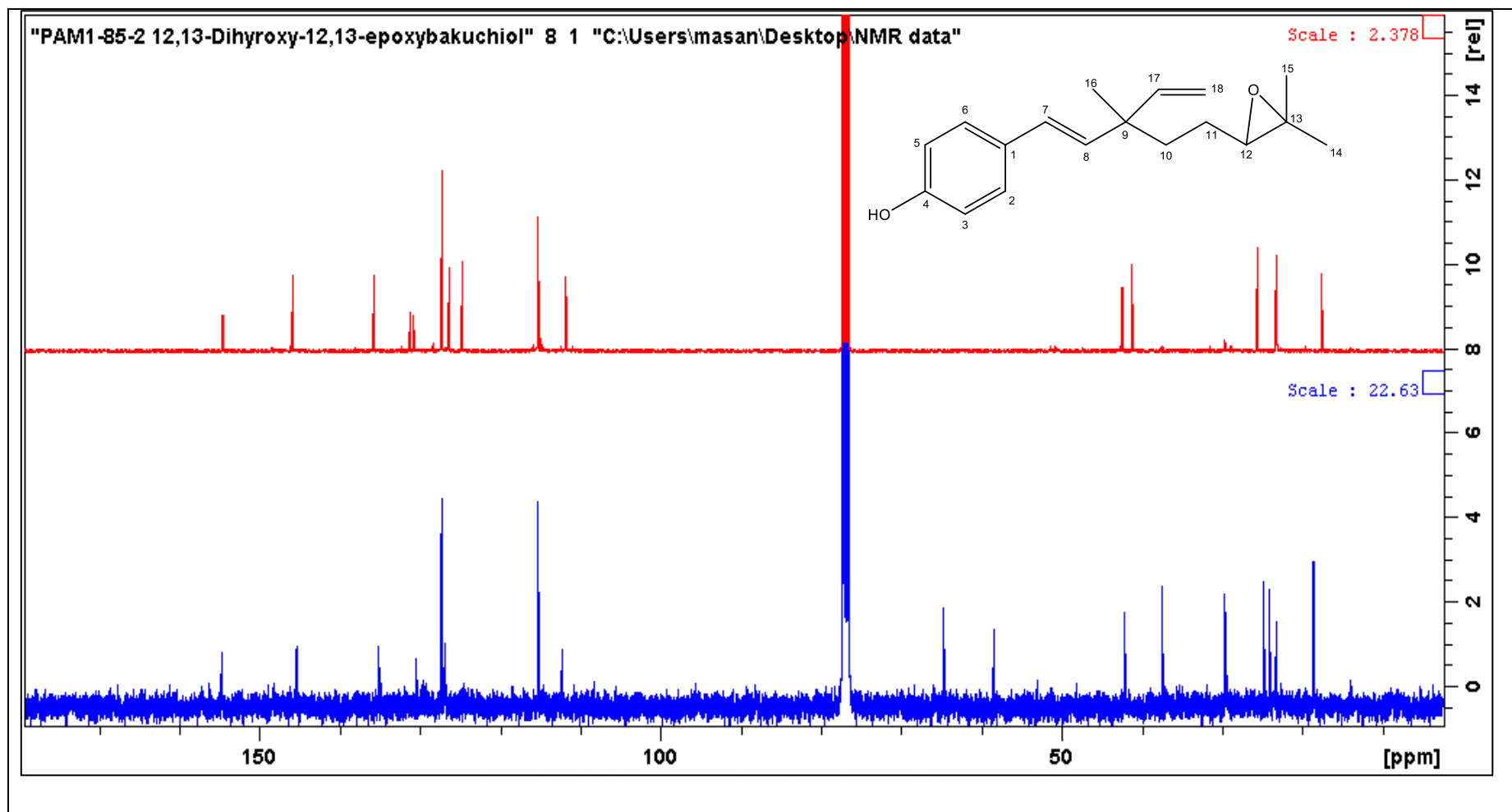


Figure 40:  $^{13}\text{C}$  NMR (400MHz,  $\text{CDCl}_3$ ) spectrum of Compound 1 and Compound 2. Where Red: compound 2 , Blue :Bakuchiol.



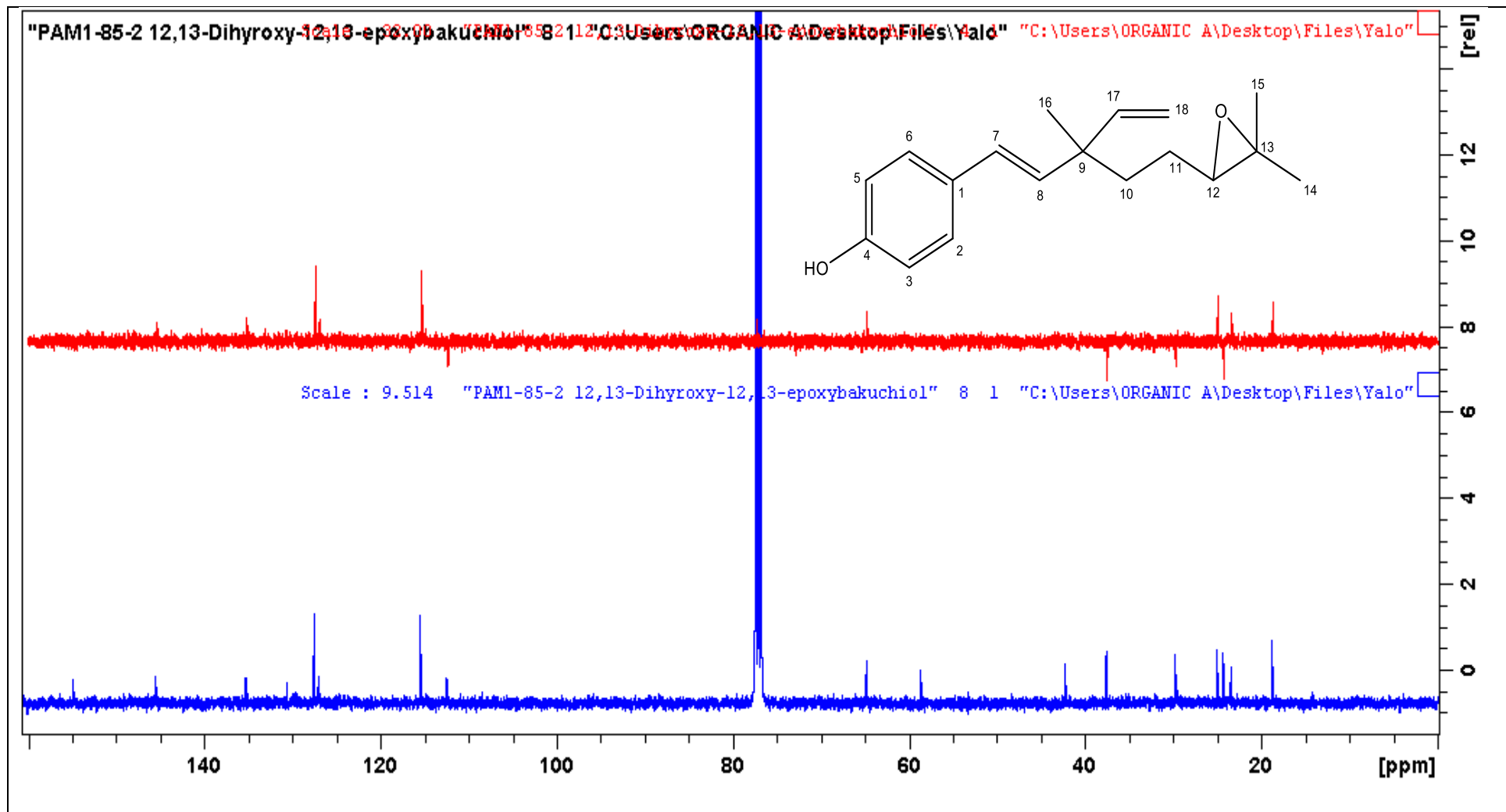


Figure 41: DEPT-135 NMR (400MHz, CDCl<sub>3</sub>) spectrum of compound 2.

The  $^1\text{H} - ^1\text{H}$  COSY spectrum (as shown in Figure 42) revealed a correlation between  $\delta$  2.71 ppm ( assigned as H-12) and a multiplet  $\delta$  1.53 ppm ( assigned as H-11) , thus, confirming the epoxide ring. The rest of the  $^1\text{H} - ^1\text{H}$  COSY correlations of Compound 2 were identical to that of Bakuchiol.



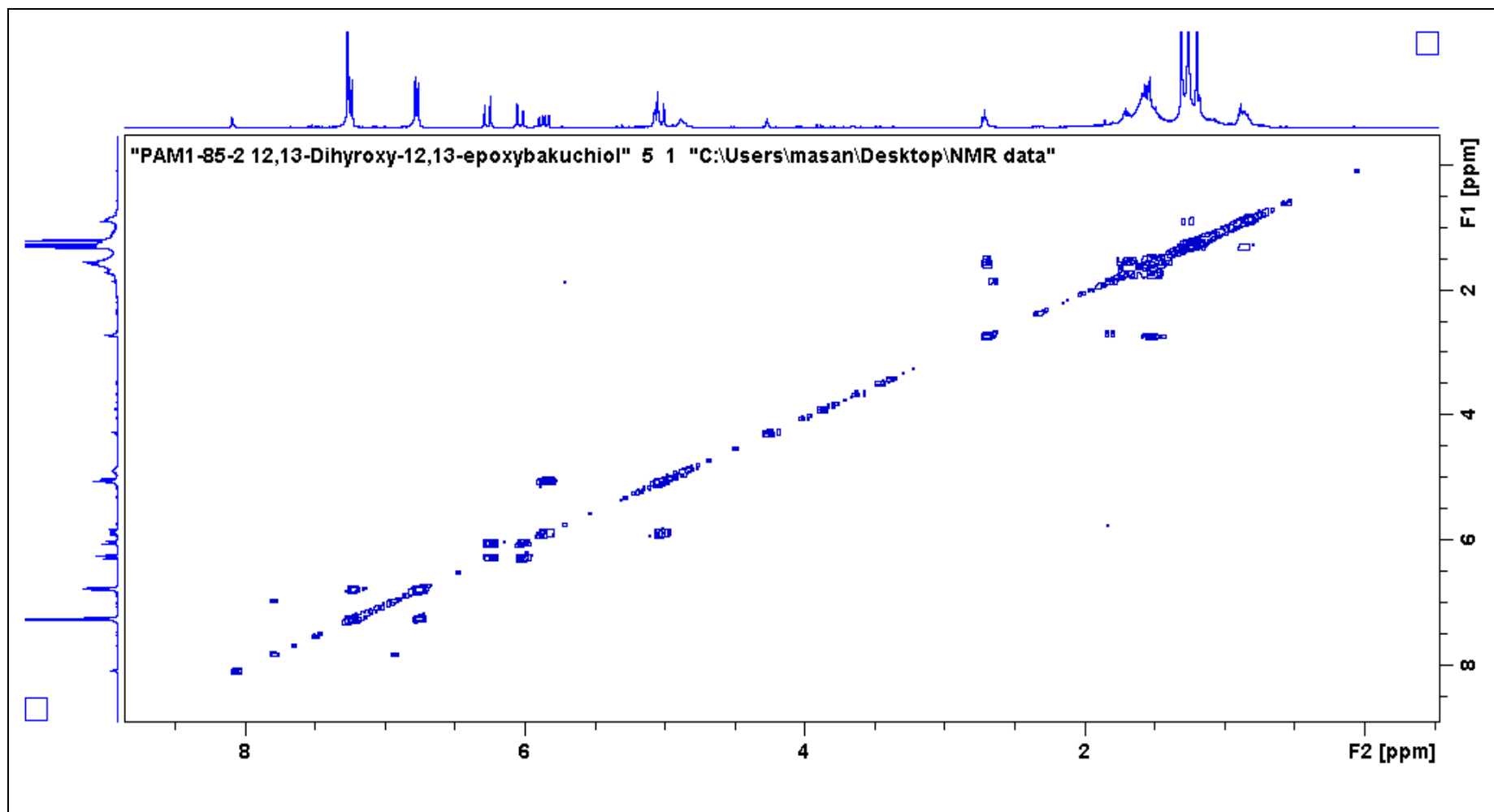
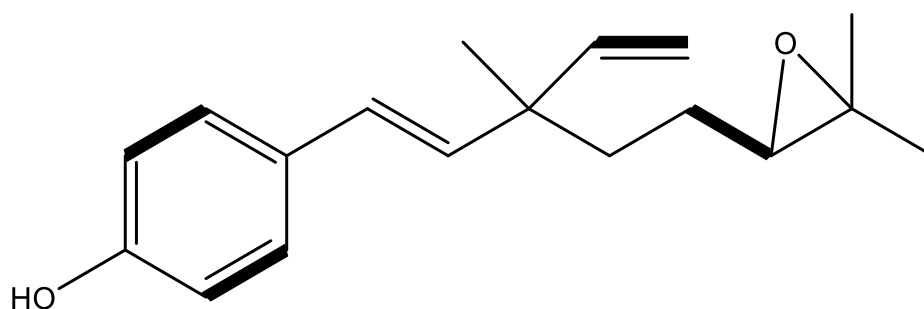
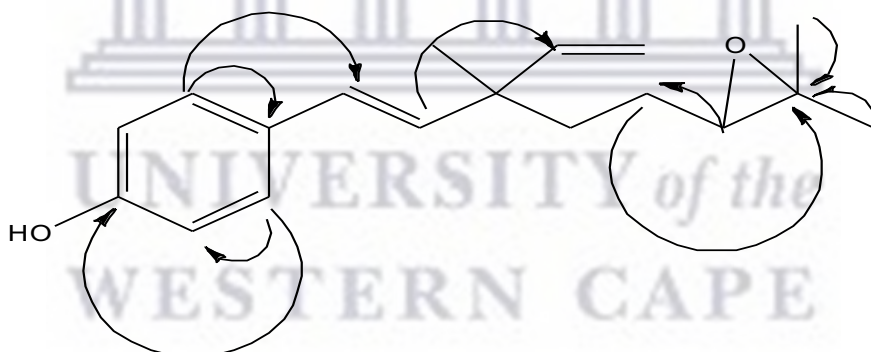


Figure 42:  $^1\text{H}$ - $^1\text{H}$  COSY (400 MHz,  $\text{CDCl}_3$ ) spectrum of Compound 2.



**Figure 43: : Important  $^1\text{H}$ - $^1\text{H}$  correlations represented by ———.**

Information from the HSQC spectrum allowed the interpretation of the  $^1\text{H} - ^{13}\text{C}$  single bond. The HMBC spectrum (as shown in Figure 45 ) was further used to confirm the structure of Compound 2. The observed correlations different to the correlations of bakuchiol were as followed: H-12 to C-11 ( $\delta_c$  41,37 ppm ) conforming the close proximity of C-11 to the epoxide, thus assisting with the assignment of C-11. Other correlations were H-14 to C-12, C-13 and C-15; and H-15 to C-12, C-13 and C-14 which also assisted in establishing the assignment of C-13 ( $\delta_c$  58.6 ppm).



**Figure 44: Important HMBC correlations of Compound 2.**

Using the HMBC spectrum correlations, the structure of this compound was fully established as 12,13-dihydro 12,13-epoxybakuchiol (compound 2). The structure was confirmed by comparing the data to those published in literature (Labbé *et al.*, 1996; Majeed *et al.*, 2012)

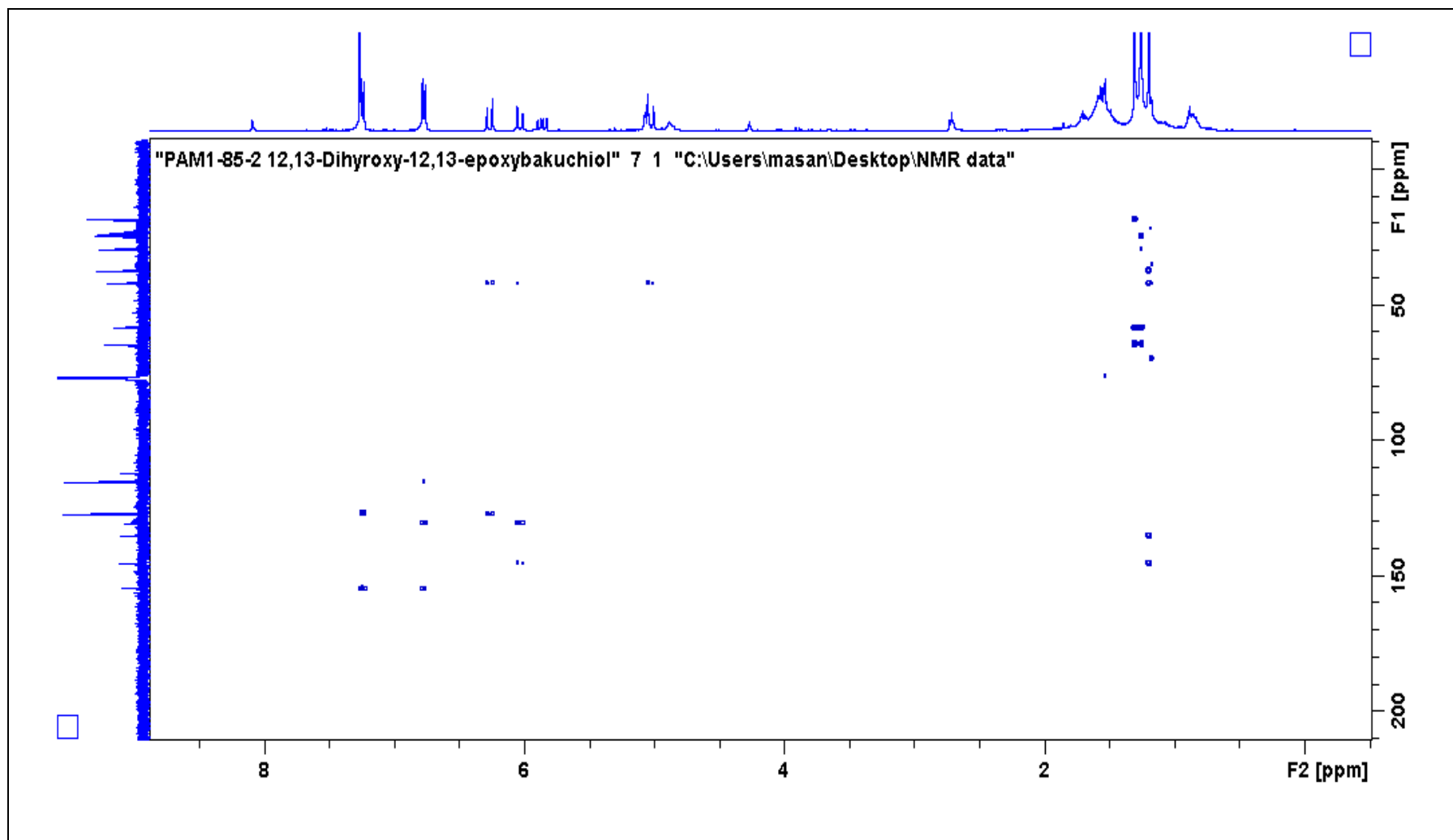


Figure 45: HMBC (400 MHz, CDCl<sub>3</sub>) spectrum of Compound 2.



**Table 18:  $^1\text{H}$  [400 MHz: m, J(Hz)] and  $^{13}\text{C}$  (100 MHz) NMR spectral data of Compound 2. Where \* presents quaternary carbons.**

Position	$^{13}\text{C}$ (ppm)	$^1\text{H}$ (ppm)
1*	130.6	-
2	127.3	7.23 (d, 8.7Hz)
3	115.4	6.77 (d, 8.4Hz)
4*	154.8	-
5	115.4	6.77 (d, 8.4Hz)
6	126.9	7.23 (d, 16Hz)
7	135.3	6.26 (d, 16Hz)
8	126.6	6.02 (dd, 1.4Hz)
9*	42.2	-
10	37.6	1.55(m)
11	24.4	1.53 (m)
12	65.0	2.72 (bt)
13*	58.6	-
14	18.5	1.26 (s)
15	18.5	1.31 (s)
16	24.7	1.20 (s)
17	145.6	6.02 (dd)
18a	112.5	5.07 (td)
18b	112.5	5.01 (d)

#### **b) FTIR analysis of 12,13-dihydro 12,13-epoxybakuchiol**

The prominent peaks are described in Table 19. The FT-IR spectrum (Figure 46) of compound 2 is closely related to Compound 1 (bakuchiol). The broad peak  $3340\text{ cm}^{-1}$  is assigned to O-H stretching vibration. In addition, the weak peak  $3082\text{ cm}^{-1}$  representing C-H stretch in the aromatic ring and the peaks  $2964$  and  $2927\text{ cm}^{-1}$  assigned to C-H vibration stretch means the compound is similar to bakuchiol. Therefore, depending on the fingerprint characters of the peak positions, intensities and shapes, the fundamental components of compound 2 may be identified and differentiated from that of bakuchiol. The strong peaks at  $1376$  and  $971\text{ cm}^{-1}$  are

assigned to C=C stretch. The strong, slightly deformed peak at 1265 cm<sup>-1</sup> suggests the presence of C-O-C, because there are often overlapping fingerprint-type bands nearby, it is very difficult to be sure about the assignment of the epoxide peak.

**Table 19: FT-IR analysis data interpretation of 12,13-dihydro 12,13-epoxybakuchiol (compound 2).**

Experiment frequency (cm <sup>-1</sup> )	Intensity	Assignment
3340	B, M	-OH stretch
3082	W	C-H stretch (Aromatic)
2964 and 2927	S, N	C-H stretching in CH <sub>2</sub> and CH <sub>3</sub>
1635	W	C=C (Conjugation)
1605 and 1514	S, M	C=C stretch (Aromatic)
1452	S, N	CH <sub>2</sub> bending (methylene group)
1376	S, N	C=C stretch
1233	M, N	C-O stretch
1265	S, slightly deformed peak	C-O-C stretch
972	S, N	C=C stretch

Key words: S=strong, N=narrow, B= broad, M= medium, W = weak

UNIVERSITY of the  
WESTERN CAPE

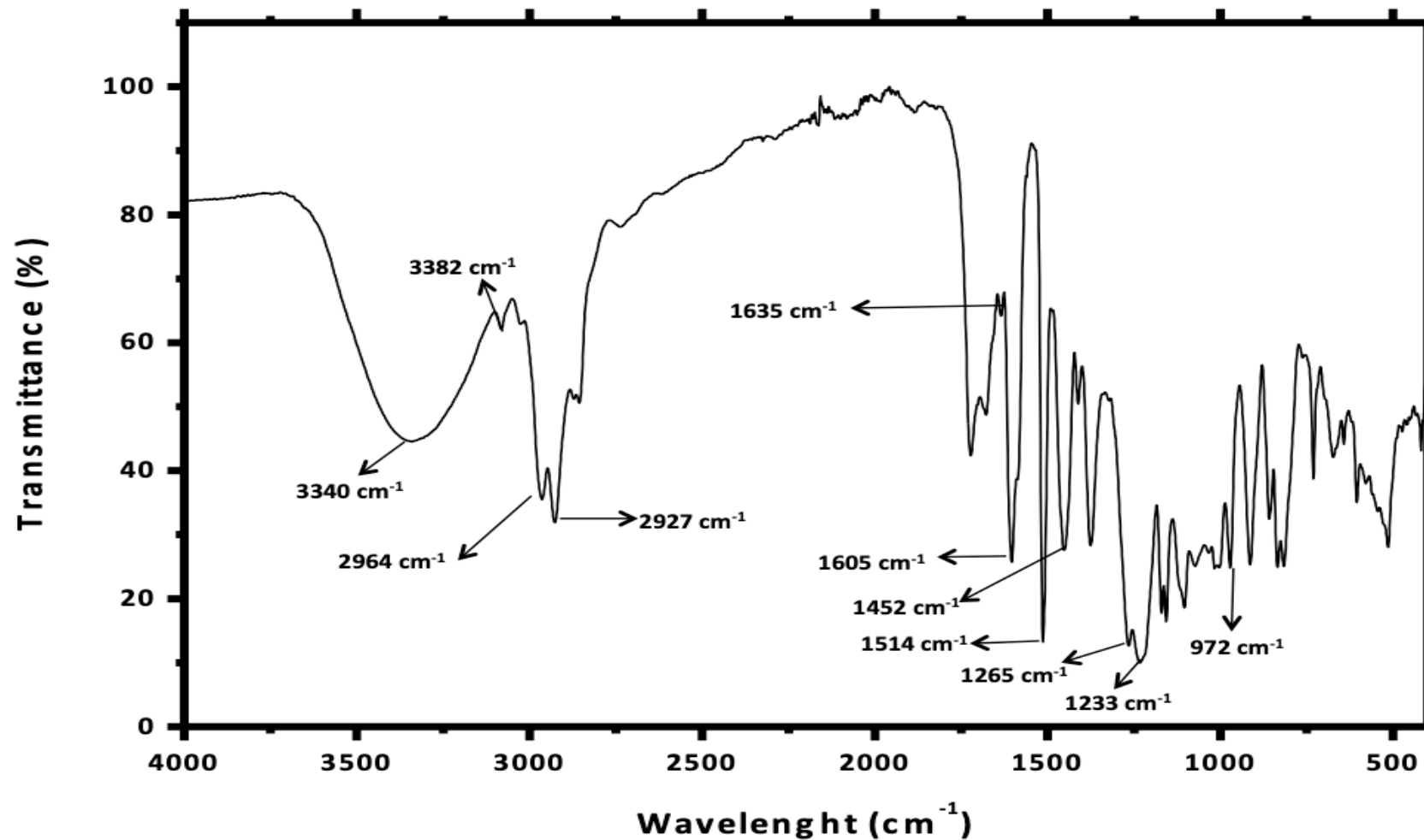


Figure 46: FTIR spectrum of 12,13-dihydro 12,13-epoxybakuchiol (Compound 2).

**c) UV analysis of 12,13-dihydro 12,13-epoxybakuchiol**

Ultraviolet (UV) spectra (Figure 47) was recorded using a NICOLET EVOLUTION 100 instrument, and methanol was used as solvent and a quartz cuvette was used. 12,13-dihydro 12,13-epoxybakuchiol has maximum absorption at 275nm in its UV spectrum.

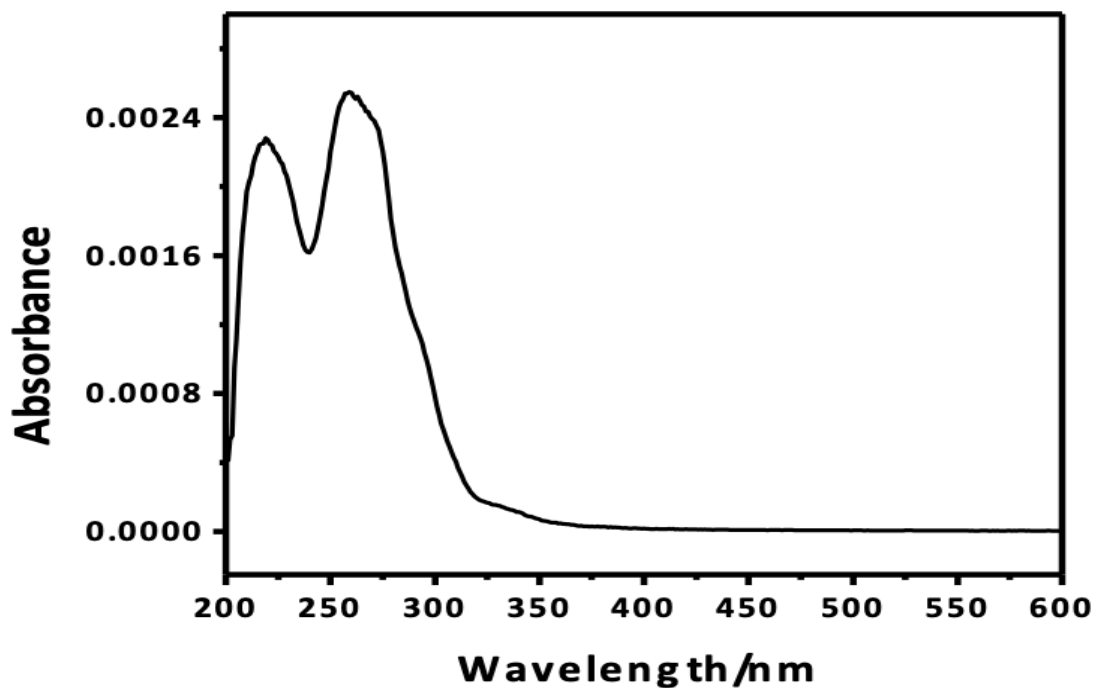
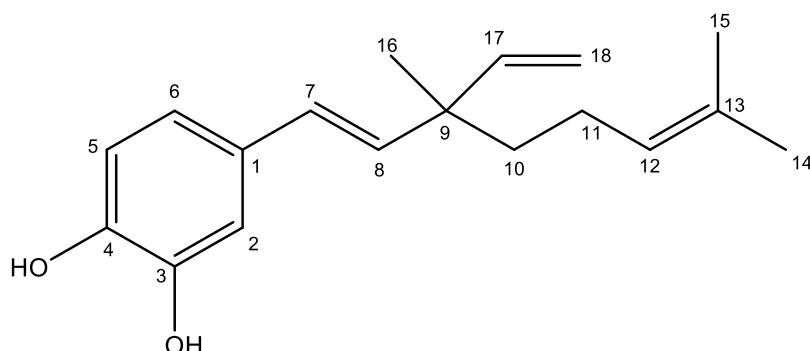


Figure 47: UV spectrum of 12,13-dihydro 12,13-epoxybakuchiol.

### 5.1.3. Structural elucidation of 3-hydroxybakuchiol



**Figure 48: Proposed structure of compound 3.**

#### a) NMR analysis of 3-hydroxybakuchiol

Compound 3 was isolated as yellow oil. The NMR spectroscopic data of Compound 3 (mass = 7.5 mg) showed a similar spectrum to those of Compound 1 (Bakuchiol). While the olefinic side chain attached to the aromatic ring was identical to that of Compound 1, the substitution pattern of the aromatic ring is different from that of Compound 1.

$^1\text{H}$  NMR data (Figure 49) showed signals of two aromatic protons at  $\delta$  6.72 (bs, 2H, H-5 and H-6) and  $\delta$  6.85 (1H, s, H-2), which suggested the existence of a 1,3,4 trisubstituted benzene ring, H-5 and H-6 being equivalent protons.

$^{13}\text{C}$  NMR (Figure 50) spectrum showed eighteen carbon peaks corresponding to 18 carbons. DEPT-135 spectrum revealed five quaternary carbons at  $\delta_c$  143.6, 142.8, 131.6 and 42.4 ppm.

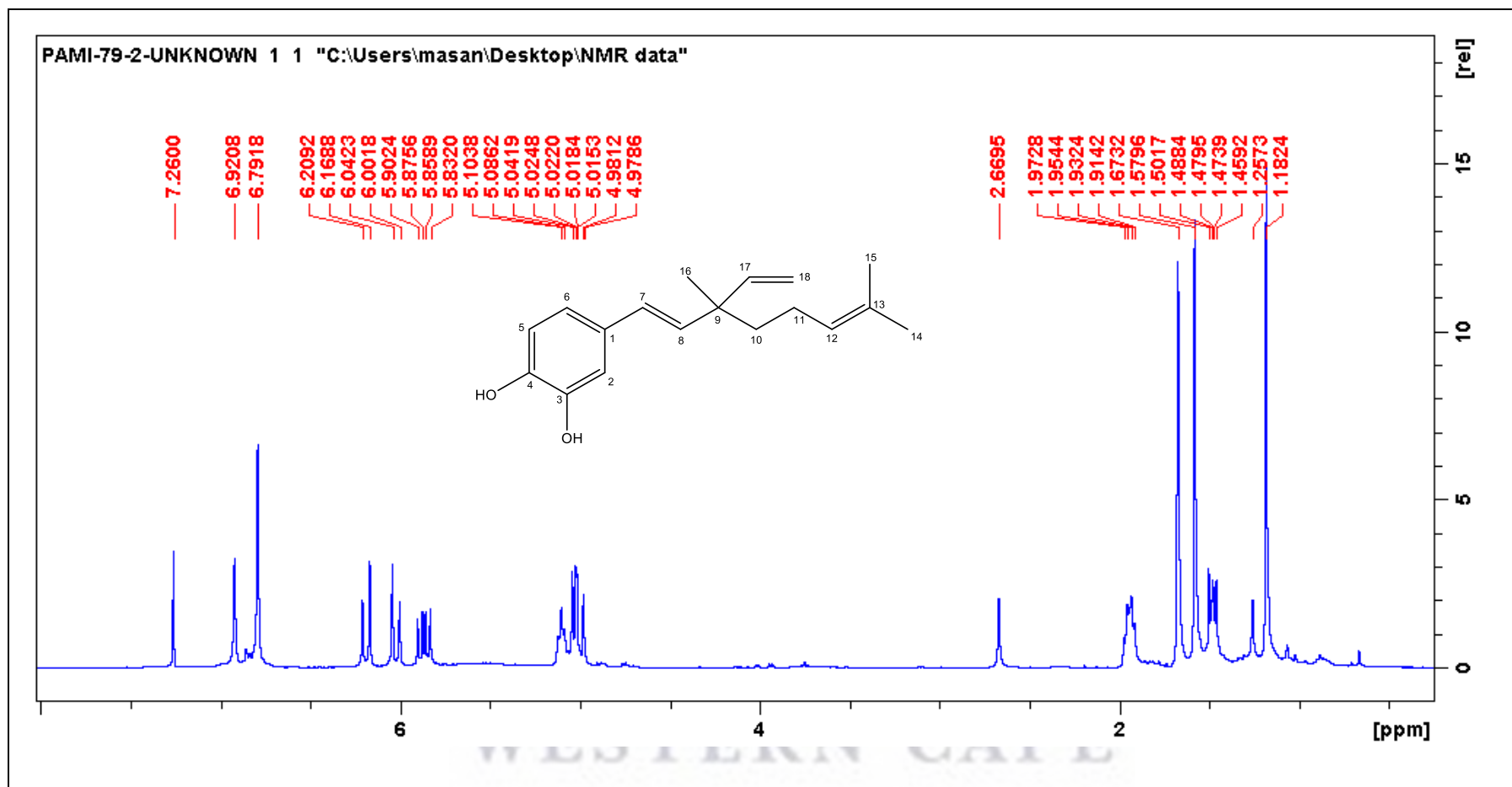


Figure 49:  $^1\text{H}$  NMR ( 400 MHz ,  $\text{CDCl}_3$ ) spectrum of compound 3.



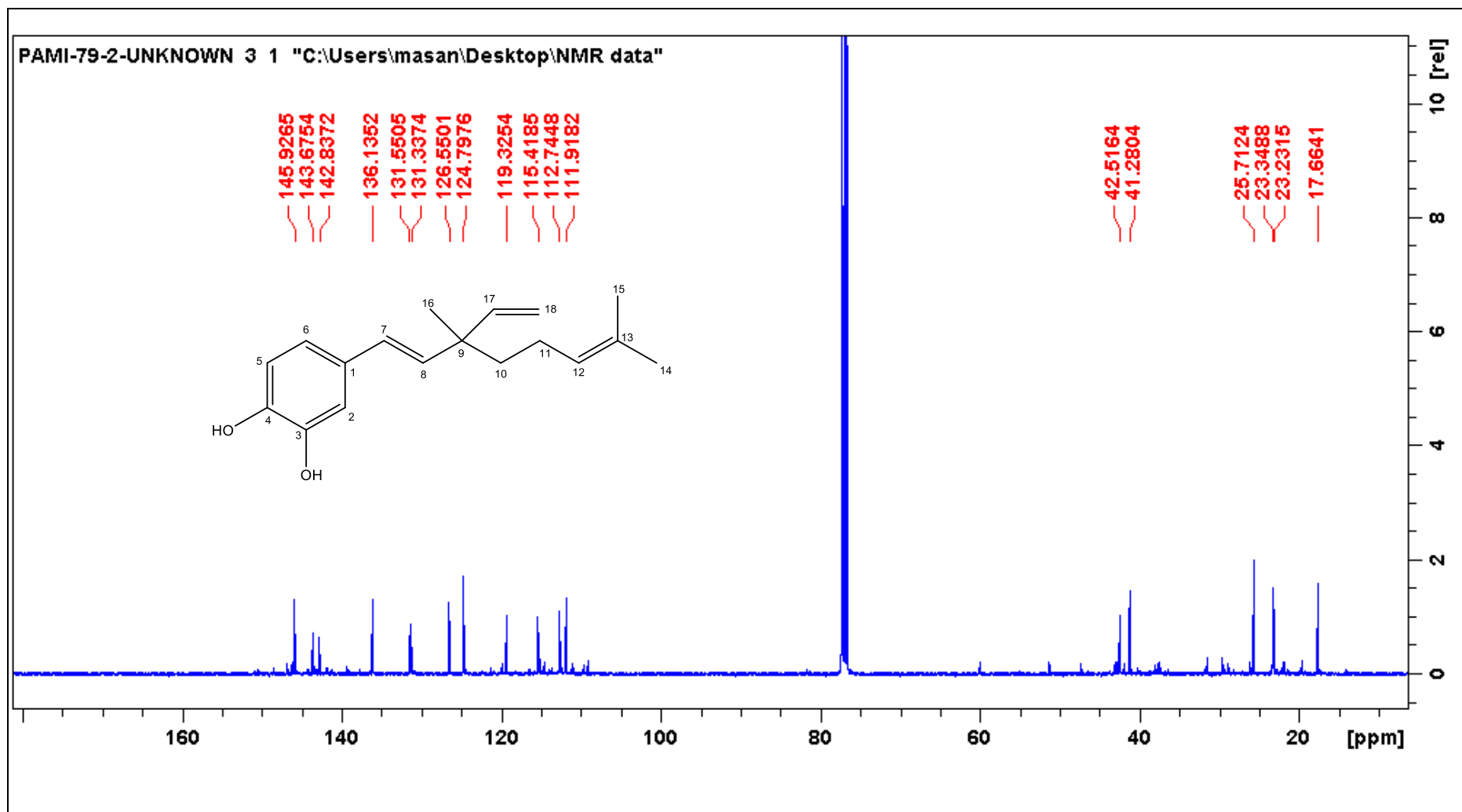


Figure 50: <sup>13</sup>C NMR ( 400 MHz , CDCl<sub>3</sub>) spectrum of compound.

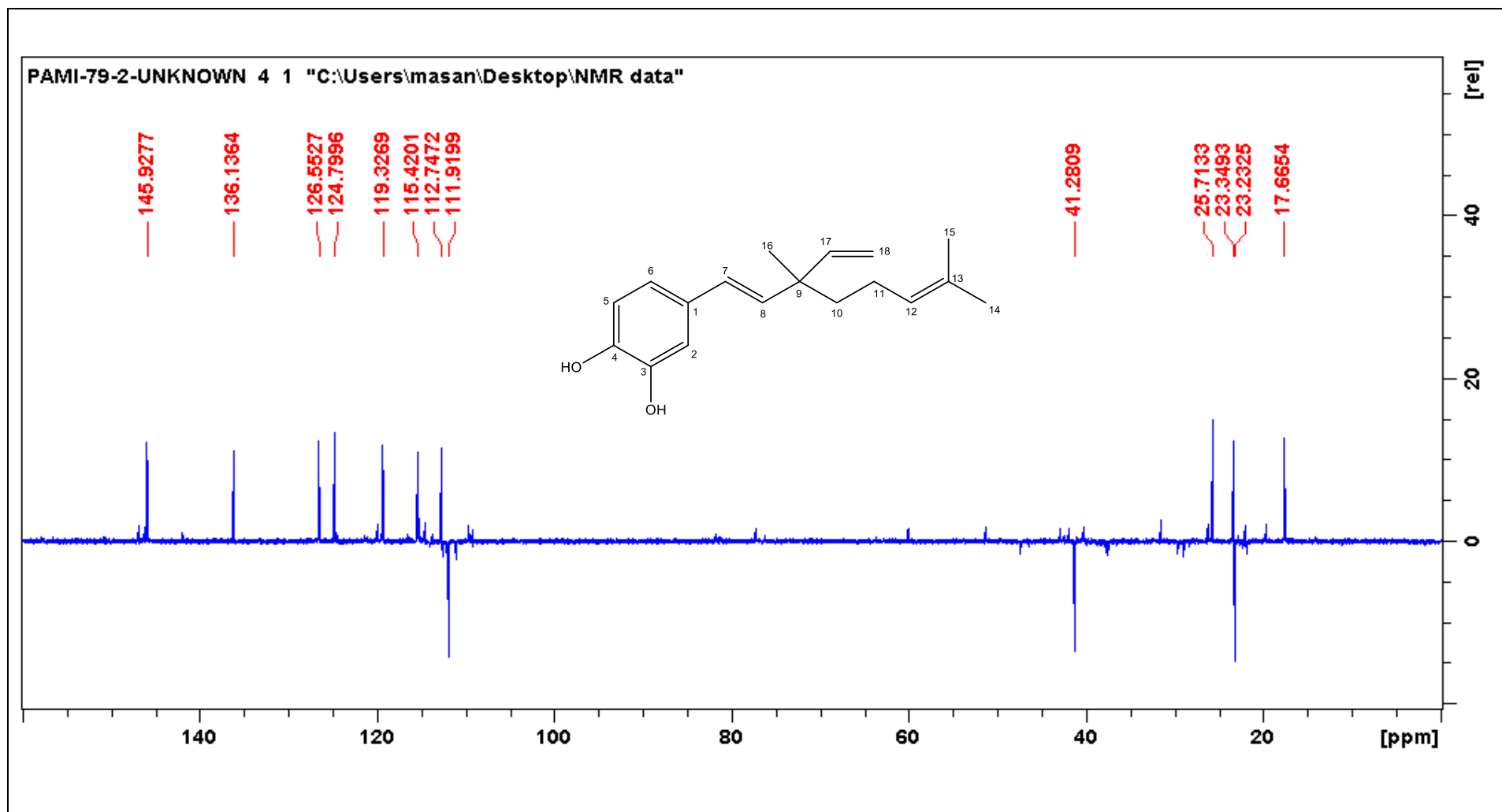


Figure 51: DEPT 135 NMR ( 400 MHz , CDCl<sub>3</sub>) spectrum of compound 3.

The HSQC allowed the interpretation of  $^1\text{H} - ^{13}\text{C}$ , showing correlations between H-2 to  $\delta_c$  112.0 ppm (C-2) and correlations H-5 and H-6 to  $\delta_c$  115.6 and 119.5 ppm confirming a *meta*-hydroxyl group substitution.

The HMBC spectrum ( Figure 46) was further used to confirm the structure of compound 3. The following correlations were observed: H-2 to C-3, C-6, C-6 and H-5 and H-6 to C-1, C2 , C-3 and C-8.



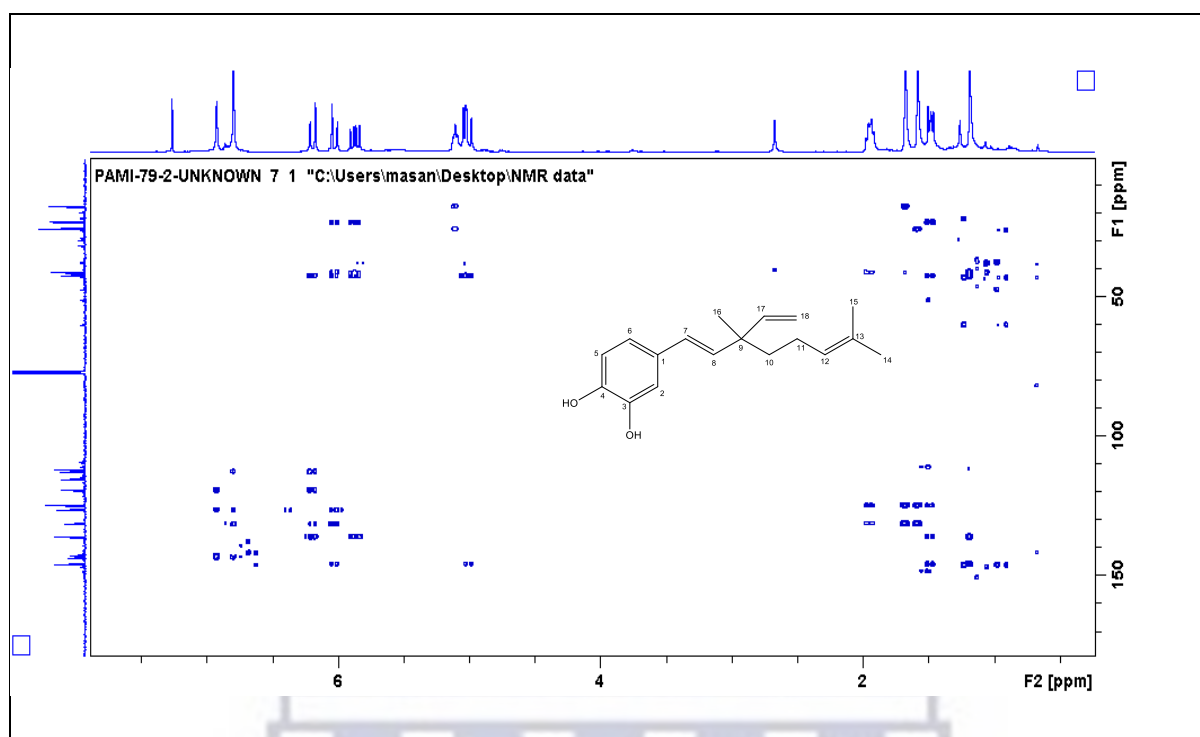
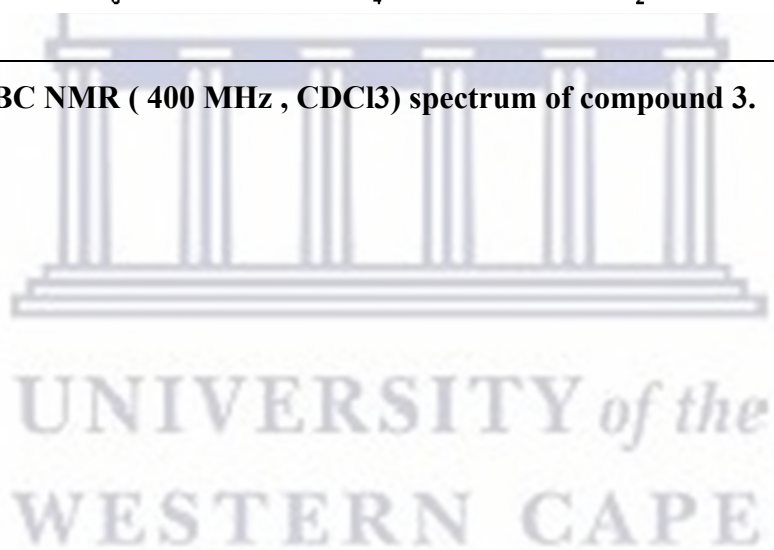


Figure 52: HMBC NMR ( 400 MHz , CDCl<sub>3</sub>) spectrum of compound 3.



From the HMBC the structure of this compound was fully established.

**Table 20:  $^1\text{H}$  [400 MHz: m, J(Hz)] and  $^{13}\text{C}$  (100 MHz) NMR spectral data of Compound 3. The \* represent quaternary carbons.**

Position	$^{13}\text{C}$ (ppm)	$^1\text{H}$ (ppm)
1*	131.5	-
2	112.8	7.60(d, 8.7Hz)
3	115.4	6.77(d, 8.4Hz)
4	154.8	-
5	115.4	6.77(d, 8.4Hz)
6	126.9	6.26(d, 16Hz)
7	135.3	6.26(d, 16Hz)
8	126.6	6.03(dd, 1.4Hz)
9*	42.1	-
10	37.6	1.55(m)
11	24.4	1.53(m)
12	65.0	2.71 (bt)
13*	58.6	-
14	18.5	1.25(s)
15	18.5	1.30(s)
16	24.7	1.20(s)
17	145.6	5.86(dd)
18a	112.5	5.05(td)
18b	112.5	5.01(d)

The above data confirmed the structure of Compound 3 as 3-hydroxybakuchiol. The spectra data and structure agreed with literature (Labbé *et al.*, 1996).

#### b) FTIR analysis of compound 3

FT-IR spectrometry was used to further characterize compound 3. The spectra is expected to be the same as for Compound 1, with slight changes in peak positions and intensities. There is a significant change observed is the intensity peak  $3343\text{ cm}^{-1}$  assigned to the OH group, it

should be more than of bakuchiol because there is two –OH groups present in the compound, unlike in bakuchiol.

**Table 21:FT-IR analysis data interpretation of 3-hydroxybakuchiol.**

Experiment frequency ( $\text{cm}^{-1}$ )	Intensity	Assignment
3343	B, M	-OH stretch
3082	W	C-H stretch (Aromatic)
2958 and 2922	N, S	C-H stretching in $\text{CH}_2$ and $\text{CH}_3$
1605 and 1508	N, M	C=C stretch (Aromatic)
1449	N, M	$\text{CH}_2$ bending(methylene group)
1373	N, M	C=C stretch
1279	N, M	C-O stretch
970	N, M	C=C stretch

Key words: S=strong, N=narrow, B= broad, M= medium, W = weak



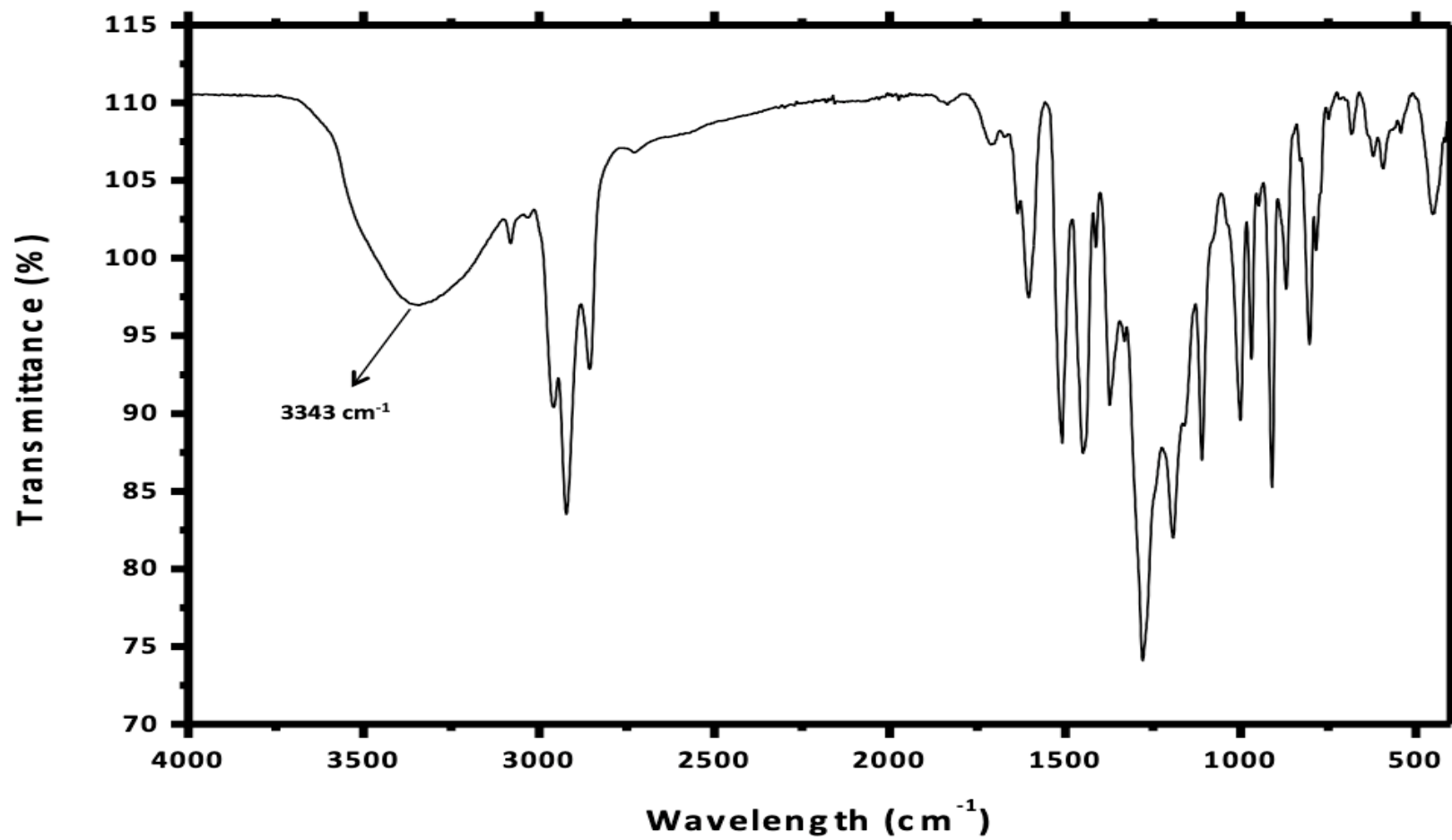


Figure 53: FTIR spectrum of 3-hydroxybakuchiol (Compound 3).

**c) UV analysis of 3-hydroxybakuchiol**

Ultraviolet (UV) spectra (Figure 54) was recorded using a NICOLET EVOLUTION 100 instrument, and methanol was used as solvent and a quartz cuvette was used. 3-hydroxybakuchiol has maximum absorption at 275 nm in its UV spectrum.

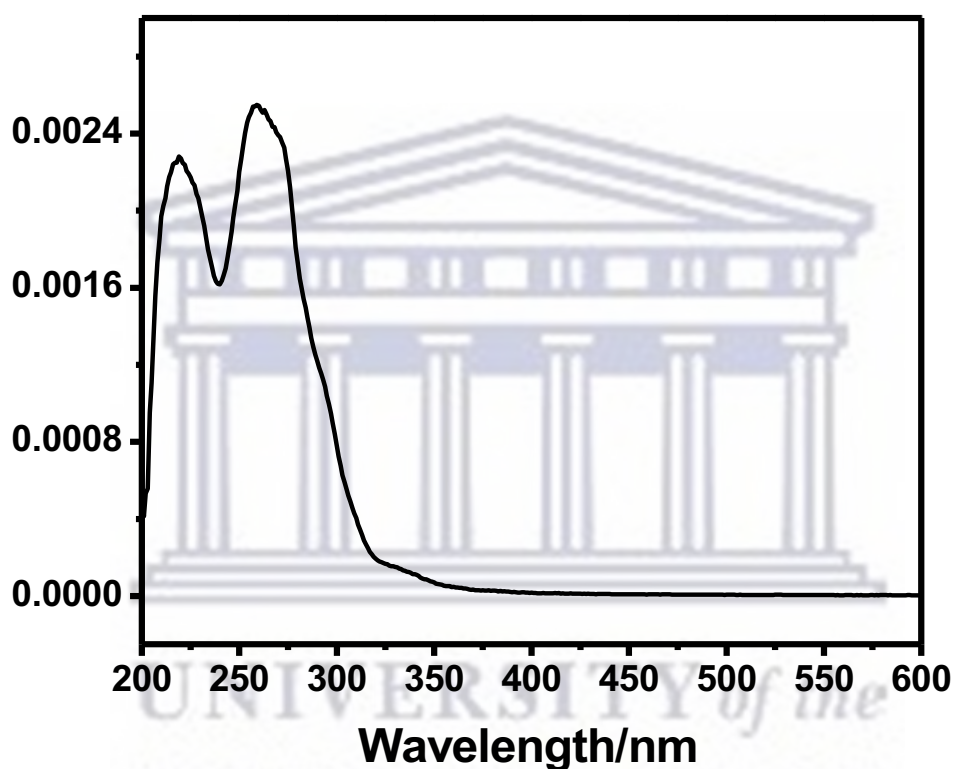
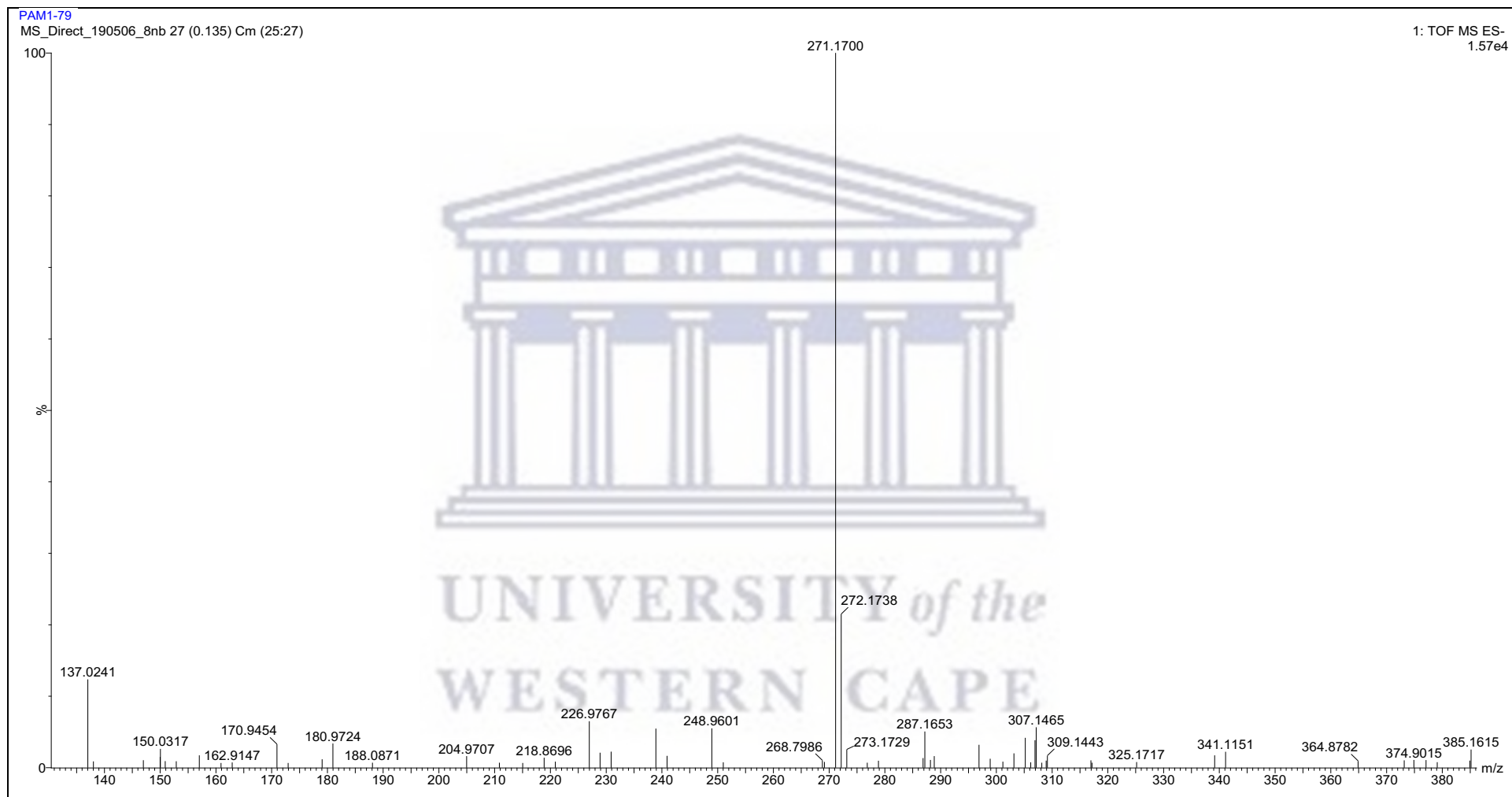


Figure 54: UV spectrum of 3-hydroxybakuchiol.

**d) Mass Spectrometry of 3-hydroxybakuchiol.**

Based on the chemical structure (Figure 48), 3-hydroxybakuchiol readily loses a proton in electrospray ionization. Hence, the negative electrospray ionization mode was used. As shown in Figure 55, the compound produced a deprotonated molecular ion  $[M-H]^-$  at  $m/z$  271.17.



**Figure 55:** The mass spectra of 3-hydroxybakuchiol isolated from the methanolic extract of *Psoralea aphylla* plan

#### 5.1.4. Structural elucidation of Compound 4 - Steroids.

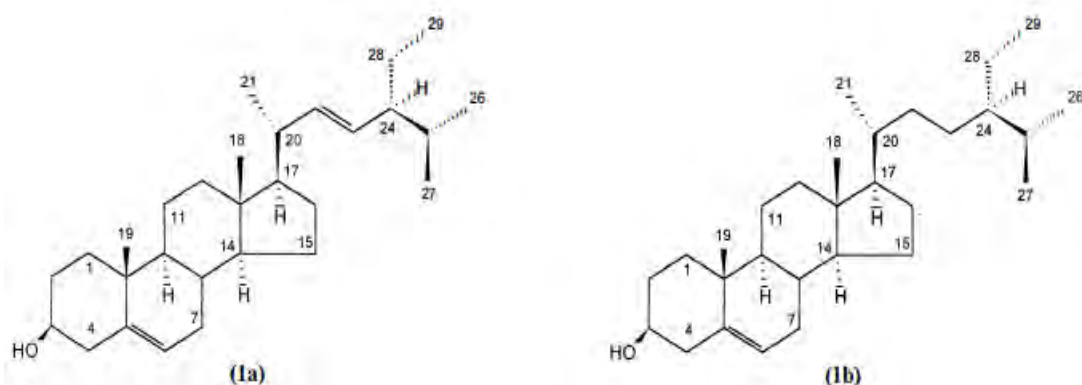


Figure 56: Proposed structures of Compound 4 (1a is stigmasterol and 1b is sitosterol).

##### a) NMR analysis of a mixture stigmasterol and sitosterol.

The  $^1\text{H}$  NMR spectrum (Figure 57) showed olefinic protons  $\delta$  5.28 (d,  $J = 4.7$  Hz, H-6),  $\delta$  5.08 (dd, H- 22) and 5.01 (dd,  $J = 8.4$  Hz, H- 23). A triplet of a doublet appeared at  $\delta$  3.42 (tdd, H-6) suggesting a presence of a sterol moiety. Other peaks of high intensity were  $\delta$  0.93 (s), 0.85 (d,  $J = 6.6$  Hz, H-26), 0.77 (s), 0.91 (d,  $J = 1.8$  Hz, H-19), 0.73 (s, H- 28) and  $\delta$  0.61 (s, H-18) ppm, which indicated the presence of six methyl groups.

The  $^{13}\text{C}$  NMR spectrum (Figure 58) showed resonance for 29 signals. Four olefinic carbons appeared at  $\delta_c$  121.7, 129.2, 138.3 and 140.7 ppm; with signals at  $\delta_c$  140.7 and 121.7 ppm as two carbon double bonds. A hydroxyl group at  $\delta_c$  71.8 ppm (C-3); three quaternary carbons at  $\delta_c$  140.7, 46.9 and 36.2 ppm; eleven methylene carbons at  $\delta_c$  42.3, 39.8, 36.2, 37.2, 31.9, 31.6, 28.9, 25.4, 23.1, 24.3 and 21.1 ppm, which is more methylene carbons than expected in a sterol. Thus, indicating a mixture of two compounds.

According to literature, Compound 4 was revealed to be a mixture of stigmasterol and sitosterol (Cayme *et al.*, 2004). Literature also shows that it is very difficult to obtain and sitosterol in its pure state. The only difference between the two sterols is that stigmasterol has two olefinic carbons at C-22 and C-23, while sitosterol has two methylene carbons at C-22 and C-23.



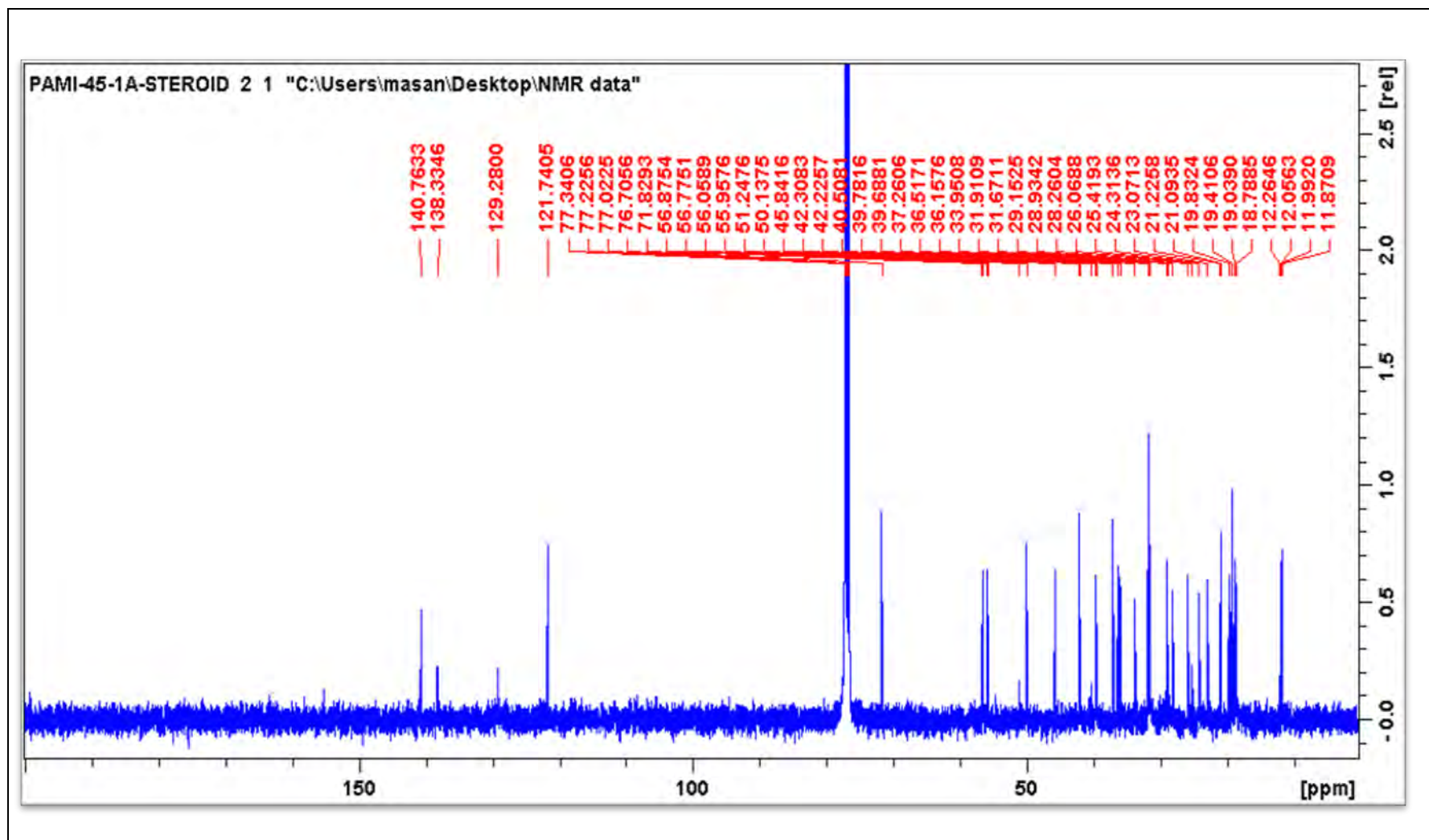


Figure 58:  $^{13}\text{C}$  NMR (400 MHz,  $\text{CDCl}_3$ ) spectrum of compound 4.



Therefore, from the above  $^1\text{H}$  and  $^{13}\text{C}$  NMR , compound 4 is the mixture of mixture of stigmasterol and sitosterol. The structures and data agreed with those of literature ( Cayme *et al.*, 2004; Pierre *et al.*, 2015; Rajput and Rajput, 2012).



**Table 22:**  $^1\text{H}$  [400 MHz: m, J(Hz)] and  $^{13}\text{C}$  (100 MHz) NMR spectral data of Compound 4, which is a mixture of stigmasterol and sitosterol.

Position	Stigmasterol $^1\text{H}$ (ppm)	$^{13}\text{C}$ (ppm)	Sitosterol $^1\text{H}$ (ppm)
1		37.2	
2		31.6	
3	3.42 (tdd, J = 4.5,4.2, 3.8Hz, 1H)	71.8	3.42 (tdd, J = 4.5,4.2, 3.8Hz, 1H)
4		42.3	
5		140.8	
6	5.28 (d, J = 4.7 Hz, 1H)	121.7	5.28 (d, J = 4.7 Hz, H1)
7		31.9	
8		31.1	
9		50.1	
10		36.2	
11		21.1	
12		39.8	
13		42.3	
14		Stigmasterol- 56.9 Sitosterol - 56.1	
15		24.3	
16		29.2 28.9	
17		56.1	
18	0.61 (s, 3H)	12.06	0.61 (s, 3H)

(continued)

Position	Stigmasterol <sup>1</sup> H (ppm)	<sup>13</sup> C (ppm)	Sitosterol <sup>1</sup> H (ppm)
19	0.71 (d, J = 1.8 Hz, 3H)	19.8	0.93 (d, J=6.5 Hz, 3H)
20	4.98 (m, 1H)	39.8 36.2	
21		23.1	
22	5.08 (dd, J=8.4, 15.1 Hz)		
23	5.02 (dd, J=8.4, 15.1 Hz)	Stigmasterol- 129.2 Sitosterol – 26.1	
24	0.83 (t, J = 7.1 Hz, 3H)	Stigmasterol- 51.2 Sitosterol - 56.1	
25		Stigmasterol- 31.9 Sitosterol – 29.2	
26	0.85 (d, J = 6.6 Hz, 3H)	Stigmasterol- 21.1 Sitosterol – 19.0	
27	0.80 (d, J=6.6. HZ, 3H)	Stigmasterol- 18.8 Sitosterol – 19.8	
28	0.73 (s, 3H)	Stigmasterol- 25.4 Sitosterol – 23.1	
29	1.03 (s, 3H)	Stigmasterol – 12.0 Sitosterol - 11.9	

**b) UV analysis of stigmasterol and sitosterol.**

Ultraviolet (UV) spectra were recorded using a NICOLET EVOLUTION 100 instrument, and methanol was used as solvent and a quartz cuvette was used. The steroids have maximum absorption at 212 nm in the UV spectrum (Figure 59)

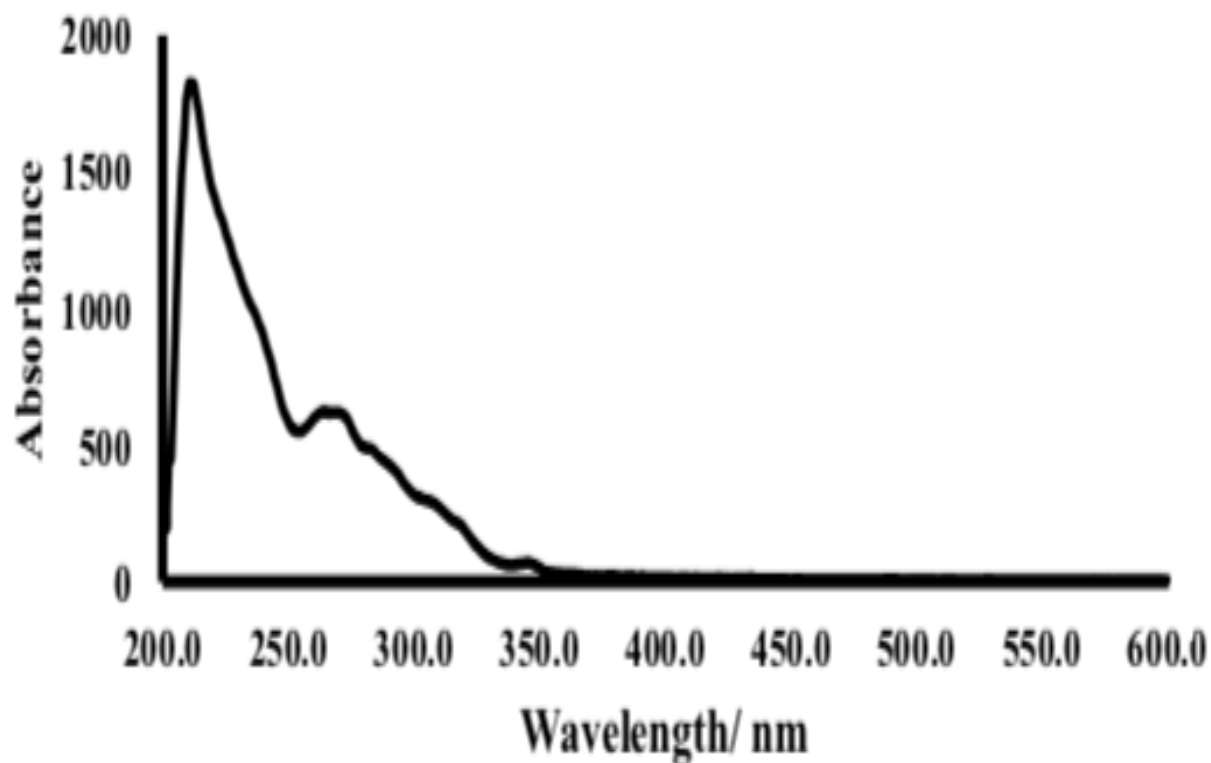


**Figure 59: UV spectrum of stigmasterol and  $\beta$ -sitosterol**

### 5.1.5. Summary of analysis of isolated compounds

In summary, the isolated compounds were characterised by recording NMR, UV and IR. Compound 3 was characterised by MS for more clarity on its structure. The information gathered provide good information about the nature and type of products. In NMR, some of the assignments are interchangeable and only resolvable signals are shown.

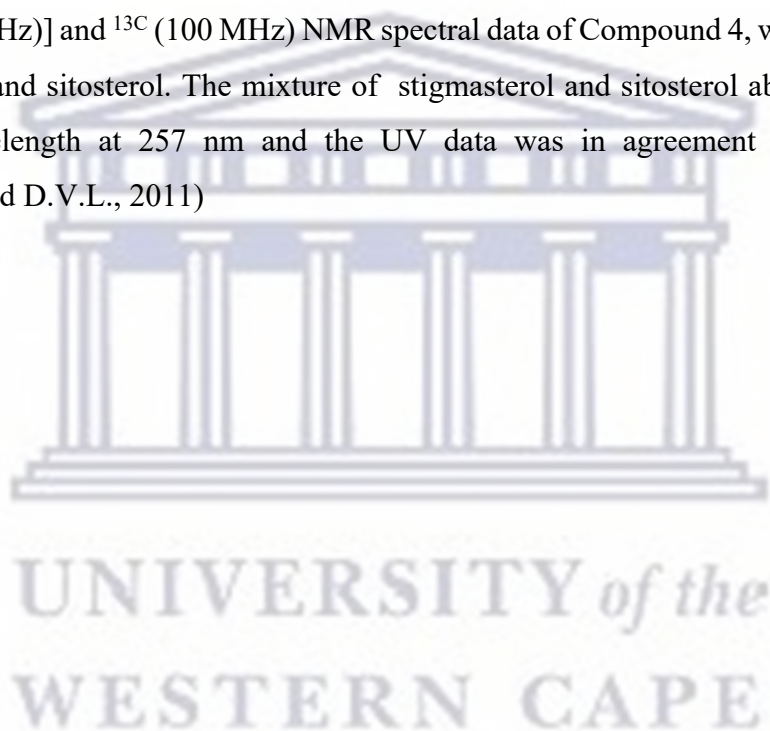
**Compound 1 (Bakuchiol):** A yellowish oil; UV ( $\lambda_{\max}$ ): 225.0 nm, 275 nm; IR: 3302, 3082, 2917, 1605, 1514, 1462, 1376, 1236, 971  $\text{cm}^{-1}$ ;  $^1\text{H}$  and  $^{13}\text{C}$  see Table 16:  $^1\text{H}$  [400 MHz: m, J(Hz)] and  $^{13}\text{C}$  (100 MHz) NMR spectral data of Compound 1. Where \* presents quaternary carbons.  $^1\text{H}$  NMR spectrum showed aromatic signals at  $\delta$  7.22 ppm and  $\delta$  6.75 ppm which correlated with the observed on the FT-IR spectrum showing an aromatic C-H stretched peaks at 3082  $\text{cm}^{-1}$ . The FTIR spectra showed an C-O stretch, which was attributed to the hydroxyl group validated by the quaternary carbon at  $\delta_c$  154.6 ppm (C4) showed in the  $^{13}\text{C}$  NMR spectra. Bakuchiol absorbed light at a maximum wavelength at 275 nm and the UV data was in agreement with literature (Labbé *et al.*, 1996)

**Compound 2 (12,13-Dihydro-12,13-epoxybakuchiol):** A yellowish oil; UV ( $\lambda_{\max}$ ): 240.0 nm, 260 nm ; IR: 3340, 3082, 2964, 2927, 1635, 1605, 1514, 1452, 1376, 1233, 1265, 972;  $^1\text{H}$  and  $^{13}\text{C}$  see Table 18:  $^1\text{H}$  [400 MHz: m, J(Hz)] and  $^{13}\text{C}$  (100 MHz) NMR spectral data of Compound 2. Where \* presents quaternary carbons. 12,13-Dihydro-12,13-epoxybakuchiol is similar to bakuchiol. FT-IR data showed a slightly deformed peak at 1265  $\text{cm}^{-1}$  which was attributed a C-O-C stretch, the peak was validated using  $^{13}\text{C}$  spectrum. The  $^{13}\text{C}$  spectrum indicated a presence of a trisubstituted epoxide ring assigned to C-12 and C-13 at  $\delta_c$  65.0 ppm and  $\delta_c$  58.6 ppm, respectively; and C-13 was confirmed as a quaternary carbon of the oxirene ring. 12,13-Dihydro-12,13-epoxybakuchiol absorbed light at a maximum wavelength at 260 nm and the UV data was in agreement with literature (Labbé *et al.*, 1996)).

**Compound 3 (3-Hydroxybakuchiol):** A yellowish oil: UV ( $\lambda_{\max}$ ): 240.0nm, 260nm ; IR: 3343, 3082, 2958, 2922, 1605, 1508, 1449, 1373, 1279, 970  $\text{cm}^{-1}$ ; MS ( $m/z$ ): [M $^-$ ] 271.17;  $^1\text{H}$  and  $^{13}\text{C}$  see Table 20:  $^1\text{H}$  [400 MHz: m, J(Hz)] and  $^{13}\text{C}$  (100 MHz) NMR spectral data of Compound 3. The \* represent quaternary carbons.].

3-Hydroxybakuchiol showed to be similar to bakuchiol, the difference being an extra hydroxy functional group. The  $^1\text{H}$  NMR spectrum implied an existence of 1,3,4 trisubstituted benzene ring due to aromatic protons at  $\delta$  6.72 and  $\delta$  6.85. The FTIR spectrum validated the presence of hydroxyl groups by an intensified peak at a wavelength of  $3343\text{ cm}^{-1}$ . The MS spectrum showed a large deprotonated molecular ion 271.17 [M-] corresponding to a molecular formula  $\text{C}_{18}\text{H}_{23}\text{O}_2$ , thus in agreement with NMR data. 3-Hydroxybakuchiol absorbed light at a maximum wavelength at 260 nm and the UV data was in agreement with literature (Labbé *et al.*, 1996)).

**Compound 4 (stigmasterol and sitosterol)** : White crystals; UV ( $\lambda_{\text{max}}$ ): 257.0 nm ;IR: 3340, 3082, 2964, 2927, 1635, 1605, 1514, 1452, 1376, 1233, 1265, 972.  $^1\text{H}$  and  $^{13}\text{C}$  see Table 22:  $^1\text{H}$  [400 MHz: m, J(Hz)] and  $^{13}\text{C}$  (100 MHz) NMR spectral data of Compound 4, which is a mixture of stigmasterol and sitosterol. The mixture of stigmasterol and sitosterol absorbed light at a maximum wavelength at 257 nm and the UV data was in agreement with literature ( Govindarajan and D.V.L., 2011)





## 5.2. Tyrosinase inhibition Assay

The average tyrosinase inhibition percentages of the main extract and isolated compounds screened at 25 and 50  $\mu\text{g}/\text{mL}$  are shown in Figure 60. All the samples showed not be effective inhibitors of mushroom tyrosinase compared to kojic acid (KA). The compound with higher tyrosinase inhibition percentage was compound 12,13- dihydroxy-12,13-epoxybakuchiol with an inhibition percentage of 35.9% at 50  $\mu\text{g}/\text{mL}$ , followed by bakuchiol with an inhibition percentage of 35.9% at 50  $\mu\text{g}/\text{mL}$ , main extract (MA) with an inhibition percentage of 21.7% at 100  $\mu\text{g}/\text{mL}$  and 3-hydroxybakuchiol with an inhibition percentage of 9.4% at 100  $\mu\text{g}/\text{mL}$ .

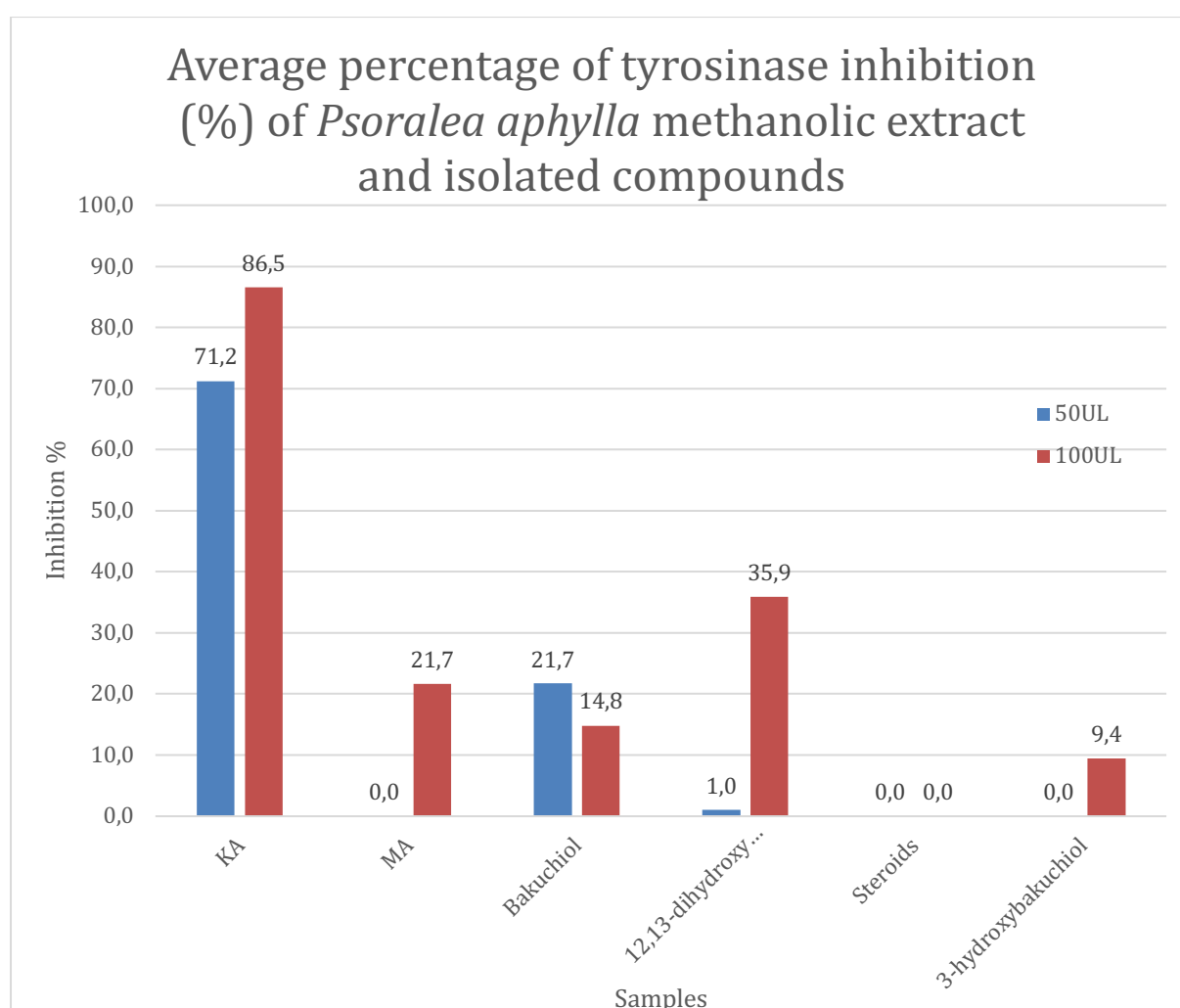


**Figure 60:** A bar graph showing average tyrosinase inhibition percentages of *Psoralea aphylla* methanol extract and isolated compound in comparison to kojic acid at different concentrations (50 UL= 25  $\mu\text{g}/\text{ml}$  and 100UL= 50  $\mu\text{g}/\text{ml}$ ). Where KA is Kojic acid, MA is the methanolic extract of *Psoralea aphylla*, C1 is bakuchiol, C2 is 12,13 – dihydro-12,13-epoxybakuchiol.

### 5.3. Tyrosinase solution biosensor

#### 5.3.1. Standard experiment: Cyclic voltammetry of Tyrosinase and L-tyrosine in PBS buffer discussion and results

The cyclic voltammetry experiments were conducted with an Ag/AgCl reference electrode, a platinum wire auxiliary electrode, and a glassy carbon working electrode. The current response of L-tyrosine substrate at different concentrations measured by cyclic voltammetry at GC in 50mM PBS pH= 6.5 vs Ag/AgCl scan rate 50mV/s is shown in Figure 61. The black cyclic voltammogram labelled as 'PBS' represents the bare GCE, which is the background response at 50mV/s scan rate. When tyrosinase is added to the PBS solution, there was no change in current response observed, which indicated that tyrosinase itself did not show any redox behaviour. The current response represented by the red cyclic voltammogram labelled as 'PBS + TYR'. Upon addition of L-tyrosine, the cyclic voltammogram developed an oxidation peak that developed at 0.8 V vs Ag/AgCl. The oxidation peak at 0.8 V increased with the increase in concentration of L- tyrosine. This peak is attributed to the electrochemical oxidation of L-tyrosine by tyrosinase enzyme to form dopaquinone (Etsassala *et al.*, 2019). They reported the tyrosine oxidation peak at 890 mV and a corresponding reduction peak was observed at - 825 mV. The linear range for tyrosine oxidation by the enzyme present in solution, was determined to be 0.02 mM to 0.20 mM. The average limit of detection (LOD) was found to be 0.20 mM with a standard deviation value (STD, n=3) of 0.77 and a sensitivity of 12.64  $\mu\text{A}/\text{mM}$  (Figure 62).

UNIVERSITY of the  
WESTERN CAPE

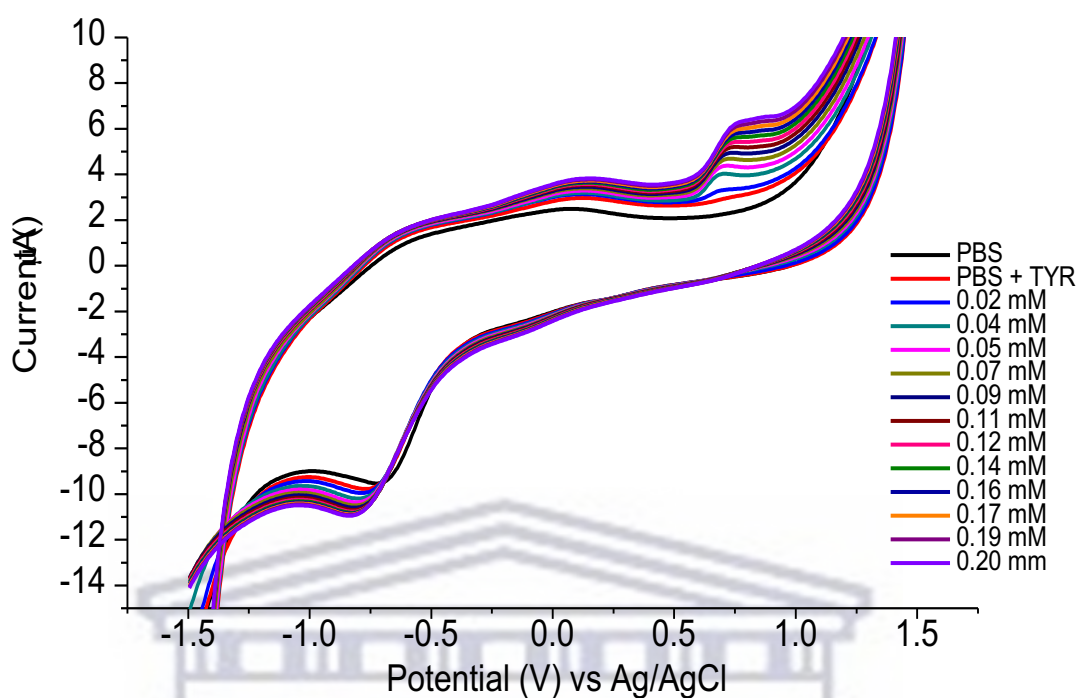


**Figure 61: Cyclic voltammetry of tyrosinase measured using a GCE in response to different concentrations of L-tyrosine in 50 mM PBS pH 6.5, vs Ag/AgCl, at a scan rate of 50mV/s.**

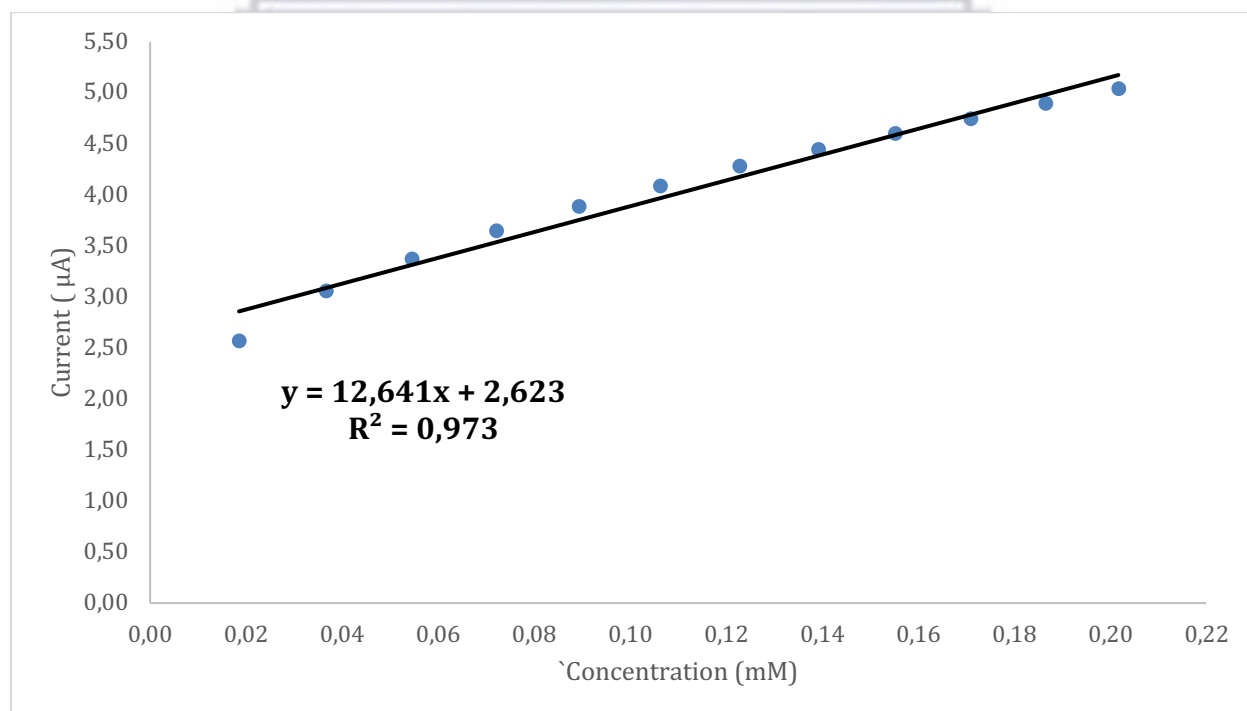


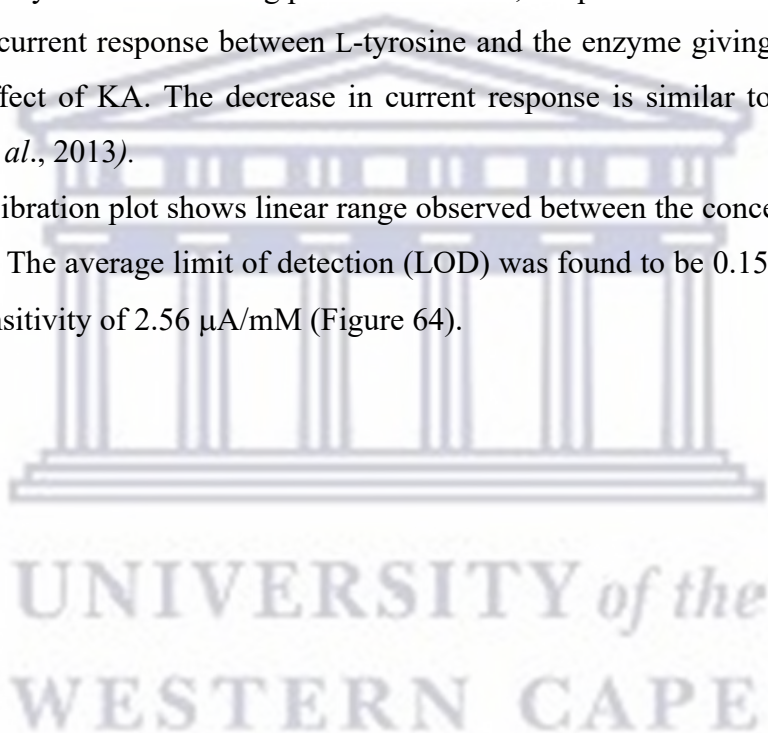
**Figure 62: Full calibration curve of current vs concentration of L-tyrosinase at GCE in 50 mM PBS pH 6.5, vs Ag/AgCl, at a scan rate of 50mV/s. , n = 3 measurements.**

### 5.3.2. Cyclic voltammetry of Tyrosinase, L-tyrosine and Kojic acid (TYR-KA-LTYR biosensor) in PBS buffer.

In Figure 63, the current response of tyrosinase and a fixed concentration of kojic acid (KA) in the presence of different concentrations of L-tyrosine substrate was measured using a GCE in 50 mM PBS pH = 6.5 vs Ag/AgCl scan rate 50mV/s is shown.

In the presence of KA which is a known competitive inhibitor for tyrosinase, we observe a decrease in current on first the addition of L-tyrosine. The decrease in current means that the KA has inhibited the enzyme response. In the previous experiment, Figure 61, in the absence of KA, a continuous increase in current for every addition of tyrosine was observed and that confirmed the catalysis reaction taking place. In this case, the presence of KA clearly effects a decrease in this current response between L-tyrosine and the enzyme giving an indication of the inhibition effect of KA. The decrease in current response is similar to that reported in literature (Xia *et al.*, 2013).

The resulting calibration plot shows linear range observed between the concentrations of 0.02 mM to 0.20mM. The average limit of detection (LOD) was found to be 0.15 mM with a STD of 0.14 and a sensitivity of 2.56  $\mu\text{A}/\text{mM}$  (Figure 64).



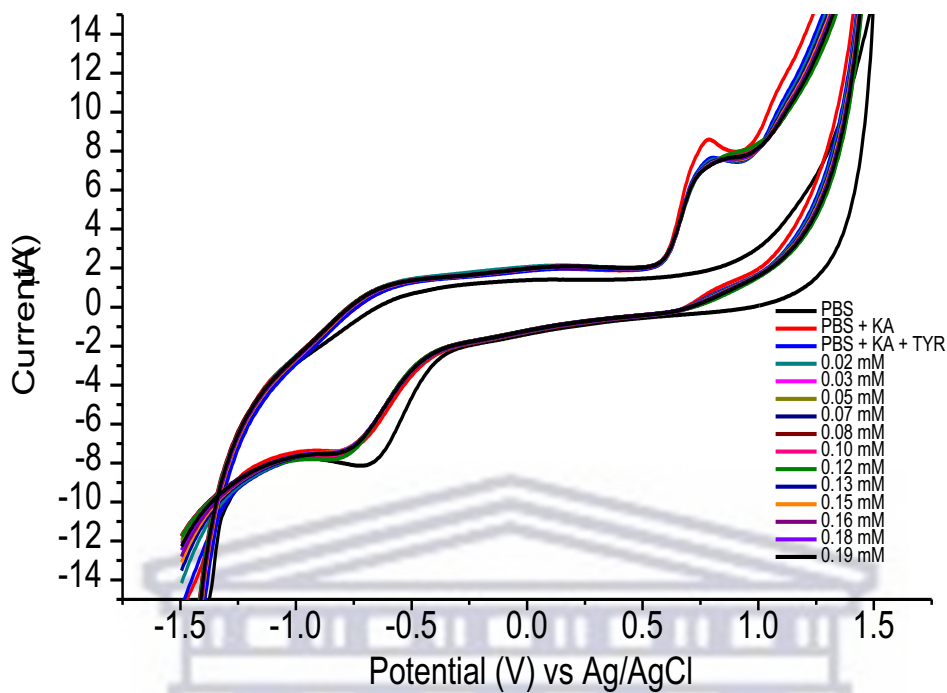


**Figure 63:** Cyclic voltammetry of tyrosinase measured using a GCE in response to a fixed concentration of KA and different concentrations of L-tyrosine in 50 mM PBS pH 6.5, vs Ag/AgCl, at a scan rate of 50mV/s.

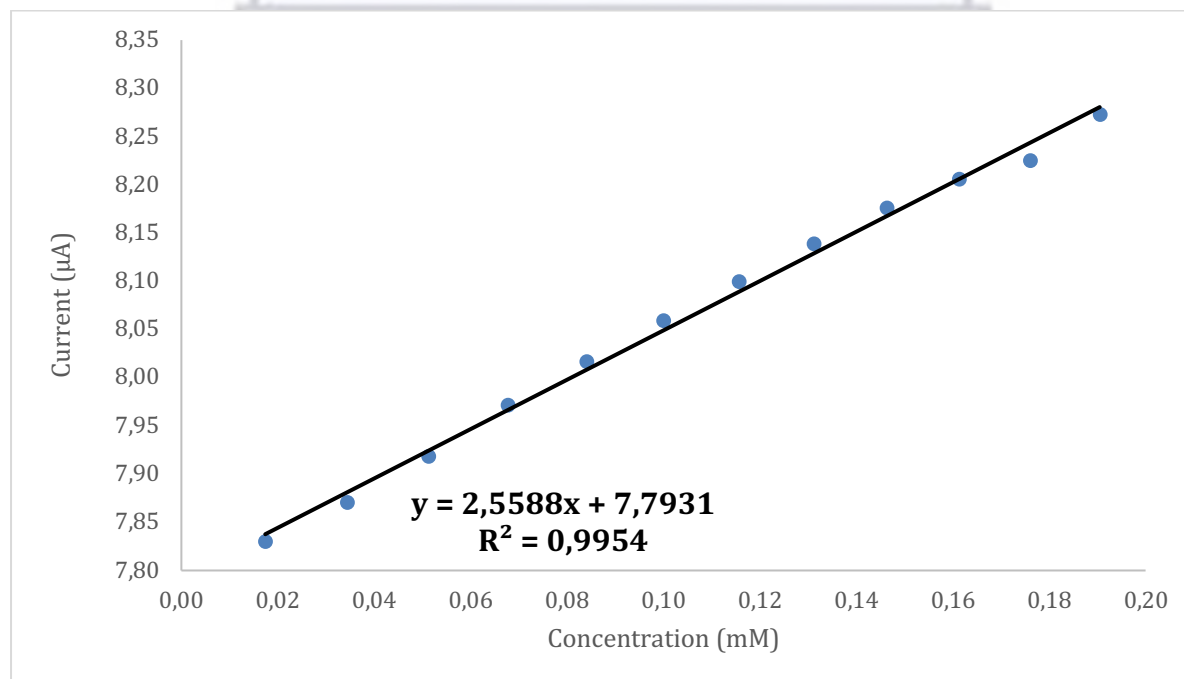


**Figure 64:** Full calibration curve of current vs concentration of L-tyrosinase at GCE in 50 mM PBS pH 6.5, vs Ag/AgCl, at a scan rate of 50mV/s. , n = 3 measurements.

### 5.3.3. Cyclic voltammetry of Tyrosinase and isolated compound in PBS buffer.

#### 5.3.3.1. Compound 1: Bakuchiol

In Figure 65, the electrochemical conversion of bakuchiol in the presence of the enzyme tyrosinase produced an oxidation peak at 0.5 V. There is a similarity in the bakuchiol chemical structure to that of L-tyrosine as the both have a hydroxyl functional group. Thus, the compound was expected to be catalysed by the enzyme. The sensor responds rapidly to the addition of bakuchiol indicating a biocatalytic activity taking place. The peak increases upon the addition of bakuchiol in the cell. However, bakuchiol chemical structure is inherently different to that of L-tyrosine and hence compared to Figure 61, the peak potential has shifted down, from 0.8 V to 0.5 V.

The resulting calibration plot Figure 66 evaluated the increase of tyrosinase current response to different concentrations of bakuchiol, from the lowest concentration 0.02 mM to 0.10 mM. The experiment was repeated  $n = 3$  times and the average LOD value of 0.10 mM with a STD value of 0.21 and sensitivity of  $6.75 \mu\text{A}/\text{mM}$ .

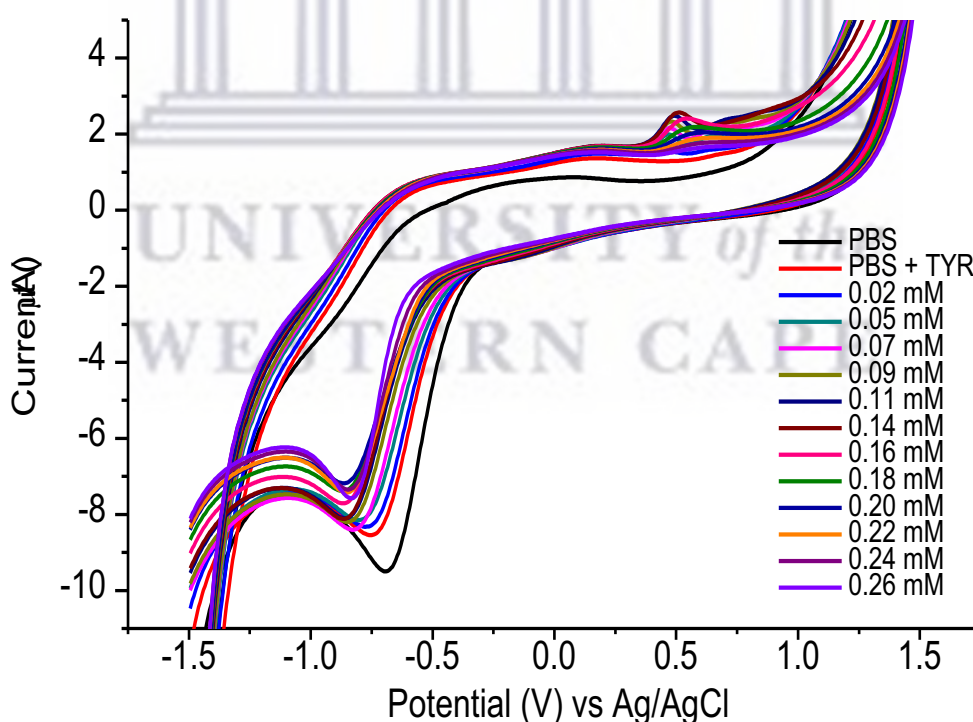


**Figure 65:** Cyclic voltammetry of tyrosinase measured using a GCE in response to different concentrations of bakuchiol in 50 mM PBS pH 6.5, vs Ag/AgCl, at a scan rate of 50mV/s.



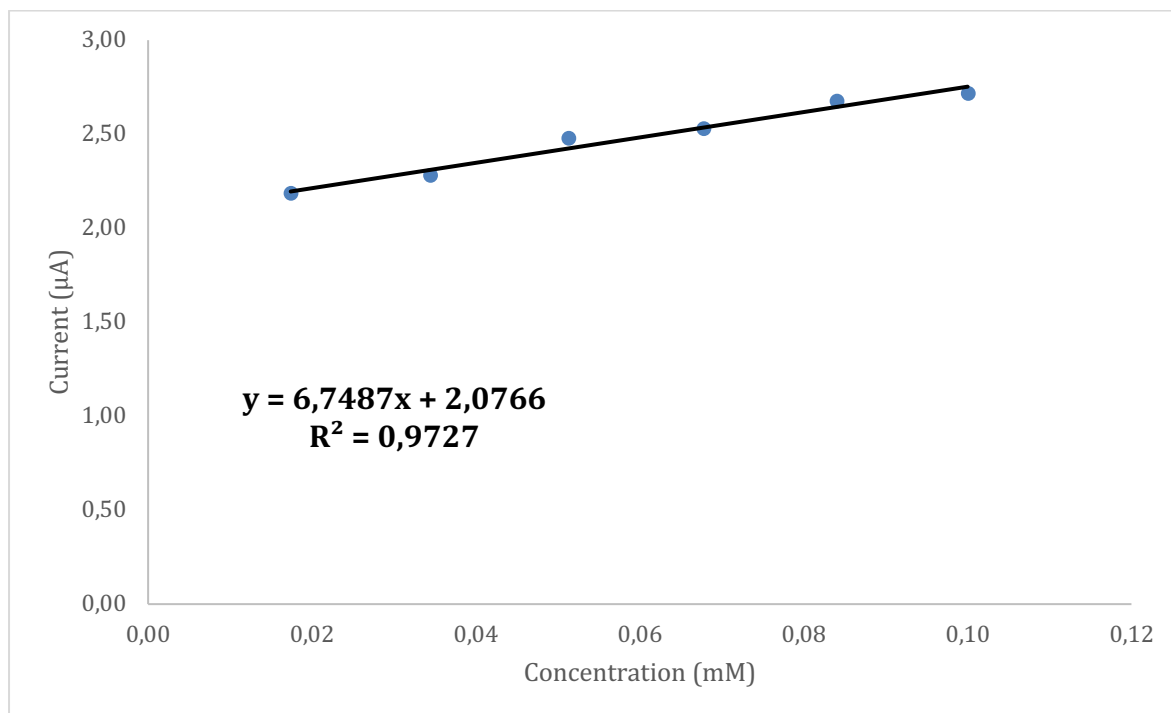


**Figure 66: Calibration curve of tyrosinase responding to different concentrations of bakuchiol as a substrate in 50 mM PBS pH = 6,5 at scan rate of 50mV/s using GCE vs Ag/AgCl.**

### 5.3.3.2. Compound 2 : 12,13-dihydro- 12,13- epoxybakuchiol

In Figure 67, the electrochemical conversion 12,13-dihydro- 12,13- epoxybakuchiol in the presence of tyrosinase enzyme produced an oxidation peak at 0.5V. 12,13-dihydro- 12,13- epoxybakuchiol has a similar chemical structure to that of bakuchiol, with the -OH functional group attached to the same position in the benzene ring. Thus, 12,13-dihydro- 12,13- epoxybakuchiol was expected to either inhibit tyrosinase enzyme similar to KA or shift the current to 0.5 V like bakuchiol. Figure 67 show the oxidation peak increases as the concentration increases to 0.10 mM. This peak was attributed to the catalytic activity of tyrosinase taking place.

The calibration curve in Figure 68 shows the current response of tyrosinase to different concentration of 12,13-dihydro- 12,13- epoxybakuchiol starting with the lowest concentration of 0.02 mM to 0.10 mM. The experiment was repeated n=3 times, the average LOD of 0.10 mM , STD value of 0.24, sensitivity of 7.75 µA/ mM and a correlation coefficient of 0.9645. The results showed a catalytic ability for the reduction of tyrosinase enzyme by 12,13- dihydro- 12,13- epoxybakuchiol. After the addition of 0.10 mM of 12,13-dihydro- 12,13- epoxybakuchiol, all of the enzyme was used up, therefore, no absorption was observed.

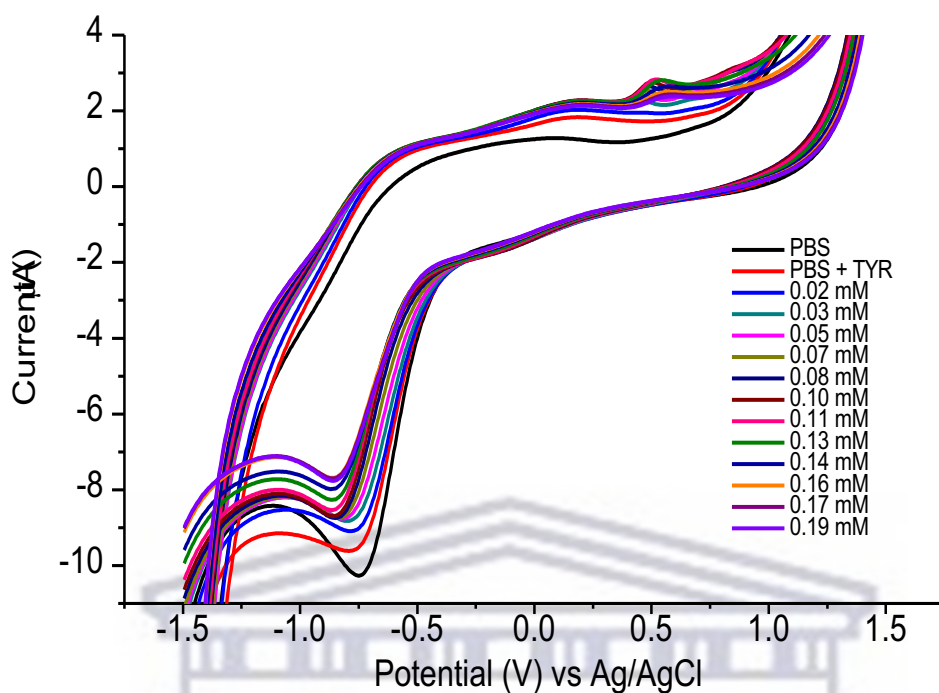


**Figure 67:** Cyclic voltammetry of tyrosinase in response to different concentrations of 12,13- dihydro- 12, 13 – epoxybakuchiol in 50 mM PBS pH = 6.5, at scan rate of 50mV/s using a GCE.

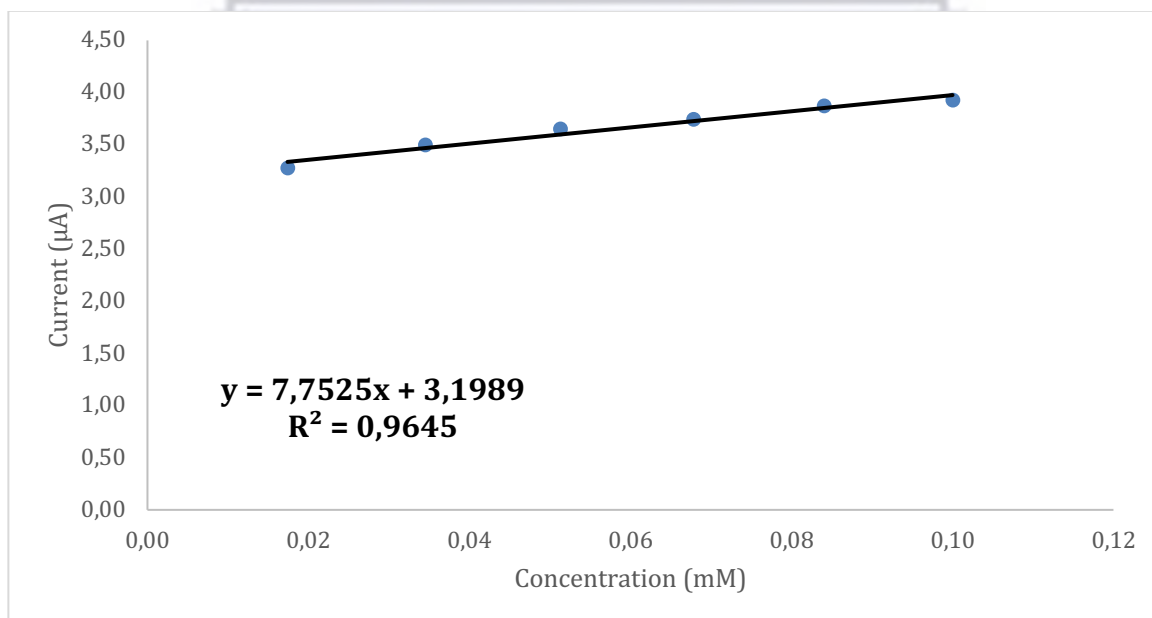


**Figure 68:** Calibration curve of tyrosinase responding to different concentrations of 12,13-dihydro- 12,13- epoxybakuchiol as a substrate in 50 mM PBS pH = 6,5 at scan rate of 50mV/s using GCE vs Ag/AgCl.

### 5.3.3.3. Compound 3: 3-Hydroxybakuchiol

3-Hydroxybakuchiol has a similar chemical structure to bakuchiol, with the difference being an additional hydroxy group attached to the benzene ring. The current response of tyrosinase in the presence of different concentrations of 3-hydroxybakuchiol was measured using a GCE in 50 mM PBS pH = 6.5 vs Ag/AgCl scan rate 50mV/s is shown in Figure 69. We observed an increase in current at a potential of 0.25V with each addition of 3-hydroxybakuchiol suggesting a catalysis reaction taking place.

The linear range was observed between the concentrations of 0.02 mM to 0.20 mM. The average limit of detection (LOD) was found to be 0.12 mM and the with a Standard deviation value (STD) of 0.49 and a sensitivity of 13.24  $\mu\text{A}/\text{mM}$  (Figure 70).

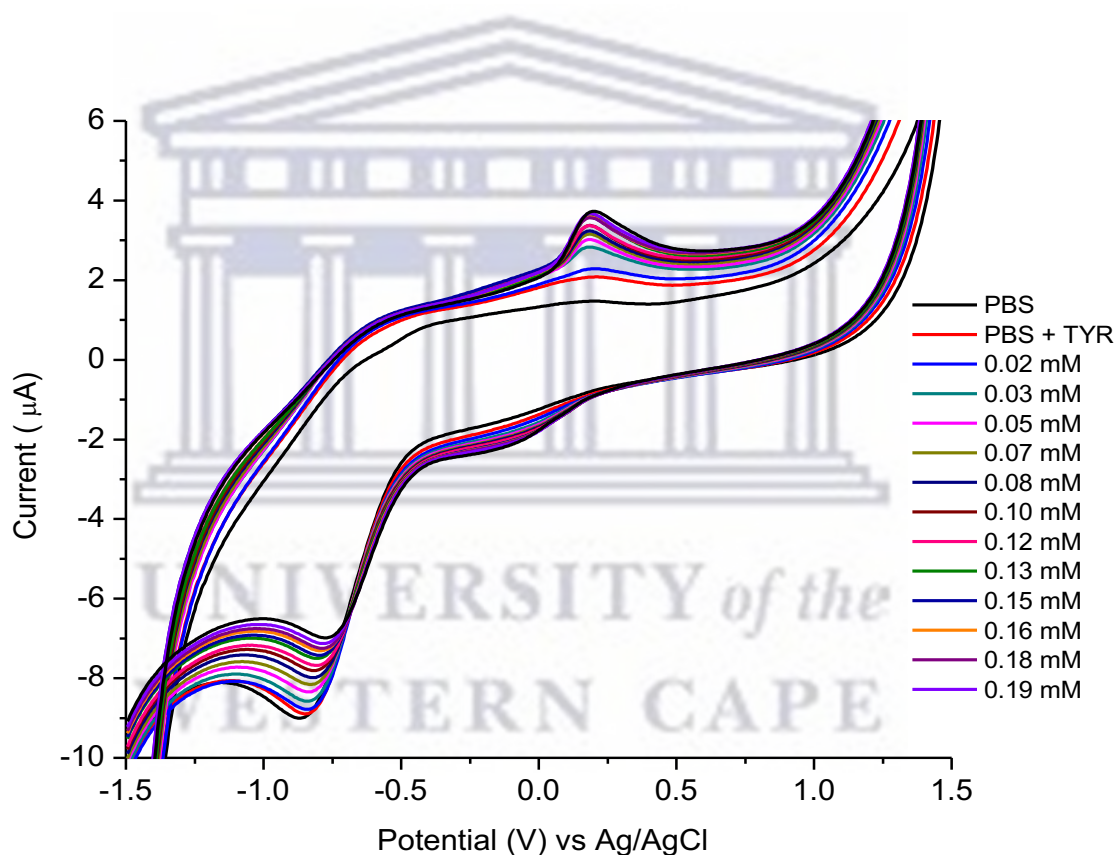


**Figure 69:** Cyclic voltammety of tyrosinase in response to different concentrations of 3-hydroxybakuchiol in 50 mM PBS pH = 6.5, at scan rate of 50mV/s using a GCE.

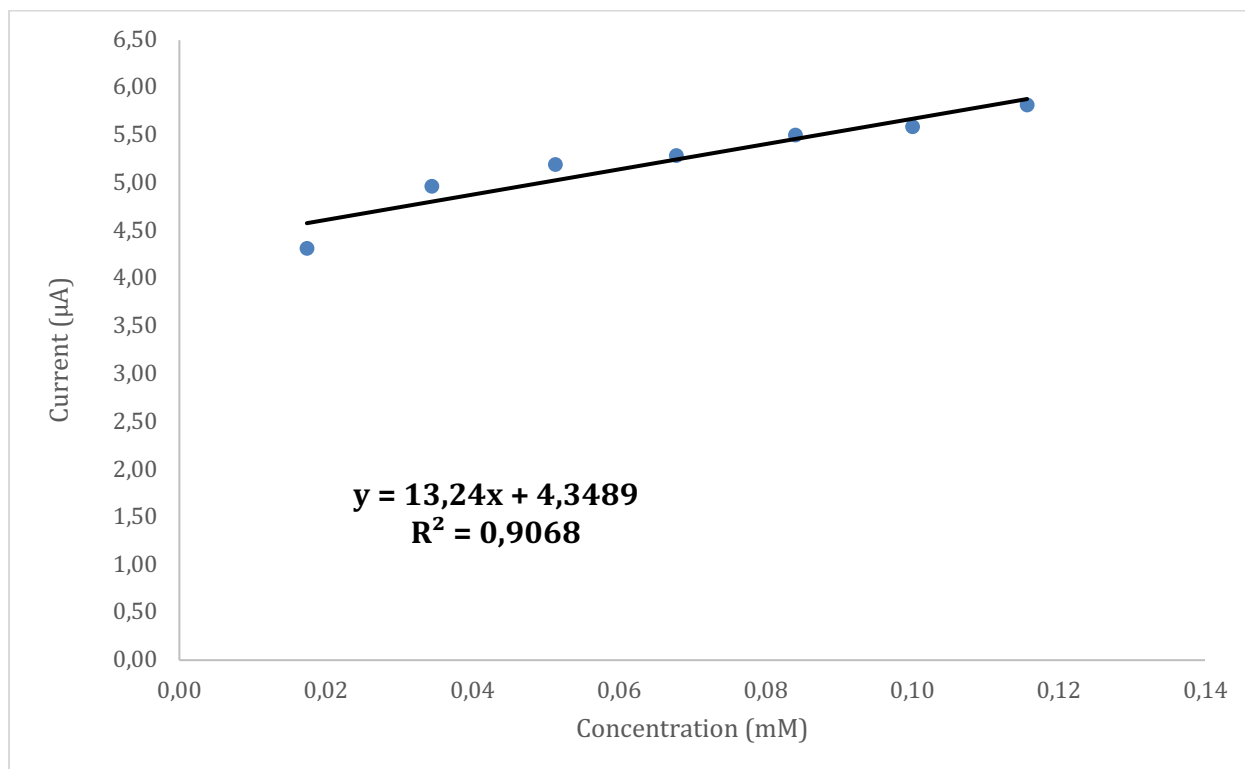


**Figure 70:** Scatter plot tyrosinase in response of different concentrations of 3-hydroxybakuchiol compound using 50 mM PBS electrolyte at scan rate of 50mV/s using a GCE.

#### 5.3.4. Summary

The table below gives a summary of tyrosinase inhibition biosensors (Table 23). We compared the sensitivity of the electrochemical oxidation response of isolated compounds as possible inhibitors in the presence of the known tyrosine/tyrosinase biosensor response established, to the effect to a known tyrosinase/ tyrosine systems established as the reference system. We used sensitivity as an indication of the selectivity towards the 3 isolated compounds and the correlation value ( $R^2$ ) to assess the liner association of the values. Kojic acid was evaluated to give the position of known inhibitor and all other compounds were compared to this reference inhibitor systems. Bakuchiol displayed the lowest sensitivity and a large positive linear association value. 12,13-dihydro-12,13-epoxybakuchiol had a sensitivity of 7.75  $\mu\text{A}/\text{mM}$  and low LOD value. The results were consistent with the reported results of the tyrosinase inhibition screening using ELISA method (in Chapter 5, 0:Tyrosinase inhibition Assay Results and Discussion; page 139).

**Table 23: Comparison of analytical electrochemical performance of isolated compounds compared to a known tyrosinase inhibitor, kojic acid and substrate L-tyrosine.**

<b>Experiment</b>	<b>Peak Potential (V)</b>	<b>LOD (mM)</b>	<b>R<sup>2</sup></b>	<b>Sensitivity (μA/ mM)</b>	<b>% Inhibition (%)</b>
<b>Tyrosinase + L-Tyrosine (uninhibited)</b>	0.8	0.20	0.9727	12.64	No inhibition
<b>Tyrosinase + KA + L-Tyrosine (known inhibitor)</b>	0.8	0.19	0.9954	2.56	79.74
<b>Tyrosinase+ Bakuchiol</b>	0.5	1.10	0.9727	6.75	46.59
<b>Tyrosinase + 12,13-dihydro- 12,13-epoxybakuchiol</b>	0.5	0.10	0.9645	7.75	38.69
<b>Tyrosinase + 3-Hydroxybakuchiol</b>	0.25	0.12	0.9068	13.24	No inhibition

Most tyrosinase inhibition studies reported in literature, report screen printed electrodes modified with tyrosinase enzyme by incubation or drop coating, for various biosensing applications, based on catalysis or inhibition (Zia *et al.*, 2013; Wang *et al.*, 1996 ). However, we have adopted the approach of a solution biosensor to eliminate transducer effects in the evaluation of the extracted compounds behavior.

## 5.4. Cytotoxicity of bakuchiol

Bakuchiol is a compound that was isolated from the methanolic extract of the indigenous South African plant *Psoralea aphylla*. The compound was evaluated to determine cytotoxic effect on B16 melanoma cells. B16 melanoma cells have been used in studies for discovering potent skin depigmenting agents (Tai *et al.*, 2009). Figure 71 shows the cytotoxicity of bakuchiol on B16 melanoma cells. The cell viability was reduced progressively with the increase in the bakuchiol concentration. The cell viability was completely inhibited at 100  $\mu\text{g}/\text{mL}$  of bakuchiol.

The Dose-Response-Inhibition of bakuchiol on B16 melanoma cells is shown in Figure 72. The graph shows that bakuchiol has an  $\text{IC}_{50}$  value of 11.66  $\mu\text{g}/\text{mL}$ .

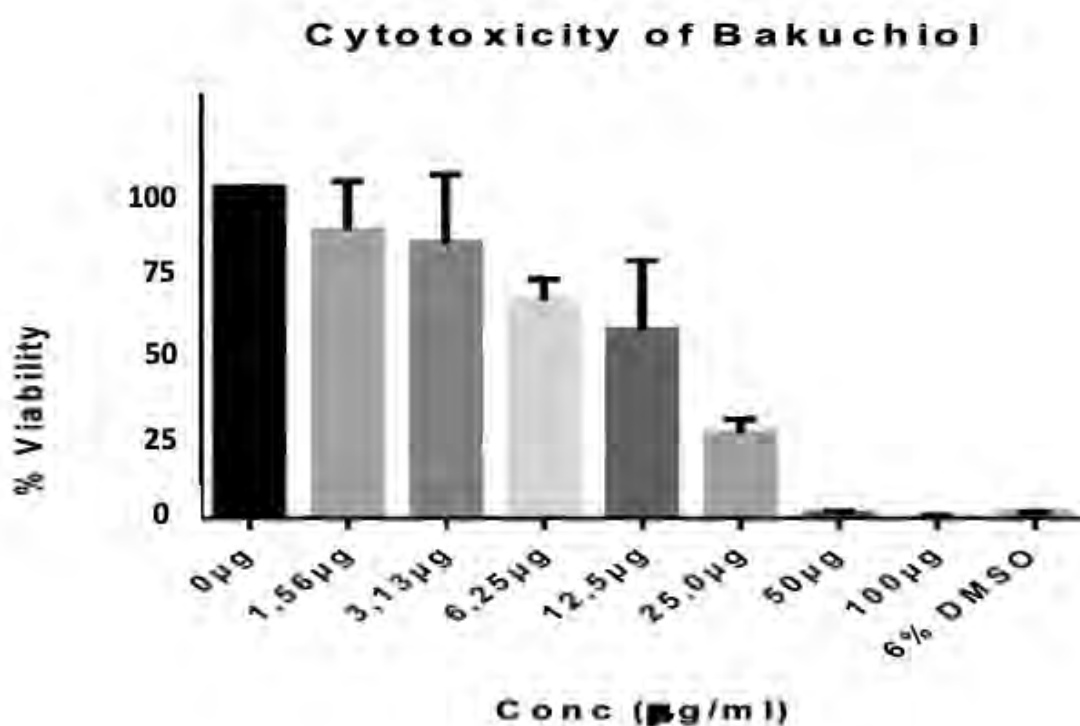


**Figure 71: Cytotoxicity of Bakuchiol on B16 Melanoma cells. The cells were treated with concentration between 1.56 – 100  $\mu\text{g}/\text{mL}$ , for 48 hours. Data are expressed as mean  $\pm$  SEM ( $n = 3$ ).**



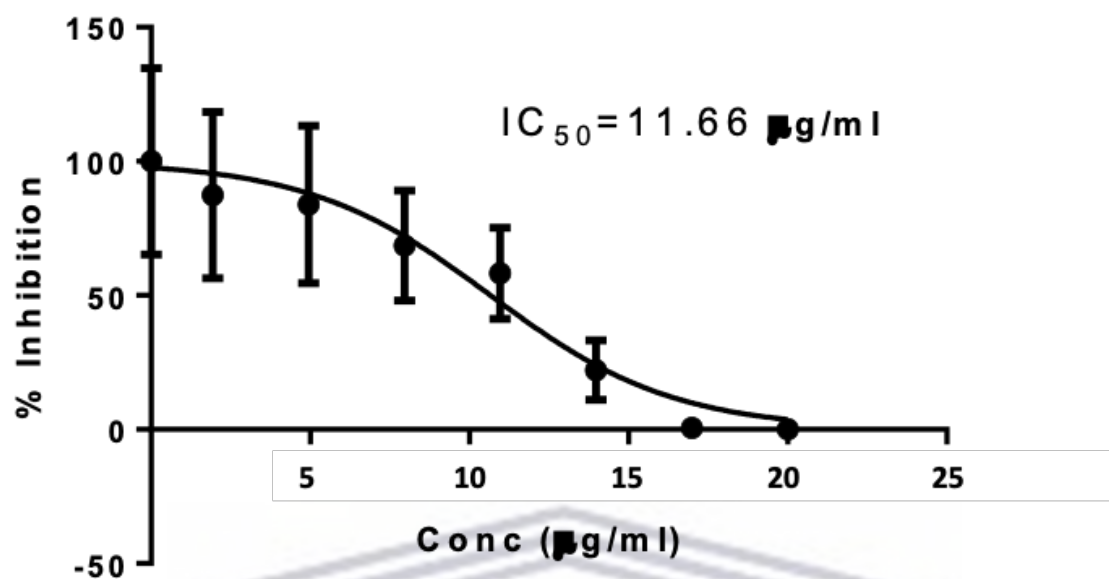


**Figure 72: Dose-Response-Inhibition of Bakuchiol on B16 Melanoma cells.**

Over the years, the usage of bakuchiol in skin care products has grown and keeps increasing.

In this study, the compound bakuchiol was found to be highly toxic to B16 melanoma cells.

---

# Chapter 6: Conclusion and recommendations

---

*This chapter presents the combined conclusion of the thesis work and of the results obtained as well as recommendations and future work.*

## 6.1. Discussion and Conclusion

In Part A, *Psoralea aphylla* plant was collected in Paarl, Western Cape in February 2018. The botanical specimens of the plant sample was submitted and identified by Prof. Christopher Cupido of Fort Hare University, Eastern Cape. The fresh plant was ground (664.5 g) and extracted using methanol and then filtered. The filtrate was concentrated in rotary evaporator to afford a crude extract (200.0 g) which was chromatographed by silica gel chromatography. Which led to isolation of compounds using column chromatography, high performance liquid chromatography and crystallization. The isolated compounds were identified as (C1) bakuchiol, (C2) 12,13- dihydro-12,13-epoxybakuchiol, (C3) 3-hydroxybakuchiol and a mixture of stigmasterol and  $\beta$ -sitosterol; on the basis of spectroscopic analysis and by comparing their physical properties reported in literature. This is the first time compounds have been isolated from a *Psoralea aphylla* plant.

In Part B, the methanolic extract and all four compounds were preliminarily screened using the ELISA tyrosinase inhibition assay for their tyrosinase inhibition activity and a new assay based on electrochemical reporting, was developed for the rapid screening of tyrosinase inhibitors. In both methods a known tyrosinase inhibitor, kojic acid was used as a positive control and L-tyrosine as the substrate. The ELISA assay results showed kojic acid to have a inhibition percentage 86.5 % at 50  $\mu\text{g/mL}$ , (C2) 12,13- dihydro-12,13-epoxybakuchiol had the highest inhibition percentage of 35.9% at 50  $\mu\text{g/mL}$ , bakuchiol showed a tyrosinase inhibition percentage of 21.7% / at 50  $\mu\text{g/mL}$  and 14.8 % at 50  $\mu\text{g/mL}$  and (C3) 3-hydroxybakuchiol showed a tyrosinase inhibition percentage of 9.4 % at 50  $\mu\text{g/mL}$ . However, the steroid mixture (C4) stigmasterol and sitosterol did not show any tyrosinase inhibition activity.

Electrochemistry was used to explore a possibility of a tyrosinase biosensor by testing the inhibition activity of monoterpenes isolated in a methanol extract of *Psoralea aphylla* on tyrosinase enzyme. The tyrosinase enzyme is responsible for the catalysing the oxidation of L-tyrosine to a quinone. Electrochemistry confirmed that bakuchiol had the highest inhibitory effect of the three compounds isolated (46.60%) followed closely by 12,13-dihydro-12,13-epoxybakuchiol (38.69%), whereas 3-hydroxybakuchiol showed no inhibitory response.

The graph below (Figure 73) shows a comparison between the inhibition % results obtained using the ELISA assay and inhibition % based on the sensitivity established from cyclic voltammetry.

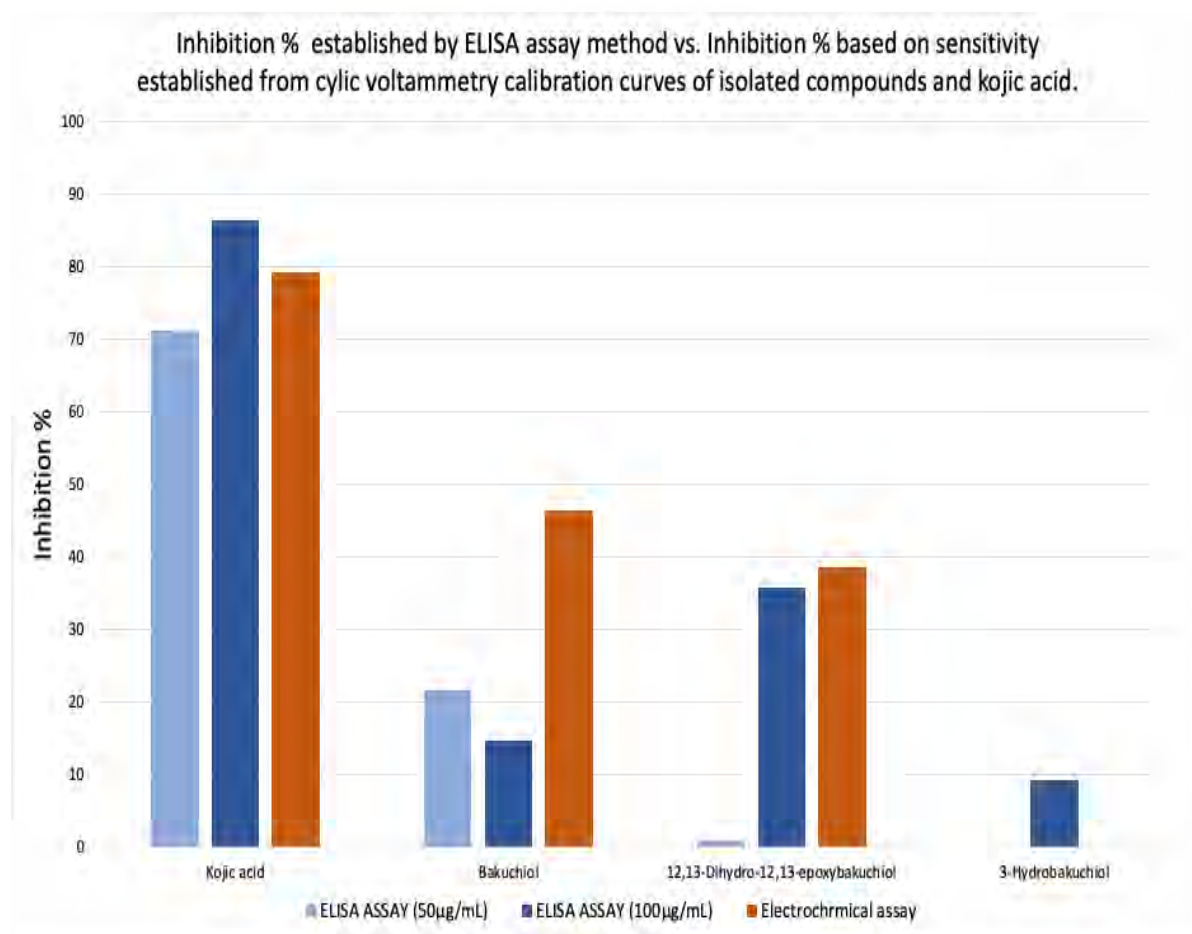


**Figure 73: Inhibition % established by ELISA assay method vs. % Inhibition based on sensitivity established from cyclic voltammetry calibration curves of isolated compounds and kojic acid.**

As expected, kojic acid showed a high inhibition effect in both methods. Bakuchiol and 3-12,13-dihydro-12,13-epoxybakuchiol showed a higher inhibition effects in the electrochemical method as compared to the ELISA method. Using the electrochemical method 3-

hydroxybakuchiol showed no inhibition effect and using the ELISA assay the compound showed low inhibition effect (9.4%).

Furthermore, the electrochemistry method was demonstrated to be quicker for pre-screening of potential tyrosinase inhibitors because it is not necessary to wait for 30 minute incubation period to check the absorbance needed to calculate the inhibition percentage. Other advantages of the electrochemistry method include simplicity, speed, sensitivity, relatively low cost and can lead to the development of portable tyrosinase inhibition screening devices. Thus, making the electrochemistry method a promising rapid method for pre-screening bioactive compounds and complex mixtures, such as plant extracts. The electrochemistry method can be amended in future to optimise the inhibition quantification. The amendments include testing other known tyrosinase inhibitors, screening more plant extracts, considering the use a paper-based tyrosinase biosensors and reducing size of biosensors.

In Part C, it was important to determine the cytotoxicity of bakuchiol to know whether bakuchiol is potentially harmful to humans and animals because bakuchiol being used in various skin products to treat skin diseases (such as wrinkles, pigmentation and anti-aging) as an alternative to retinoids (Chaudhuri and Bojanowski., 2014). Even though the compound is employed in the cosmetic industry for treatment of skin diseases, in this study the cytotoxicity of bakuchiol was investigated against B16 melanoma cells using MTT assay. Bakuchiol showed high cytotoxicity effect on B16 cells at an  $IC_{50}$  of 11.66  $\mu\text{g}/\text{mL}$ . The results agree with previous studies that evaluated the cytotoxicity effect of bakuchiol (Rangari *et al.*, 1992; Chaudhuri *et al.*, 2015).

## **6.2. Recommendations for further research**

The research efforts on *Psoralea aphylla* methanolic extracts indicate a promising potential for the native Southern African plant to provide bioactive components with potential pharmacological properties such as, antimicrobial, antifungal, antipregnancy, antiviral, antifibrogenic, anti-inflammatory, antimutagenic, antioxidant, antitumorigenic, cytotoxic, and antitumor activities. More cytotoxicity studies should be done on compounds that are already used in the cosmetic industry and skin care customers should be warned of the effects of commercialised ingredients used in skin products. A bioassay study should be done to isolate phytochemicals for specific bioactivities. Additional studies are necessary to examine the safety of topical application of bakuchiol.

Tyrosinase inhibitors are not only investigated for skin diseases but also to investigate pollutants water analysis, phenols in wine and in the medical field. Further improvement in tyrosinase biosensor includes using synthetic known tyrosinase inhibitors to work out a method that can be validated, investigating unknown samples (that could possibly have a mixture of inhibitors) as tyrosinase inhibitors . We also to need to further investigate if it would be better to immobilize the enzyme or use it while in solution. Gold nanoparticles can be incorporated in biosensors for screening tyrosinase inhibitors as they can act as nanoscale electrodes for small, simple, sensitive and stable electroanalytical procedures that can be used for faster detection of tyrosinase inhibitors (Sans *et al.*, 2005; Liu *et al.*, 2017).





### 6.3. References

1. Alam, F., Khan, G.N. and Asad, M.H.H.B., 2018. Psoralea corylifolia L: Ethnobotanical, biological, and chemical aspects: A review. *Phytotherapy research*, 32(4), pp.597-615.
2. Allen, O.N. and Allen, E.K., 1981. *The Leguminosae, a source book of characteristics, uses, and nodulation*. Univ of Wisconsin Press. pp.812. doi: 10.1007/BF02858721
3. Bequette, J.P., Jungong, C.S. and Novikov, A.V., 2009. Enantioselective synthesis of Bakuchiol using diazosulfonate C–H insertion to install the quaternary center. *Tetrahedron letters*, 50(50), pp.6963-6964.
4. Bio-rad. 2019. TC20™ Automated Cell Counter. [ONLINE] Available at: <https://www.bio-rad.com/en-za/product/tc20-automated-cell-counter?ID=M7FBG34VY>. [Accessed 18 November 2019].
5. Biosensors/Biodevice Applications. In *Non-Thermal Plasma Technology for Polymeric Materials* (pp. 409-437). Elsevier.
6. Bochot, C., Gouron, A., Bubacco, L., Milet, A., Philouze, C., Réglier, M., Serratrice, G., Jamet, H. and Belle, C., 2014. Probing kojic acid binding to tyrosinase enzyme: insights from a model complex and QM/MM calculations. *Chemical communications*, 50(3), pp.308-310.
7. Burnett, C.L., Bergfeld, W.F., Belsito, D.V., Hill, R.A., Klaassen, C.D., Liebler, D.C., Marks, J.G., Shank, R.C., Slaga, T.J., Snyder, P.W. and Andersen, F.A., 2010. Final report of the safety assessment of kojic acid as used in cosmetics. *International journal of toxicology*, 29(6\_suppl), pp.244S-273S.
8. Casey, G., 2002. Physiology of the skin. *Nursing Standard (through 2013)*, 16(34), p.47.
9. Cayme, J.M.C. and Ragasa, C.Y., 2004. Structure elucidation of  $\beta$ -stigmasterol and  $\beta$ -sitosterol from *Sesbania grandiflora* [Linn.] Pers. and  $\beta$ -carotene from *Heliotropium indicum* Linn. by NMR spectroscopy. *Kimika*, 20(1), pp.5-12.
10. Chang, T.S., 2009. An updated review of tyrosinase inhibitors. *International journal of molecular sciences*, 10(6), pp.2440-2475.
11. Chaudhuri, R.K. and Bojanowski, K., 2014. Bakuchiol: a retinol-like functional compound revealed by gene expression profiling and clinically proven to have anti-aging effects. *International journal of cosmetic science*, 36(3), pp.221-230.
12. Chaudhuri, R.K. and Marchio, F., 2011. Bakuchiol in the management of acne-affected skin. *Cosmetics and Toiletries*, 126(7), pp.502.



12. Chaudhuri, R.K., 2010. The miracle of retinol. *Soap Perfum. Cosmet*, pp.23-24.
13. Chaudhuri, R.K., 2015. Bakuchiol: A Retinol-Like Functional Compound, Modulating Multiple Retinol and Non-Retinol Targets. *Cosmeceuticals and Active Cosmetics*, pp.1-18.
14. Chen, Z., Jin, K., Gao, L., Lou, G., Jin, Y., Yu, Y. and Lou, Y., 2010. Anti-tumor effects of bakuchiol, an analogue of resveratrol, on human lung adenocarcinoma A549 cell line. *European journal of pharmacology*, 643(2-3), pp.170-179.
15. Cho, H., Jun, J.Y., Song, E.K., Kang, K.H., Baek, H.Y., Ko, Y.S. and Kim, Y.C., 2001. Bakuchiol: a hepatoprotective compound of *Psoralea corylifolia* on tacrine-induced cytotoxicity in Hep G2 cells. *Planta Medica*, 67(08), pp.750-751.
16. Chopra, B., Dhingra, A.K. and Dhar, K.L., 2013. *Psoralea corylifolia* L.(Buguchi)—folklore to modern evidence. *Fitoterapia*, 90, pp.44-56. doi: 10.1016/j.fitote.2013.06.016.
17. Chopra, B., Dhingra, A.K. and Dhar, K.L., 2013. *Psoralea corylifolia* L.(Buguchi)—folklore to modern evidence. *Fitoterapia*, 90, pp.44-56. doi: 10.1016/j.fitote.2013.06.016.
18. Clark, A.K. and Sivamani, R.K., 2016. Phytochemicals in the treatment of hyperpigmentation. *Botanics*, 6, pp.89.
19. Coleman, P.B. ed., 1993. *Practical sampling techniques for infrared analysis*. CRC Press.
20. Costin, G.E. and Hearing, V.J., 2007. Human skin pigmentation: melanocytes modulate skin color in response to stress. *The FASEB journal*, 21(4), pp.976-994.
21. Cowling, R.M. and Holmes, P.M., 1992. Endemism and speciation in a lowland flora from the Cape Floristic Region. *Biological Journal of the Linnean Society*, 47(4), pp.367-383.
22. del Torno-de Román, L., Alonso-Lomillo, M.A., Domínguez-Renedo, O. and Arcos-Martínez, M.J., 2016. Tyrosinase based biosensor for the electrochemical determination of sulfamethoxazole. *Sensors and Actuators B: Chemical*, 227, pp.48-53.
23. Deri, B., Kanteev, M., Goldfeder, M., Lecina, D., Guallar, V., Adir, N. and Fishman, A., 2016. The unravelling of the complex pattern of tyrosinase inhibition. *Scientific reports*, 6, pp.34993.
24. Dhaliwal, S., Rybak, I., Ellis, S.R., Notay, M., Trivedi, M., Burney, W., Vaughn, A.R., Nguyen, M., Reiter, P., Bosanac, S. and Yan, H., 2019. Prospective, randomized, double-blind assessment of topical bakuchiol and retinol for facial photoageing. *British Journal of Dermatology*, 180(2), pp.289-296.

25. Dlova, N.C., Hamed, S.H., Tsoka-Gwegweni, J. and Grobler, A., 2015. Skin lightening practices: an epidemiological study of South African women of African and Indian ancestries. *British Journal of Dermatology*, 173, pp.2-9
26. Dlova, N.C., Hendricks, N.E. and Martincgh, B.S., 2012. Skin-lightening creams used in Durban, South Africa. *Ethnic skin and hair disorders in kwaZulu-NataL*, p.37.
27. Dlodlu, M. N., Muasya, A. M., Chimphango, S. B. M. & Stirton, C. H. Taxonomy of the southern African Psoralea aphylla complex (Psoraleeae, Leguminosae). *South African J. Bot.* 97, 77–100 (2015).
28. Doyle, J. J. (2001) 'Leguminosae', *Encyclopedia of Genetics*, (around 3000), pp. 1081–1085. doi: 10.1006/rwgn.2001.1642.
29. Doyle, J. J., 2001. 'Leguminosae', *Encyclopedia of Genetics*, (around 3000), pp. 1081–1085. doi: 10.1006/rwgn.2001.1642.
30. Elbagory, A.M., 2015. *Chemical and biological evaluation of palythoa tuberculosa collected from the red sea* (Doctoral dissertation, University of the Western Cape).
31. Etsassala, N.G., Waryo, T., Popoola, O.K., Adeloye, A.O., Iwuoha, E.I. and Hussein, A.A., 2019. Electrochemical screening and evaluation of lamiaceae plant species from South Africa with potential tyrosinase activity. *Sensors*, 19(5), pp.1035.
32. George, J., Laing, M.D. and Drewes, S.E., 2001. Phytochemical research in South Africa. *South African Journal of Science*, 97(3-4), pp.93-105.
33. Govindarajan, P. and D.V.L, S., 2011. Isolation and characterization of stigmasterol and b-sitosterol from *Acacia nilotica* (L.) Delile ssp *Indica* (benth.)Brenan. *Journal of Pharmacy Research*, 4(10), pp. 3601-3602
34. Grieshaber, D., MacKenzie, R., Vörös, J. and Reimhult, E., 2008. Electrochemical biosensors-sensor principles and architectures. *Sensors*, 8(3), pp.1400-1458.
35. Heitz, M.P. and Rupp, J.W., 2018. Determining mushroom tyrosinase inhibition by imidazolium ionic liquids: a spectroscopic and molecular docking study. *International journal of biological macromolecules*, 107, pp.1971-1981.
36. Iwamura, J., Dohi, T., Tanaka, H., Odani, T. and Kubo, M., 1989. Cytotoxicity of corylifoliae fructus. II. Cytotoxicity of bakuchiol and the analogues. *Yakugaku zasshi: Journal of the Pharmaceutical Society of Japan*, 109(12), pp.962-965.
37. Jiangning, G. et al. (2005) 'Antioxidants from a Chinese medicinal herb - *Psoralea corylifolia* L.', *Food Chemistry*, 91(2), pp. 287–292. doi: 10.1016/j.foodchem.2004.04.029.

38. Jiangning, G., Xinchu, W., Hou, W., Qinghua, L. and Kaishun, B., 2005. Antioxidants from a Chinese medicinal herb—*Psoralea corylifolia* L. *Food chemistry*, 91(2), pp.287-292.
39. Jothi, L. and Nageswaran, G., 2019. Plasma Modified Polymeric Materials for Biosensors/Biodevice Applications. In *Non-Thermal Plasma Technology for Polymeric Materials* (pp. 409-437). Elsevier.
40. Kanitakis, J., 2002. Anatomy, histology and immunohistochemistry of normal human skin. *European journal of dermatology*, 12(4), pp.390-401.
41. Kim, J.Y., Kim, J.Y., Jenis, J., Li, Z.P., Ban, Y.J., Baiseitova, A. and Park, K.H., 2019. Tyrosinase inhibitory study of flavonolignans from the seeds of *Silybum marianum* (Milk thistle). *Bioorganic & medicinal chemistry*, 27(12), pp.2499-2507.
42. Kim, S.S., Hyun, C.G., Choi, Y.H. and Lee, N.H., 2013. Tyrosinase inhibitory activities of the compounds isolated from *Neolitsea aciculata* (Blume) Koidz. *Journal of enzyme inhibition and medicinal chemistry*, 28(4), pp.685-689.
43. Koul, B., Taak, P., Kumar, A., Kumar, A. and Sanyal, I., 2018. Genus *Psoralea* A review of the traditional and modern uses, phytochemistry and pharmacology. *Journal of ethnopharmacology*.
44. Koul, B., Taak, P., Kumar, A., Kumar, A. and Sanyal, I., 2019. Genus *Psoralea*: a review of the traditional and modern uses, phytochemistry and pharmacology. *Journal of ethnopharmacology*, 232, pp.201-226. . doi: 10.1016/j.jep.2018.11.036.
45. Kubo, M., Dohi, T., Odani, T., Tanaka, H. and Iwamura, J., 1989. Cytotoxicity of *Corylifoliae* Fructus. I. Isolation of the effective compound and the cytotoxicity. *Yakugaku zasshi: Journal of the Pharmaceutical Society of Japan*, 109(12), pp.926-931.
46. Kumar, N. and Upadhyay, L.S., 2018. Polymeric gels for biosensing applications. In *Polymeric Gels* (pp. 487-503).
47. Labbé, C., Faini, F., Coll, J. and Connolly, J.D., 1996. Bakuchiol derivatives from the leaves of *Psoralea glandulosa*. *Phytochemistry*, 42(5), pp.1299-1303.
48. Lall, N., Mogapi, E., De Canha, M.N., Crampton, B., Nqephe, M., Hussein, A.A. and Kumar, V., 2016. Insights into tyrosinase inhibition by compounds isolated from *Greyia radlkoferi* Szyszyl using biological activity, molecular docking and gene expression analysis. *Bioorganic & medicinal chemistry*, 24(22), pp.5953-5959.
49. Lampman, G.M., Kriz, G.S. and Vyvyan, J.R., 2001. *Introduction to spectroscopy: A guide for students of organic chemistry*. 3<sup>rd</sup> edn, Harcourt College Publishers, pp. 267-292.

50. Lewis G, Schrire B, Mackinder B, Lock M. (2005) 'Legumes of the world. Royal Botanical Gardens, Kew, UK Louarn
51. Li, C.C., Wang, T.L., Zhang, Z.Q., Yang, W.Q., Wang, Y.F., Chai, X., Wang, C.H. and Li, Z., 2016. Phytochemical and pharmacological studies on the genus *Psoralea*: a mini review. *Evidence-Based Complementary and Alternative Medicine*, 2016.
52. Li, J. and Zhiling, X., 1995. Review of Constituents in Fruits of *Psoralea corylifolia* L.[J]. *China Journal of Chinese Materia Medica*, 2.
53. Li, Y. G. et al. (2015) 'Fructus *Psoraleae* contains natural compounds with potent inhibitory effects towards human carboxylesterase 2', *Fitoterapia*. Elsevier B.V., 101, pp. 99–106. doi: 10.1016/j.fitote.2015.01.004.
54. Li, Y.G., Hou, J., Li, S.Y., Lv, X., Ning, J., Wang, P., Liu, Z.M., Ge, G.B., Ren, J.Y. and Yang, L., 2015. Fructus *Psoraleae* contains natural compounds with potent inhibitory effects towards human carboxylesterase 2. *Fitoterapia*, 101, pp.99-106. doi: 10.1016/j.fitote.2015.01.004.
55. Lima, C., Silva, J., de Tássia Carvalho Cardoso, É., Silva, E., Lameira, J., do Nascimento, J., do Socorro Barros Brasil, D. and Alves, C., 2014. Combined kinetic studies and computational analysis on kojic acid analogs as tyrosinase inhibitors. *Molecules*, 19(7), pp.9591-9605.
56. Liu, B.W., Huang, P.C., Li, J.F. and Wu, F.Y., 2017. Colorimetric detection of tyrosinase during the synthesis of kojic acid/silver nanoparticles under illumination. *Sensors and Actuators B: Chemical*, 251, pp.836-841.
57. Mabbott, G.A., 1983. An introduction to cyclic voltammetry. *Journal of Chemical education*, 60(9), p.697.
58. Mabona, U. and Van Vuuren, S.F., 2013. Southern African medicinal plants used to treat skin diseases. *South African Journal of Botany*, 87, pp.175-193. doi: 10.1016/j.sajb.2013.04.002.
59. Mahendra, A.A., Bandara, G.K., Rohinie, G.A. and Disala, J.C., 2012. Studies on the composition and standardization of 'Bakuchi Oil', an ayurvedic medicinal oil prepared from *psoralea corylifolia* L. used in the treatment of Vitiligo. *International journal of research in Ayurveda and pharmacy*, 3, pp.411-415.
60. Maisch, J.M.(1889) Useful plants of the genus *Psoralea*. *American J Pharm*, 61, pp 500–503.

61. Majeed, R., Reddy, M.V., Chinthakindi, P.K., Sangwan, P.L., Hamid, A., Chashoo, G., Saxena, A.K. and Koul, S., 2012. Bakuchiol derivatives as novel and potent cytotoxic agents: A report. *European journal of medicinal chemistry*, 49, pp.55-67.
62. Mapunya, M.B., Nikolova, R.V. and Lall, N., 2012. Melanogenesis and antityrosinase activity of selected South African plants. *Evidence-Based Complementary and Alternative Medicine*, 2012.
63. Masika, P.J. and Afolayan, A.J., 2002. Antimicrobial activity of some plants used for the treatment of livestock disease in the Eastern Cape, South Africa. *Journal of Ethnopharmacology*, 83(1-2), pp.129-134. doi: 10.1016/S0378-8741(02)00242-8.
64. Matos, M.J., Santana, L., Uriarte, E., Abreu, O.A., Molina, E. and Yordi, E.G., 2015. Coumarins—an important class of phytochemicals. In *Phytochemicals-Isolation, Characterisation and Role in Human Health*. IntechOpen.
65. Momtaz, S., Mapunya, B.M., Houghton, P.J., Edgerly, C., Hussein, A., Naidoo, S. and Lall, N., 2008. Tyrosinase inhibition by extracts and constituents of *Sideroxylon inerme* L. stem bark, used in South Africa for skin lightening. *Journal of Ethnopharmacology*, 119(3), pp.507-512.
66. Morgan, D.M., 1998. Tetrazolium (MTT) assay for cellular viability and activity. In *Polyamine protocols*, pp. 179-184. Humana Press.
67. Nofel, M. (2016) 'Leguminosae family tree', ResearchGate, (February), pp. 11–29.
68. Noh, J.M., Kwak, S.Y., Seo, H.S., Seo, J.H., Kim, B.G. and Lee, Y.S., 2009. Kojic acid–amino acid conjugates as tyrosinase inhibitors. *Bioorganic & medicinal chemistry letters*, 19(19), pp.5586-5589.
69. Nostro, A., Germano, M.P., D'angelo, V., Marino, A. and Cannatelli, M.A., 2000. Extraction methods and bioautography for evaluation of medicinal plant antimicrobial activity. *Letters in applied microbiology*, 30(5), pp.379-384.
70. Pae, H.O., Cho, H., Oh, G.S., Kim, N.Y., Song, E.K., Kim, Y.C., Yun, Y.G., Kang, C.L., Kim, J.D., Kim, J.M. and Chung, H.T., 2001. Bakuchiol from *Psoralea corylifolia* inhibits the expression of inducible nitric oxide synthase gene via the inactivation of nuclear transcription factor- $\kappa$ B in RAW 264.7 macrophages. *International immunopharmacology*, 1(9-10), pp.1849-1855.
71. Palchetti, I., Hansen, P.D. and Barcelo, D., 2017. *Past, Present and Future Challenges of Biosensors and Bioanalytical Tools in Analytical Chemistry: A Tribute to Professor Marco Mascini* (Vol. 77). Elsevier.



72. Park, M.H., Kim, J.H., Chung, Y.H. and Lee, S.H., 2016. Bakuchiol sensitizes cancer cells to TRAIL through ROS-and JNK-mediated upregulation of death receptors and downregulation of survival proteins. *Biochemical and biophysical research communications*, 473(2), pp.586-592.
73. Parkhey, P. and Mohan, S.V., 2019. Biosensing Applications of Microbial Fuel Cell: Approach Toward Miniaturization. In *Microbial Electrochemical Technology* (pp. 977-997). Elsevier.
74. Patrick, G.L. 2005. An Introduction to Medicinal Chemistry. Oxford University Press Inc., New York, pp. 161-184.
75. Peng, G.P., Wu, P.H., Li, H.Y. and Yuan, Y.T., 1996. Chemical studies on *Psoralea corylifolia*. *Journal of Chinese Medicine Materia*, 25(11), pp.563-565.
76. Pierre, L.L. and Moses, M.N., 2015. Isolation and characterisation of stigmaterol and  $\beta$ -sitosterol from *Odontonema strictum* (acanthaceae). *Journal of Innovations in Pharmaceuticals and Biological Sciences*, 2(1), pp.88-95.
77. Qu, Z., Na, W., Liu, X., Liu, H. and Su, X., 2018. A novel fluorescence biosensor for sensitivity detection of tyrosinase and acid phosphatase based on nitrogen-doped graphene quantum dots. *Analytica chimica acta*, 997, pp.52-59.
78. Rajput, A.P. and Rajput, T.A., 2012. Isolation of stigmaterol and  $\beta$ -sitosterol from chloroform extract of leaves of *Corchorus fascicularis* Lam. *Int J Biol Chem*, 6(4), pp.130-135.
79. Rangari, V.D. and Agrawal, S.R., 1992. Chemistry & Pharmacology of *Psoralea Corylifolia*. *Indian drugs-bombay-*, 29, pp.662-662.
80. Riss, T.L., Moravec, R.A., Niles, A.L., Duellman, S., Benink, H.A., Worzella, T.J. and Minor, L., 2016. Cell viability assays. In *Assay Guidance Manual [Internet]*. Eli Lilly & Company and the National Center for Advancing Translational Sciences.
81. Riviere, J.E. and Monteiro-Riviere, N.A., 2005. *Dermal absorption models in toxicology and pharmacology*. CRC Press. pp. 3-4.
82. Sanz, V.C., Mena, M.L., González-Cortés, A., Yanez-Sedeno, P. and Pingarrón, J.M., 2005. Development of a tyrosinase biosensor based on gold nanoparticles-modified glassy carbon electrodes: Application to the measurement of a bioelectrochemical polyphenols index in wines. *Analytica Chimica Acta*, 528(1), pp.1-8.
83. Sawant, S.N., 2017. Development of Biosensors From Biopolymer Composites. In *Biopolymer Composites in Electronics* (pp. 353-383). Elsevier.



84. Schutte, A.L., 2000. Fabaceae. In: Goldblatt, P., Manning, P. (Eds.), *Plants of the Cape Flora*. Strelitzia, vol. 9, p. 505.
85. Scognamiglio, V., Rea, G., Arduini, F. and Palleschi, G., 2016. *Biosensors for Sustainable Food-New Opportunities and Technical Challenges* (Vol. 74). Elsevier.
86. Sendovski, M., Kanteev, M., Ben-Yosef, V.S., Adir, N. and Fishman, A., 2011. First structures of an active bacterial tyrosinase reveal copper plasticity. *Journal of molecular biology*, 405(1), pp.227-237.
87. Shukla, S.K., Govender, P.P. and Tiwari, A., 2016. Polymeric Micellar Structures for Biosensor Technology. In *Advances in Biomembranes and Lipid Self-Assembly* (Vol. 24, pp. 143-161). Academic Press.
88. Shukla, S.K., Govender, P.P. and Tiwari, A., 2016. Polymeric Micellar Structures for Biosensor Technology. In *Advances in Biomembranes and Lipid Self-Assembly* (Vol. 24, pp. 143-161). Academic Press.
89. Stapelberg, J., Nqephe, M., Lambrechts, I., Crampton, B. and Lall, N., 2019. Selected South African plants with tyrosinase enzyme inhibition and their effect on gene expression. *South African journal of botany*, 120, pp.280-285.
90. Talukdar, D., 2013. Leguminosae, in Stanley Maloy and Kelly Hughes (ed.) *Brenner's Encyclopedia of Genetics*. 2nd edn. University of Calcutta, Uttarpara, West Bengal, India: Elsevier, pp. 212–216. doi: 10.1016/B978-0-12-374984-0.00854-8.
91. Tai, S.S.K., Lin, C.G., Wu, M.H. and Chang, T.S., 2009. Evaluation of depigmenting activity by 8-hydroxydaidzein in mouse B16 melanoma cells and human volunteers. *International journal of molecular sciences*, 10(10), pp.4257-4266.
92. Tan, G., Yang, T., Miao, H., Chen, H., Chai, Y. and Wu, H., 2015. Characterization of compounds in *Psoralea corylifolia* using high-performance liquid chromatography diode array detection, time-of-flight mass spectrometry and quadrupole ion trap mass spectrometry. *Journal of chromatographic science*, 53(9), pp.1455-1462.
93. Tang, L., Zeng, G., Liu, J., Xu, X., Zhang, Y., Shen, G., Li, Y. and Liu, C., 2008. Catechol determination in compost bioremediation using a laccase sensor and artificial neural networks. *Analytical and bioanalytical chemistry*, 391(2), pp.679-685.
94. Taylor, J. E., Lee, S. & Crous, P. W. Biodiversity in the Cape Floral Kingdom: Fungi occurring on Proteaceae. *Mycol. Res.* 105, 1480–1484 (2001).
95. Truong, D.H., Nguyen, D.H., Ta, N.T.A., Bui, A.V., Do, T.H. and Nguyen, H.C., 2019. Evaluation of the use of different solvents for phytochemical constituents, antioxidants,

- and in vitro anti-inflammatory activities of *Severinia buxifolia*. *Journal of food quality*, 2019
96. Tsai, Y.C. and Chiu, C.C., 2007. Amperometric biosensors based on multiwalled carbon nanotube-Nafion-tyrosinase nanobiocomposites for the determination of phenolic compounds. *Sensors and Actuators B: Chemical*, 125(1), pp.10-16.
  97. Ullah, S., Park, C., Ikram, M., Kang, D., Lee, S., Yang, J., Park, Y., Yoon, S., Chun, P. and Moon, H.R., 2019. Tyrosinase inhibition and anti-melanin generation effect of cinnamamide analogues. *Bioorganic chemistry*, 87, pp.43-55.
  98. Van Wyk, B.E., 2011. The potential of South African plants in the development of new food and beverage products. *South African Journal of Botany*, 77(4), pp.857-868.
  99. Van Wyk, B.E., Oudtshoorn, B.V. and Gericke, N., 1997. *Medicinal Plants of South Africa*, pp. 7-22. Briza
  100. Wanda, G. J. M. K., Njamen, D. and Gamo, F. Z., 2015. Medicinal plants of the family of Fabaceae used to treat various ailments', in Garza, W. *Fabaceae classification, nutrient composition and health benefits*, 1, pp. 1–20.
  101. Wang, J., 2006. *Analytical electrochemistry*. 3rd ed. Hoboken, N.J.: Wiley-VCH, pp.29-30.
  102. Wang, J., 2006. Electrochemical biosensors: towards point-of-care cancer diagnostics. *Biosensors and Bioelectronics*, 21(10), pp.1887-1892.
  103. Wang, J., 2006. Electrochemical biosensors: towards point-of-care cancer diagnostics. *Biosensors and Bioelectronics*, 21(10), pp.1887-1892.
  104. Wang, J., Nascimento, V.B., Kane, S.A., Rogers, K., Smyth, M.R. and Angnes, L., 1996. Screen-printed tyrosinase-containing electrodes for the biosensing of enzyme inhibitors. *Talanta*, 43(11), pp.1903-1907.
  105. Wang, Y., Curtis-Long, M.J., Lee, B.W., Yuk, H.J., Kim, D.W., Tan, X.F. and Park, K.H., 2014. Inhibition of tyrosinase activity by polyphenol compounds from *Flemingia philippinensis* roots. *Bioorganic & medicinal chemistry*, 22(3), pp.1115-1120.
  106. Wee, Y., Park, S., Kwon, Y.H., Ju, Y., Yeon, K.M. and Kim, J., 2019. Tyrosinase-immobilized CNT based biosensor for highly-sensitive detection of phenolic compounds. *Biosensors and Bioelectronics*, 132, pp.279-285.
  107. Wojciechowski M.F., 2003. Reconstructing the phylogeny of legume (Leguminosae): an early 21st century perspective In: B.B. Klitgaard and A. Bruneau (editors). *Advances in legume Systematics*, part 10, Higher Level Systematics. Royal Botanic Gardens, Kew. 5-35.

108. Xi-yuan, W. and Jian-xin, W., 2007. Synergistic Effect of Psoralen Cooperated with Substrates on Tyrosinase Activation. *Natural Product Research & Development*, 19(1).
109. Xia, N., Zhang, L.P., Feng, Q.Q., Deng, D.H., Sun, X.L. and Liu, L., 2013. Amplified voltammetric detection of tyrosinase and its activity with dopamine-gold nanoparticles as redox probes. *Int J Electrochem Sc*, 8(4), pp.5487-5495.
110. Yan, X., Hu, T., Wang, L., Zhang, L. and Su, X., 2016. Near-infrared fluorescence nanoprobe for enzyme-substrate system sensing and in vitro imaging. *Biosensors and Bioelectronics*, 79, pp.922-929.
111. Yáñez, J., Vicente, V., Alcaraz, M., Castillo, J., Benavente-García, O., Canteras, M. and Teruel, J.A.L., 2004. Cytotoxicity and antiproliferative activities of several phenolic compounds against three melanocytes cell lines: relationship between structure and activity. *Nutrition and cancer*, 49(2), pp.191-199.
112. Yang, Z., Zhang, Y., Sun, L., Wang, Y., Gao, X. and Cheng, Y., 2012. An ultrafiltration high-performance liquid chromatography coupled with diode array detector and mass spectrometry approach for screening and characterising tyrosinase inhibitors from mulberry leaves. *Analytica chimica acta*, 719, pp.87-95.
113. Yi, N. and Abidian, M.R., 2016. Conducting polymers and their biomedical applications. In *Biosynthetic Polymers for Medical Applications* (pp. 243-276). Woodhead Publishing.
114. Zhang, F.X., Qiu, Z.C., Yao, Z.H., Wong, M.S., Yao, X.S. and Dai, Y., 2016. Isolation and identification of metabolites of bakuchiol in rats. *Fitoterapia*, 109, pp.31-38.
115. Zhu, Y.C., Mei, L.P., Ruan, Y.F., Zhang, N., Zhao, W.W., Xu, J.J. and Chen, H.Y., 2019. Enzyme-Based Biosensors and Their Applications. In *Advances in Enzyme Technology* pp. 201-223. Elsevier.